DEVELOPMENT OF PREDICTIVE ROCKFALL RUNOUT MAPS BASED ON CALIBRATED ROCKFALL MODELS

by

Olivia Tabor

A thesis

submitted in partial fulfillment

of the requirements for the degree of

Master of Science in Civil Engineering

Boise State University

August 2023

BOISE STATE UNIVERSITY GRADUATE COLLEGE

DEFENSE COMMITTEE AND FINAL READING APPROVALS

of the thesis submitted by

Olivia Tabor

Thesis Title: Development of Predictive Rockfall Runout Maps Based on Calibrated Rockfall Models

Date of Final Oral Examination: July 14, 2023

The following individuals read and discussed the thesis submitted by student Olivia Tabor, and they evaluated the student's presentation and response to questions during the final oral examination. They found that the student passed the final oral examination.

Nick Hudyma, Ph.D., P.E.	Chair, Supervisory Committee
Bhaskar Chittoori, Ph.D., P.E.	Member, Supervisory Committee
Mary MacLaughlin, Ph.D., P.E.	Member, Supervisory Committee

The final reading approval of the thesis was granted by Nick Hudyma, Ph.D., Chair of the Supervisory Committee. The thesis was approved by the Graduate College.

ACKNOWLEDGMENTS

Foremost, I would like to acknowledge and thank my advisor, Dr. Nick Hudyma, who made this work possible. He provided knowledge and support throughout the writing process. I cannot say enough thanks for the time and effort that he has put into helping me craft this research.

I would also like to thank my two committee members, Dr. Bhaskar Chittoori and Dr. Mary MacLaughlin. Thank you Dr. Chittoori for your time spent reviewing my thesis. You have been very helpful throughout my academic career, and I cannot give you enough thanks. Thank you, Dr. MacLaughlin, for your time on my committee board and for answering my questions. Your knowledge of rockfall has helped me understand the limitations I faced throughout my thesis and has guided me toward solutions.

I also want to thank Rocscience for their support and for providing access to RocFall2. This software was the foundation of my research, and I could not have completed it without the support of Rocscience.

Lastly, I'd like to thank my peers who have helped me gather information in the field: Nathaniel Walker, Russell Gray, and McKenna Roan. Thank you all so much for the time spent gathering data even when there was horrible weather. This was truly a group effort, and I could not have done this without all of you. Cheers!

ABSTRACT

Cliffs formed in columnar jointed basalt have the proper geometry and discontinuities to initiate rockfall events. There are a number of locations in Boise, Idaho that may experience rockfall events from columnar jointed basalt cliffs. Publicly available LiDAR data coupled with site reconnaissance activities were used to develop calibrated two-dimensional rockfall models at a study site in southeast Boise. Photogrammetry was used to determine the volume of seven calibration boulders. The study site, located on Whitney Terrace, consists of a columnar jointed basalt cliff followed by a slope with a subdivision at the toe of the slope.

The two common approaches used to generate rockfall models are the Lumped Mass and Rigid Body methods. At this site, the Rigid Body method that incorporated vegetative properties was demonstrated to be the most appropriate method for the rockfall model. Rockfall model calibration was performed by comparing the model-simulated runout distances and geolocations of the seven calibration boulders. The rockfall models were considered calibrated when the location of the calibrated boulder was within one-half of the standard deviation of the mean runout distance of the furthest traveling grouping of simulated rocks. The calibration provided a range of restitution coefficients that were used to develop predictive runout maps for rocks of various masses for the site. The rock sizes used for the predictive runout maps are based on the range of sizes of runout boulders at the site.

The predictive runout maps showed site vegetation acts as a barrier or energy dissipater for 50 kg and 100 kg simulated rocks. This mass of rocks had shorter runout distances compared to the 400 kg, 800 kg, and 1500 kg simulated rocks. There was only

one location within the study area where large, 800 kg and 1500 kg, simulated rocks would runout past the study area and into the subdivision.

Three recommendations are provided for future work. Firstly, since size and shape are important inputs to Rigid Body rockfall models, more effort should be used to accurately determine these properties. Second, publicly available LiDAR data had to be augmented with field data. Future studies should incorporate site-specific LiDAR data collected with either a terrestrial LiDAR scanner or UAV LiDAR. Finally, three-dimensional rockfall models should be used because they incorporate full-site topography and allow simulated rocks to spread downslope and laterally.

TABLE OF CONTENTS

LIST OF TABLES

LIST OF FIGURES

LIST OF ABBREVIATIONS

2D	Two-Dimensional
3D	Three-Dimensional
CRSP	Colorado Rockfall Simulation Program
DEM	Digital Elevation Model
F_n	Normal Friction
F_d	Dynamic Friction
LiDAR	Light Detecting and Ranging
NPS	National Parks Service
R	Restitution Coefficient
R_n	Normal Coefficient of Restitution
R_t	Tangential Coefficient of Restitution
RTK	Real-Time Kinematics
σ	Standard Deviation
STDV	Standard Deviation
UAV	Unmanned Aerial Vehicle
USDA	United States Department of Agriculture
V_{fN}	Final Normal Velocity
V_{ft}	Final Tangential Velocity
V_{iN}	Impact Normal Velocity
V_{iT}	Final Impact Tangential Velocity

CHAPTER ONE: INTRODUCTION

Rockfall is a geohazard that poses a threat to infrastructure. Rockfall is common in areas with steep and/or undercut rock slopes with steeply dipping or daylighting discontinuities. Rockfall events can be triggered by seismic activity, increases in pore water pressures, freeze-thaw cycles, or the growth of vegetation within discontinuities. There are many strategies to protect infrastructure from rockfall hazards which include barriers, ditches, fences, nets, and rock sheds (Wyllie 2017). Before mitigation methods can be applied, the rock slope must be assessed. One of the greatest challenges of rockfall prediction is knowing how the rock slope and detached rocks will behave. A calibrated rockfall model is essential to understanding the behavior.

A rockfall model can be used to understand rockfall mechanics and behaviors. The models can be used to predict the runout distances, types of movements, and associated energy of rockfall events. This information can be used to identify areas that may be affected by rockfall events and design mitigation strategies. Producing a rockfall model is a complicated task because of the numerous factors that must be incorporated. These factors include slope materials, slope geometry, discontinuities, rock block size, and rock block shape. These factors along with the locations of rockfall initiation and the event causing the rock detachment have effects on the model results. Rockfall models can be performed using a Lumped Mass method or Rigid Body method. The Lumped Mass method is the most widely used method.

The results of the rockfall model can be used to understand future hazards for a particular site. Models can predict the distance a detached rock will travel or the energy associated with any size and shape of a detached rock. This can help to design barriers and other mitigation strategies. The ability to run models with different input parameters can account for many variations in slope and rock behavior. The models can be used to find locations of hazards across an area. Knowing where hazardous areas lie can decrease threats to safety and infrastructure damage.

1.1 Research Objective

The research objective is to use the commercially available program, RocFall2, to develop a mass-based predictive rockfall runout map based on calibrated rockfall models. The calibrated rockfall models will provide accurate runout distances of boulders present in the study area. Based on the calibrated model, a series of mass-based rockfall runout maps will be developed. These maps will display the range of locations where certain-sized rocks will run out after detaching from the face of the rock slope.

1.2 Research Questions

The following research questions are established to achieve the research objectives:

- Can publicly available LiDAR data be used for a calibrated rockfall model and the development of predictive rockfall maps?
- Is the Lumped Mass or Rigid Body analysis method more appropriate for the columnar jointed basalt at the study site?
- How is a rockfall model considered calibrated?

- What is the best way to produce a predictive runout map when the potential block size at the site is variable?

1.3 Limitations of the Research

The limitations of this research are associated with using publicly available LiDAR data, the effect of vegetation, calibration of a rockfall model, and two-dimensional versus three-dimensional analyses. Each of these limitations is discussed below.

1.3.1 Use of Publicly Available LiDAR Data

One of the goals of this research project was to use publicly available LiDAR data. Publicly available LiDAR data often has a lower resolution than site-specific LiDAR data because of the large areas over which data is collected. This study used airborne LiDAR data with a resolution of greater than 8 points per square meter. The type of collection method used sends the laser pulses downwards so it can be difficult to capture vertical features, such as the cliff face at the study area.

1.3.2 Effect of Vegetation

The effect of vegetation on rockfall events is not well established. Vegetation will dissipate energy and reduce the runout distance of detached boulders. The type and size of vegetation, as well as the size and mass of the detached boulders, will influence runout distances. For example, large dense vegetation will reduce runout distances and may cause certain-sized boulders to come to rest in areas of vegetation. While vegetation affects all boulder sizes, it has a greater influence on the runout distance of smaller boulders. There may also be a seasonal aspect to vegetation. In the winter months, the

effect of the vegetation may be reduced, and during the summer months, the effect of vegetation may be enhanced. These uncertainties may lead to inaccuracies when calibrating the rockfall model.

1.3.3 Model Calibration

Calibration is an essential step in developing an accurate and realistic hazard map. Most rockfall models in the literature completely lack calibration or verification (Frattini et al. 2013). Calibrations are conducted using either historical data or full-scale field tests. For this study, historical data was used consisting of geolocated boulders with sizes determined through photogrammetry. An informed calibration technique was implemented, meaning that previously published results from similar sites and information from site reconnaissance narrowed the range of possibilities for the slope parameters.

For a model to be completely calibrated, the rockfall simulation would determine that the runout distance of the rock would be in the exact centroid of the observed boulder. This is not a realistic expectation because of variability in ground parameters, seasonal vegetation changes, and temporal vegetation changes, among others. In order to address these uncertainties, a method will be developed to determine the calibration parameters for each boulder. A model will be considered calibrated when the grouping of the furthest traveling rocks is analyzed. The mean and standard deviation of the grouping's runout distance will be taken. The mean of this grouping must fall within half a standard deviation of the true geolocation of the observed boulder.

1.3.4 Two-Dimensional and Three-Dimensional Analyses

Rockfall analyses can be conducted using either two-dimensional or three-dimensional analyses. For this research, a two-dimensional analysis was used. This assumes detached boulders move downslope along a straight line. The two-dimensional models do not account for the potential spread or lateral movement of a boulder moving downslope. A three-dimensional model accounts for topographic variations across a site, not just along a straight line, which would provide a more realistic estimate of runout boulder locations. One potential limitation of the two-dimensional analysis over the more realistic three-dimensional analysis is the estimation of the slope parameters for the calibration of the rockfall model. Slope parameters such as the coefficient of restitution were determined for two-dimensional analysis and may not be appropriate for three-dimensional analyses.

1.4 Structure of the Thesis

This thesis contains six chapters. The first chapter, the introduction, discusses the overview of rockfall modeling and hazard prediction. The introduction also acknowledges the limitations of the research while laying out the objectives and research questions.

Chapter Two is a literature review focusing on rock-based geological hazards with a focus on rock instability and rockfall. Within this chapter, the rockfall site conditions and rockfall models are discussed. Two case histories of rockfall in columnar jointed basalt are presented because the study site for this research is within this type of rock. Finally, the development of rockfall hazard maps and their importance is discussed.

Chapter Three describes the study site. It begins with a general discussion of the geology of southwest Idaho and finishes with a detailed description of the study site. This chapter also presents and describes the data used for this research. This includes an overview of the publicly available LiDAR data, using the LiDAR data to obtain slope geometries and site reconnaissance activities. These activities include geolocating runout boulders and using photogrammetry to determine the volumes of boulders used to calibrate rockfall models.

Chapter Four describes the process of rockfall model calibration. It presents the variables that are required for rockfall modeling. Three rounds of calibrations were performed, and their associated results are described. The multiple calibrations needed to be performed because the results did not match the observed data at the study site. Ultimately, the rockfall models were calibrated using the Rigid Body method with vegetation. Finally, the impact of the calibrated properties and their impact on the development of predicted rockfall runout maps is discussed.

Chapter Five describes the ranges and distributions of the parameters from the calibrated rockfall models that were used to generate the predictive runout maps. The predictive runout maps are presented and discussed.

Chapter Six presents the findings and limitations of the research conducted. It also includes ideas for future research and expansion. These ideas include altering the LiDAR collection method, utilizing smart rocks, and considering a three-dimensional rockfall analysis.

CHAPTER TWO: LITERATURE REVIEW

Rockfall is a geologic hazard that is complex and difficult to predict. Research on rock slope instability and rockfall behavior helps to understand the mechanics behind rock block detachment. This literature review presents background information on rock slope instability with a focus on rockfall. A discussion on rockfall simulations and variables associated with the simulations is presented with a focus on the commercially available computer program RocFall2, which is used in this research. Finally, information is presented on hazard maps and previous studies of rockfall in jointed columnar basalt. Previous studies are important because columnar jointed basalt is found at the study site for this research.

2.1 Geologic Hazards

Geologic hazards, or geohazards, are types of hazards that occur due to geologic events or conditions (Parkash and Gupta 2014)**.** While most of these hazards are naturally occurring, they can also be anthropogenically induced. Geohazards include seismic events, earth movement downslope, volcanism, expansive soils, and others. The damage and associated costs caused by geohazards are categorized as both direct and indirect. Direct costs include loss of life and damage to infrastructure. Indirect costs include disruption of transportation routes and economies.

Rock slope instability is just one type of earth movement downslope. Exposed rock faces challenges posed by physical, chemical, and biological processes. These processes have the potential to degrade rock and cause new fractures or extend current ones. Since rock masses have nonlinear properties, it can be difficult to understand and

predict rock slope instability compared to a soil slope. This poses a significant challenge to better understand and predict rock slope instability since cases of rock slope failure are on the rise. Studies have implicated that there is an increasing trend in rock slope failure, most likely caused by a rise in global temperatures (Krautblatter and Moore 2014).

2.2 Rock Slope Instability

There are four main types of rock slope instabilities: planar, wedge, circular, and toppling. These instabilities are shown in Figure 2.1.

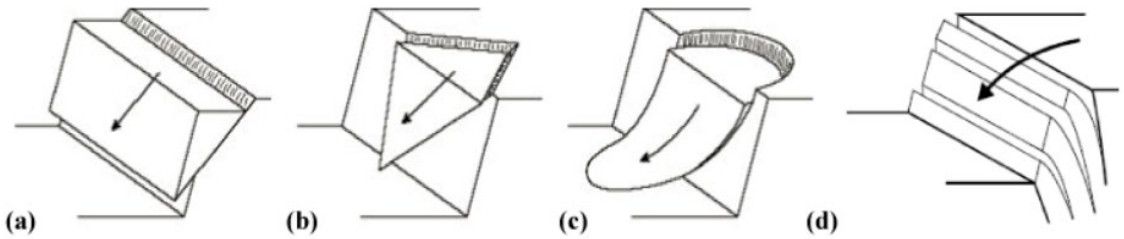

Figure 2.1: Failure Types: (a) Planar, (b) Wedge, (c) Circular, and (d) Toppling (Andrew et al. 2011)

Planar failure occurs when a rock plane slides along a discontinuity that is flatter than the overlying slope face. Wedge failure occurs when there is sliding along an intersection of discontinuities in the rock mass where the sliding block plunges downwards along an inclination flatter than the slope face. Circular failure is more prevalent with softer materials such as weathered rock. When the slope material becomes weakened, the failure surface is able to find the path of least resistance through the slope, causing a failure, usually in a circular shape. Lastly, toppling failure is when the rotation of columns or blocks cause failure (Alade and Abdulazeez 2014). Columns and thinly

bedded layers have closely spaced discontinuities causing them to be prone to failure. Within the category of toppling, there are three modes of failure: flexural, block, and block-flexure failure, shown in Figure 2.2.

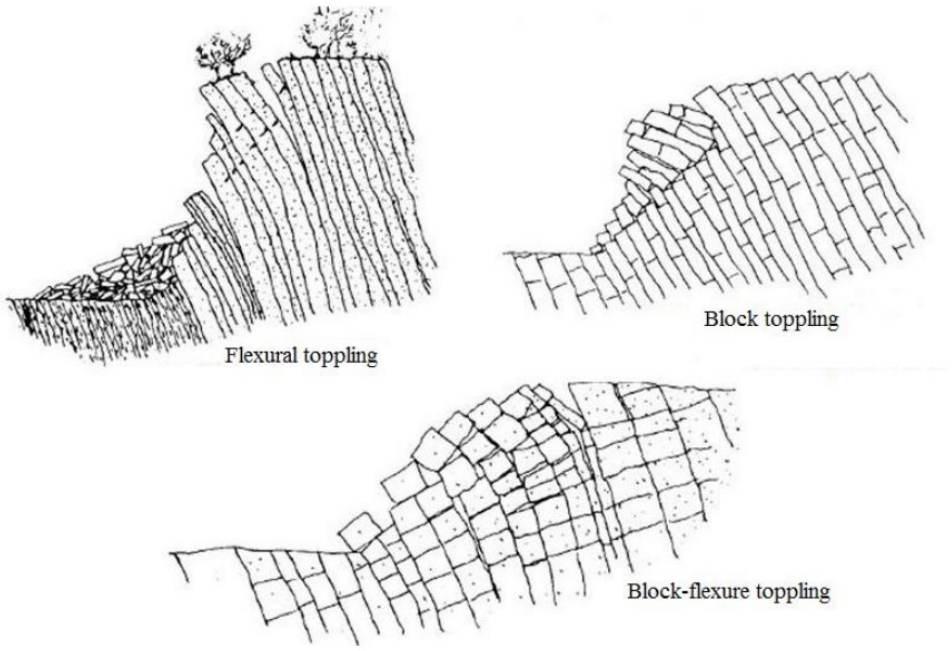

Figure 2.2: Types of Rock Toppling Failure (Andrew et al. 2011)

Flexural toppling occurs when there are steeply dipping discontinuities in the rock mass and orthogonal joints are not well developed. Block toppling is a very common failure that occurs when there are two discontinuity sets. These two sets involve one dipping steeply into the face and the other with perpendicular joints cutting into the first set of discontinuities. This type of failure pushes the small blocks forward from the larger columns pressing forward, causing the blocks to detach and pile on one another. Block-flexure toppling is when flexure occurs along pseudo-continuous columns (Cláudia

Pereira et al. 2013). The movement across the cross joints causes the rock blocks to topple.

The failure mechanisms of rock slopes mentioned above primarily involve sliding movements, but rock slope instability does not necessarily lead to detached rock blocks traveling downslope. For detached rock to travel downslope, slope instability must occur along with specific site conditions that allow rockfall motions to occur. These site-specific conditions are discussed below.

2.3 Anatomy of Rockfall Sites

Some important factors that influence rockfall behavior include slope angle and materials. The anatomy of a rockfall site can generally be categorized into the rock slope, colluvium slope, talus slope, and run-out zones. These features are displayed in Figure 2.3. The rock slope will have widely spaced impact areas and high-angle trajectories. The rockfall behavior over rock slopes will include high translational and rotational velocities. The colluvium slope is defined as the area just steeper than the angle of repose which depends on the material type. For loose rock fragments, the angle of repose is typically 37 degrees; therefore, the colluvium slope is defined as the area that is inclined greater than 37 degrees. The rockfall behavior over colluvium slopes will have closely spaced areas of impact with shallow trajectories. While the areas of impact are close together, this slope type does not cause rocks to accumulate on one another during rockfall. Talus slopes are flatter than colluvium slopes with an inclination about 32 to 37 degrees. Because of the smaller slope angle, rocks begin to accumulate on one another. While they accumulate, they begin to spread with the smaller rocks coming to rest at the beginning of

the talus slopes and the larger rocks traveling to the end of the talus slope area. These groups of rocks that accumulate over the talus slope are called scree and form talus deposits. Lastly, the run-out zone is where the most high-energy blocks come to rest. These blocks can move beyond the talus deposit and come to rest on a flatter area. The maximum angle of the runout zone near the base of the slope in this example is approximately 27.5 degrees. This angle represents the rolling friction coefficient of rockfalls (Wyllie 2017). Within this zone type, the rockfall behavior involves closely spaced impacts or rolling. Rocks in this zone can be easily stopped with barriers, ditches, or other remediation methods.

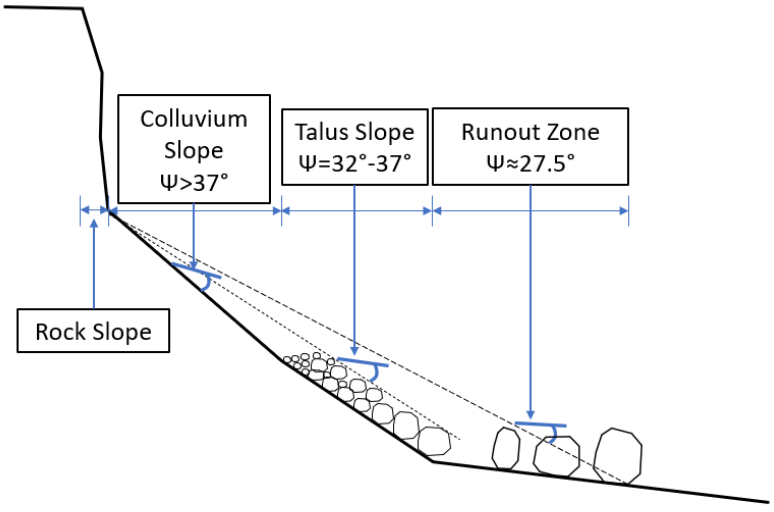

Figure 2.3: Example Slope Configuration (after Wyllie 2017)

2.4 Rockfall Events

Rockfall events are a compilation of impacts and trajectories. For each individual impact, there is a different trajectory. Rockfall trajectories are based on Newtonian mechanics. These mechanics use parabolas to define the trajectory paths. Impact mechanics are influenced by rock shape, material, and rotation (Wyllie 2017). These impacts are complex and hard to fully account for when building a model; therefore, during rockfall modeling the impacts are simplified.

Rockfall behavior can be simplified into four different types of movement: free fall, bouncing, rolling, and sliding. Free fall is when a rock detaches from the source area and falls down a steep cliff without any disruption, only being influenced by gravity. Bouncing is a type of movement that occurs when the detached rock block impacts the slope surface. The behavior of this rockfall movement is defined by the characteristics of the slope. Rolling occurs when angular velocity is present, causing the rock to roll along the slope. Lastly, sliding is when the rock block slides along the slope. The sliding velocity is influenced by kinetic friction and slope geometry (Peng 2000). Usually in areas of flatter slope, rockfall will experience both sliding and rolling before coming to rest. All of these rockfall movements are influenced by slope geometry. In a study, bouncing occurred when the slope angle was 60 degrees while rolling and sliding occurred when the slope angle was equal to or less than 45 degrees (Ritchie 1963). The rockfall behaviors and slope geometry are shown in Figure 2.4. Since the slope influences the motion of rockfall, it is vital to understand the slope properties and geometry to accurately predict rockfall behavior.

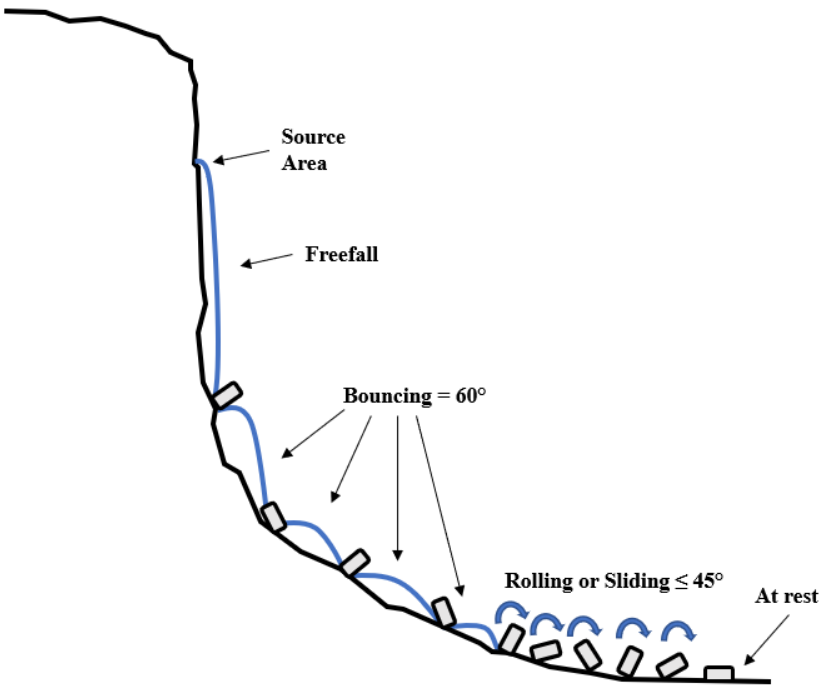

Figure 2.4: Rockfall Behavior (after Peng 2000)

2.5 Rockfall Simulation and Assessment

When facing a rock slope instability issue, creating a rockfall simulation is a useful first step in identifying hazards. A rockfall simulation can be used to produce a myriad of results. The simulation can deliver outputs on runout distance, impact velocity, rotational velocity, and more. These results can be used to help create mitigation infrastructure such as barriers or nets. Rockfall simulations can also be used to back-calculate properties of the slope, such as friction and restitution coefficients. Immense understanding can come from rockfall simulations which can provide valuable information on hazard prediction and prevention.

2.5.1 Rockfall Simulation Software

There are many types of rockfall and rock slope analysis software, such as RocFall, RocTopple, Colorado Rockfall Simulation Program, Rapid Mass Movement Simulation (RAMMS), and others. The most common rockfall simulation software are Colorado Rockfall Simulation Program (CRSP) and RocFall. CRSP was originally developed for the construction of I-70 in Glenwood Canyon, Colorado. Its theories were originally based on the research of Pfeiffer and Bowen (1989) and Pfieffer et al. (1991; 1995). This program simulates rockfall events using four main components: rock size and slope irregularities, material, and profile (CRSP Manual Version 4.0).

Rocscience produces both RocFall2 and RocFall3. RocFall2 is the most commonly used of the two and performs a 2D statistical analysis to obtain information on the behavior of the rockfall. RocFall3 is similar but considers a three-dimensional aspect to the site while RocFall2 uses a 2D cross-sectional slope. RocFall2 can determine many characteristics of the rockfall behavior such as energy, velocities, and bounce height (RocFall2 User Guide 2023). Similarly to CRSP, RocFall2 also utilizes data based on rock size and slope geometry and materials. RocFall2, which will be used in this research, is unique in that the user can choose between Lumped Mass Analysis and Rigid Body Analysis.

2.5.2 Analysis Methods in RocFall2

Lumped Mass and Rigid Body analysis methods use very different inputs and computational methods. The Lumped Mass method does not consider size or shape, only mass. This method requires a friction angle, which can be set to zero or calculated from

the coefficients of restitution. The Lumped Mass method is far more researched than the Rigid Body method; however, it is a very simplified analysis.

The Rigid Body method considers the shapes of the rocks and has a myriad of shapes available to choose from in the preset software library. User-defined shapes can also be used. The shapes are two-dimensional and extrude into the third dimension based on size and mass. The Rigid Body method also considers impulse reaction during the contact period between the rock and slope (RocFall2 User Guide 2023). This consideration is able to determine behavior such as slip, sticking, and reversal behavior. A list comparing input parameters for Lumped Mass and Rigid Body Models based on the Rocscience User Guide is found in Table 2.1.

Table 2.1: Comparison of Input Parameters for Rockfall Models in RocFall2

Parameter	**Lumped Mass**	**Rigid Body**
Rock Shape	Modeled as a particle	Rock shape is modeled
Normal coefficient of Restitution (Rn)	Velocity based	Energy based
Tangential coefficient of restitution (Rt)	Must be used	Not used unless the "Tangential CRSP Damping" option is selected
Dynamic friction	Used when rock is sliding	Applied when rock is impacting slope and when sliding
Rolling friction	Not used	Used and applied when rock rolls
Special Options	Option to consider rotational velocity if desired	Option to consider Tangential CRSP Damping, advanced friction parameters, viscoplastic ground drag, and forest damping

Both analysis methods have been validated but tend to produce different results. When modeling rock as a very small sphere and holding all other inputs the same, both analysis methods produce very similar results (RocFall2 User Guide 2023). This is due to the Lumped Mass method modeling all simulated rocks as small particles. Modeling the rocks as very small spheres in the Rigid Body method results in the most similar results between the two analysis methods.

2.5.3 Inputs into Rockfall Models

There are numerous factors that influence the behavior of rockfall events. For this thesis, four are discussed: friction coefficients, restitution coefficients, vegetation, and mass versus shape.

2.5.3.1 Friction Coefficients

The energy lost during rockfall events from friction can be represented by friction coefficients. There are two different types of friction coefficients, dynamic and rolling friction. Dynamic friction, F_d, is related to the friction angle of the material (RocFall2 User Guide 2023). The rolling friction, Fr, is used to represent energy lost from sources outside of F_d. During rockfall simulation, the friction coefficients affect the rockfall behavior; however, they do not have nearly the same influence as the coefficients of restitution.

2.5.3.2 Coefficients of Restitution

Rockfall behavior over specific site conditions can be represented by the coefficient of restitution. This coefficient can be separated into two parameters, Rn and Rt. These two coefficients help to understand how slope and conditions affect the rock's velocity and behavior during impact. The normal coefficient of restitution, Rn, represents the change of normal velocity during a rock's impact on the slope. Rn is related to the impact angle as well as the inelastic compression of the slope materials. The tangential coefficient of restitution, Rt, represents the reduction in tangential velocity during impact with the slope. It is related to friction between the slope and the rock body (Wyllie 2017).

Newton first developed the concept of a coefficient of restitution. His ideas have been expanded on to develop a formula for the normal coefficient of restitution (Wyllie 2017). It can be expressed as:

$$Normal\ coefficient\ of\ restitution, R_n = \frac{final\ normal\ velocity,\ v_{fN}}{impact\ normal\ velocity, v_{iN}} = \left(\frac{rebound\ height,\ h_f}{drop\ height, h_i}\right)^{1/2}$$

Equation 2.1

This formula suggests that a coefficient could be obtained by dropping a rock and recording its drop height and rebound height. While this seems to be a simple method of calculating the coefficient, it does not always seem to provide accurate results when using these coefficients in a rockfall simulation. This inaccuracy is likely due to the angle of impact into the slope material that changes the behavior of the rock, which this simplified method does not account for. It may be necessary to back-calculate the normal coefficient of restitution by using real observed data and rockfall simulation software.

The tangential coefficient of restitution can be expressed as:

$$Tangential\ coefficient\ of\ restitution, R_T = -\frac{final\ tangential\ velocity,\ v_{fT}}{impact\ normal\ velocity, v_{iT}}$$

Equation 2.2

The tangential coefficient of restitution does not change throughout the rockfall processes and there appears to be no relationship with the impact angle. The tangential coefficient appears to be analogous to the coefficient of friction, μ. In a study, a tractor was used to estimate the coefficient of friction by pulling on a 433 kg rock over concrete, gravel, and soil. The average friction coefficients were calculated as 0.59, 0.68, and 0.90,

respectively (Wyllie 2017). The coefficients of restitution, R_t and R_n, have a negative correlation with one another; a high R_t value means a low R_n value and vice versa.

2.5.3.3 Effects of Mass and Shape

Mass is known to play a factor in rockfall behavior. Rocks with large masses tend to have higher energy and longer runout distances. The shape is also known to play a factor in rockfall behavior; however, this is not a highly researched topic. RocFall2 offers the ability to pick rock shapes in the Rigid Body analysis mode. According to the RocFall2 User Guide, smooth shapes tend to run further down the slope than polygonal shapes. Polygonal shapes tend to slide on the slope, causing them to slow down and stop high up the slope. Lastly, rounder shapes tend to travel further than oblong shapes.

Researchers conducted experiments in Switzerland to better understand how rock block mass, size, and shape influence rockfall hazards (Caviezel et al. 2021). This experiment was conducted in Chant Sura, Flüelapass, Switzerland, over 12 snow-free days between 2017-2019. This experiment involved designing rocks using heavily reinforced concrete and dropping the rocks down the slope to represent rockfall events. In this experiment, man-made rocks used were either equant or wheel-shaped blocks. While these rocks had two different shape categories, they were designed with the same masses: 45, 200, 800, and 2670 kg. The goal of this experiment was to quantify the influence that rock shape and mass played in rockfall runout and spreading distances. The results are shown in the hazard map in Figure 2.5.

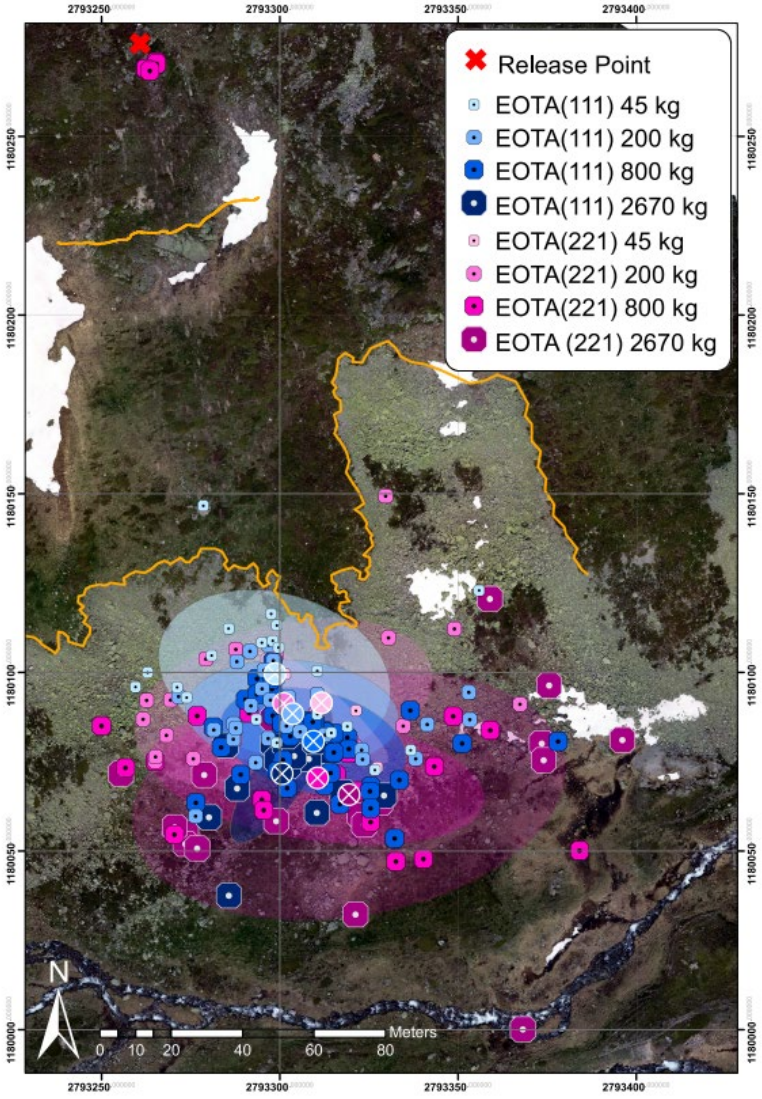

Figure 2.5: Mass vs. Shape Experiment in Switzerland (Caviezel et al. 2021)

A total of 183 drops were conducted. The wheel-shaped rocks are plotted as magenta points on the map, while blue points are the equant rocks. Based on the provided hazard map in Figure 2.5, it can be seen that the wheel-shaped rocks travel significantly further with runout distance and spread. This aligns with Rocscience's statement in the RocFall2 User Guide stating that smooth-shaped rocks will travel further than polygonal

shapes. Another observation based on the hazard map is that generally, the larger the mass, the further the distance traveled down the slope. This is due to the higher energy and velocities that larger mass rocks experience. Another observation that can be made based on the hazard map is that the spread of the wheel-shaped rocks is much higher while the equant rocks are closely grouped together, and the small-to-large runout distances of equant rocks are much less prominent than the wheel-shaped rocks. Overall, this experiment proved that shape plays a large factor in the behavior of rockfall. Rock mass also appears to affect the runout results of both shapes, but largely affects wheel-shaped rocks.

2.5.3.4 Vegetation

Vegetation on rockfall slopes can greatly affect the results of rockfall behavior and runout. Vegetation can tend to decrease rock velocities and dissipate their energy which causes them to come to rest much sooner than a vegetation-free slope would. Understanding vegetation on site is valuable when evaluating the risk of rockfall on a large-scale scope (Masuya et al. 2009). Typically, vegetation is not accounted for to take conservative measures since the vegetation slows down rockfall. Usually, vegetation is accounted for in rockfall simulations by using a friction coefficient.

2.6 Rockfall Studies in Columnar Jointed Basalt

The focus of this thesis is rockfall in columnar jointed basalt. Two important rockfall studies, described below, have been conducted in columnar jointed basalt.

2.6.1 Oregon Quarry Site

The Oregon Department of Transportation Quarry Test Site is described as hard durable basalt that rebounds well after both impact and rolling (Wyllie 2017). At least 11,250 rocks were rolled during the research including at least 750 rocks per each slope angle and height. The researchers used a suite of sizes ranging from 0.3 to 0.9 meters in diameter, measured across the longest point. Both the impact distance and rollout distance were recorded. The impact distance is defined as the slope distance from the toe of the cut slope to the area where the rock first strikes the ground. The rollout distance is the distance between the toe of the cut slope and the furthest point the rock reaches (Pierson et al. 2001). One outcome researchers found was that during rockfall, the rock would have the same impact distance and rollout distance. This occurred when dealing with steeper sloped catchment areas. This is shown below in Figure 2.6. As the catchment slope increased, rollout distances decreased.

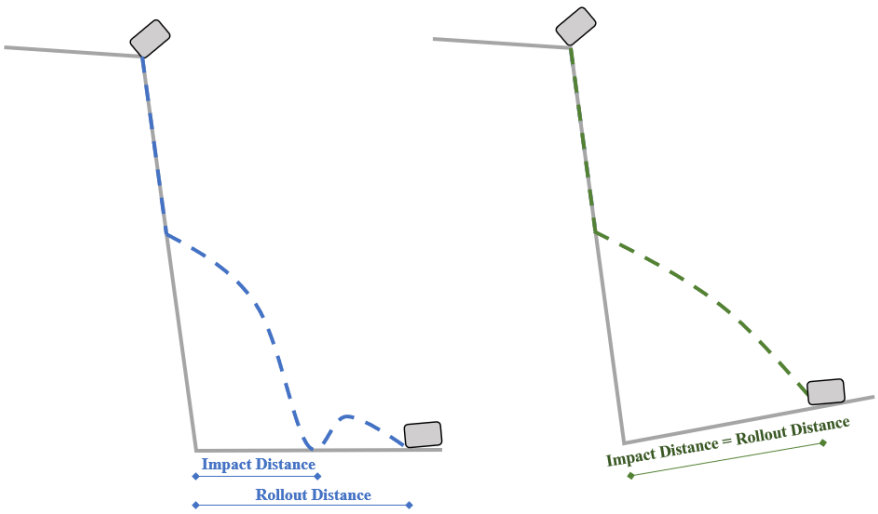

Figure 2.6: Impact and Rollout Distance (after Pierson et al. 2001)

The main takeaway from this study was that the cut and catchment areas of the slope appeared to have the greatest effect on the rockfall path. The cut slope would determine where the detached rock block first impacted the catchment area. It was determined that rockfall velocities were a function of cut slope angle, height, and amount of time spent in contact with the slope. When the slope was steeper there would be less contact with the slope, resulting in less friction. The lack of friction caused an increase in the velocity and energy of the rocks. In order to reduce rock runout, steeper catchment area slopes seemed to be the best solution to reduce rockfall runout. The results from the simulations resulted in the creation of design guidelines based on catchment area and cumulative percent of retention.

This experiment was taken and expanded on by Duncan C. Wyllie. Wyllie used RocFall 4.0 to model this site for two 580 kg rocks. The 95th percentile 1st impact location was found at 11.8 meters while the 95th percentile roll out distance is found at 19.4 meters. The Rn and Rt values for the rock slope were 1.00 and 0.59, respectively, with a standard deviation of 0.04 (Wyllie 2017).

2.6.2 Mumbai-Pune Expressway

The Mumbai-Pune Expressway in India was built to reduce accidents and accommodate the increase in traffic on an existing highway in Mumbai. The expressway opened on March 1, 2002. Soon after the opening, the expressway faced many issues with rockfall events due to monsoons. The rockfalls occurred after the detachment of rock blocks from the discontinuities with little or no shear displacement. The rock blocks descended at very high speeds up to 30 m/s (Kumar et al. 2010).

Geologic and geotechnical investigations were performed to better understand the site conditions and protection measures needed. One observation was the basalt had seepage in the top of the columns which likely made it susceptible to slope failure. The most prominent plane of weakness was the columnar (vertical) joint. The geotechnical investigation showed a thin veneer of soil ranging from a few centimeters to one meter in depth. The soil on site was classified as nonplastic.

The vertical face of the cliff was most vulnerable to detaching rock blocks. The rock face was improved by removing the loose overhanging blocks. Due to columnar jointing, the number of joints in the rock mass poses a danger with the likelihood of joint expansion over time. The remediation method proposed for this was the application of steel fiber-reinforced shotcrete. This would be applied to the rock mass along with a steel cable net displayed in Figure 2.7.

Figure 2.7: Cliff Face with Shotcrete and Steel Cable Net for Remediation

2.7 Hazard Maps for Rockfall

Hazard maps can help visualize past rockfall events and help identify areas that are at risk of future events. In some areas, accurate mapping and risk assessment are required for the government to make decisions regarding infrastructure planning for hazards. Two examples are described below.

2.7.1 Example of Rockfall Hazard Assessment and Mitigation

Yosemite National Park is one area that frequently faces rock slope instability issues, specifically rockfall. There is a rockfall inventory database for the park that has kept records since the 1800s. According to this database, from 1857 to 2011 there were a total of 925 rockfall events that were witnessed and recorded. These led to 15 fatalities, 85 injuries, and damage to infrastructure throughout the park (Stock and Collins 2014). In response to a large number of rockfall events, the National Park Service (NPS) decided to take action to reduce the risk of rockfall to tourists throughout the park.

The NPS decided to launch hazard assessments throughout certain areas of the park. This study involved terrain mapping, cosmogenic dating, and rockfall runout simulations. The final product of this study was the determination of where hazard zones were located. The NPS defined these hazard zones as an area where there was a 10% chance that in 50 years a boulder would travel through the zone. Many of these hazard zones were found to be located in highly populated areas of the park. For example, Curry Village had a third of its structures located in a hazard area.

While the NPS determined that mitigation methods were needed throughout the park, one of their major missions is to preserve the natural scenery and processes of their

parks. Due to the construction and appearance of the possible mitigation methods, these were deemed incompatible, and a different approach was taken. This resulted in the removal of structures located within high-hazard areas. Buildings were relocated or repurposed to low-occupancy structures. This mitigation decision resulted in the removal of 200 buildings and the repurposing of three buildings in 2013.

Understanding the rockfall runout and hazard areas proved successful with a 95% reduction in human occupancy-related risk compared to their 2008 levels. In 2014, a large rockfall event occurred in Curry Village, and multiple boulders were found in previously populated areas. One boulder, approximately 1 cubic meter in volume, impacted the footprint of one of the buildings removed and came to rest in the footprint of another removed building. Figure 2.8 displays the success of the mitigation technique. Figure 2.8(a) displays damage in 2008 before any mitigation measures were taken. Figure 2.8(b) shows the same general area as Figure 2.8(a). This figure also demonstrates the effect of vegetation, in this case, trees, on rockfall as the large boulder came to rest between two trees. Figure 2.8(c) shows the outline of two buildings that were removed and the location where a boulder impacted (highlighted in yellow) and where the boulder came to rest (indicated by the yellow arrow). Removing the two buildings was successful in preventing damage from a rockfall event.

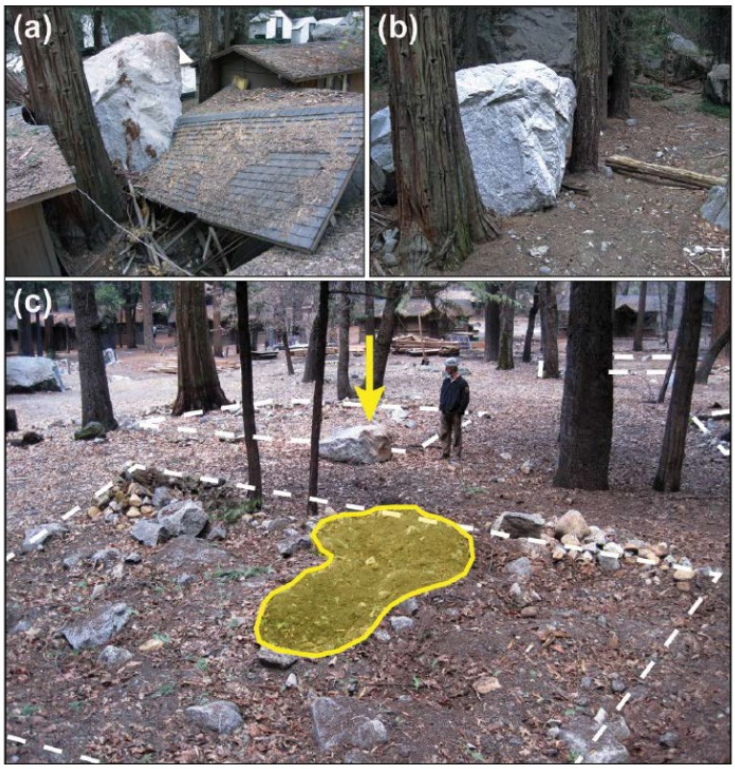

Figure 2.8: (a) Area Before Mitigation (b) Area After Mitigation (c) Area After Mitigation Showing Footprint of Rock Impacting in Old Structure Area

This rockfall event could have been extremely destructive and deadly had the mitigation process never taken place. Yosemite National Park is one of the few examples of successful rockfall analysis and mitigation.

2.7.2 Veyrier-du-Lac, France

France has developed and implemented a Risk Prevention Plan for any towns that are subjected to natural hazards, which include rockfall, avalanches, and floods. It is a requirement that these plans are updated every ten years (Monnet et al. 2010).

In the town of Veyrier-du-Lac situated in the Auvergne-Rhône-Alpes region of south-eastern France, residential areas are located along the footslope of the surrounding

mountains. The footslope in the area of the town is heavily forested with approximately 80% of the slope being vegetated. Trees and vegetation act as barriers to rockfall and infrastructure expansion into the slopes will require the removal of forested areas. In this area, rockfall occurs a moderate amount with 23 recorded events since 1950.

Researchers used historical data, field data, airborne laser scanning (ALS), and 3D rockfall simulations to create a 3D rockfall trajectory model to determine risk zoning. For the 3D rockfall simulations, the researchers used Rockyfor3D, a software that can simulate the barrier effect of trees on falling rocks.

Within the software, vegetation is modeled using a stand parameter which represents the number, position, and diameter of the trees. Forest stand parameters were estimated on a scale and then projected on the entire area using established models and ALS data. Researchers defined the hazard levels by using a cross-analysis of frequency and intensity classes. The rockfall area was divided into nine zones for analysis: seven zones of 1 m^3 sized blocks, one zone of 2 m^3 blocks, and one zone of 3 m^3 blocks. 1000 rockfall trajectories were computed; 500 for bare soil conditions and 500 for forest integration. Researchers found that the zone defined by the 1 m^3 category was impacted by forest integration. Rockfall in these zones resulted in significantly reduced rock runout distances. When comparing the two hazard maps, Figure 2.9 and Figure 2.10, it appears that forest integration had a profound effect on the lateral deviation of blocks. The energy of the rockfall significantly increased without the consideration of vegetation. There was an increased prevalence of “high” hazard areas without vegetation. The expanded lateral distance and increase in energy and frequency will likely cause more damage to

infrastructure. The hazard maps help visualize the necessity of vegetation in the area to help prevent dangerous high-energy rockfall in the area.

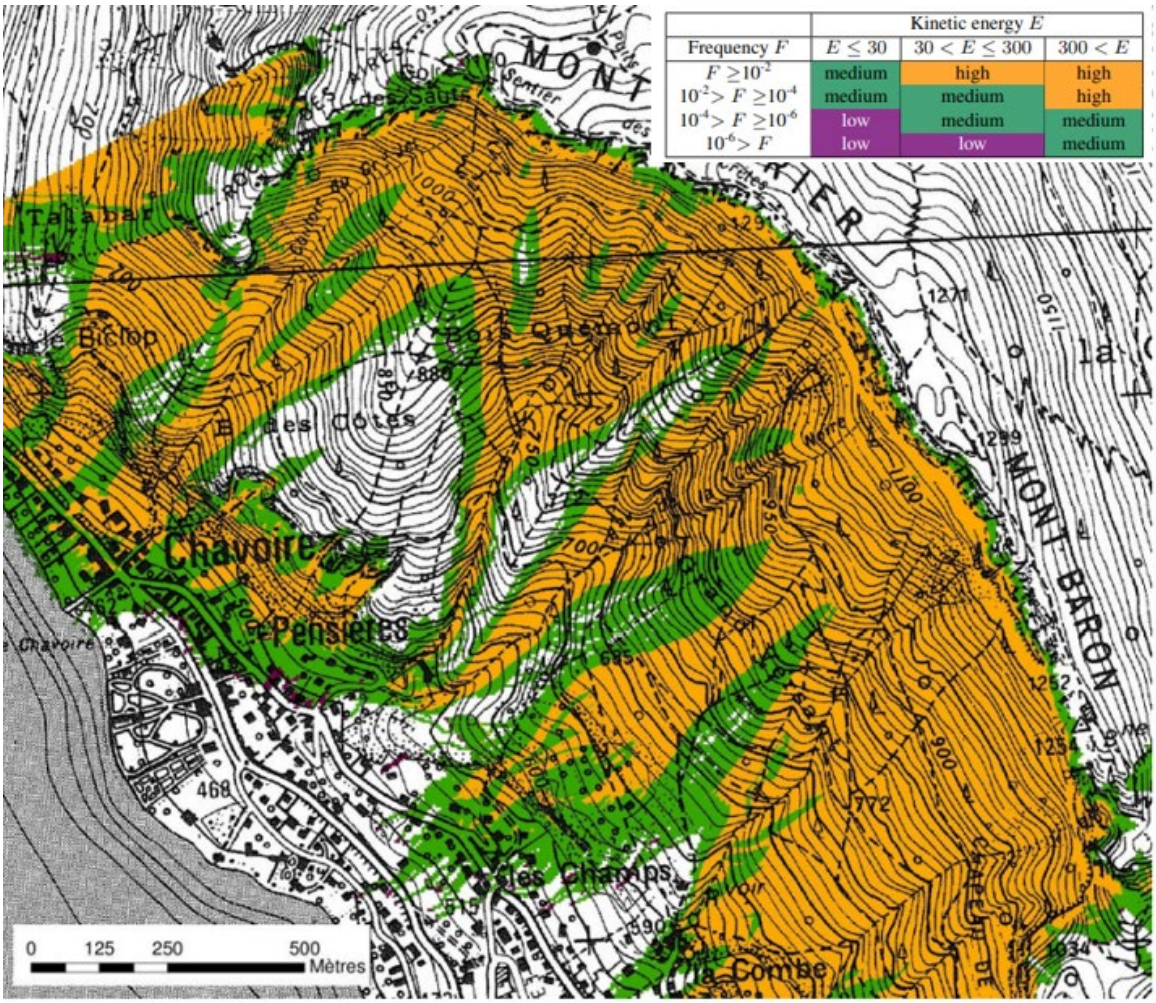

Figure 2.9a: Hazard Map without the Effect of Vegetation Considered

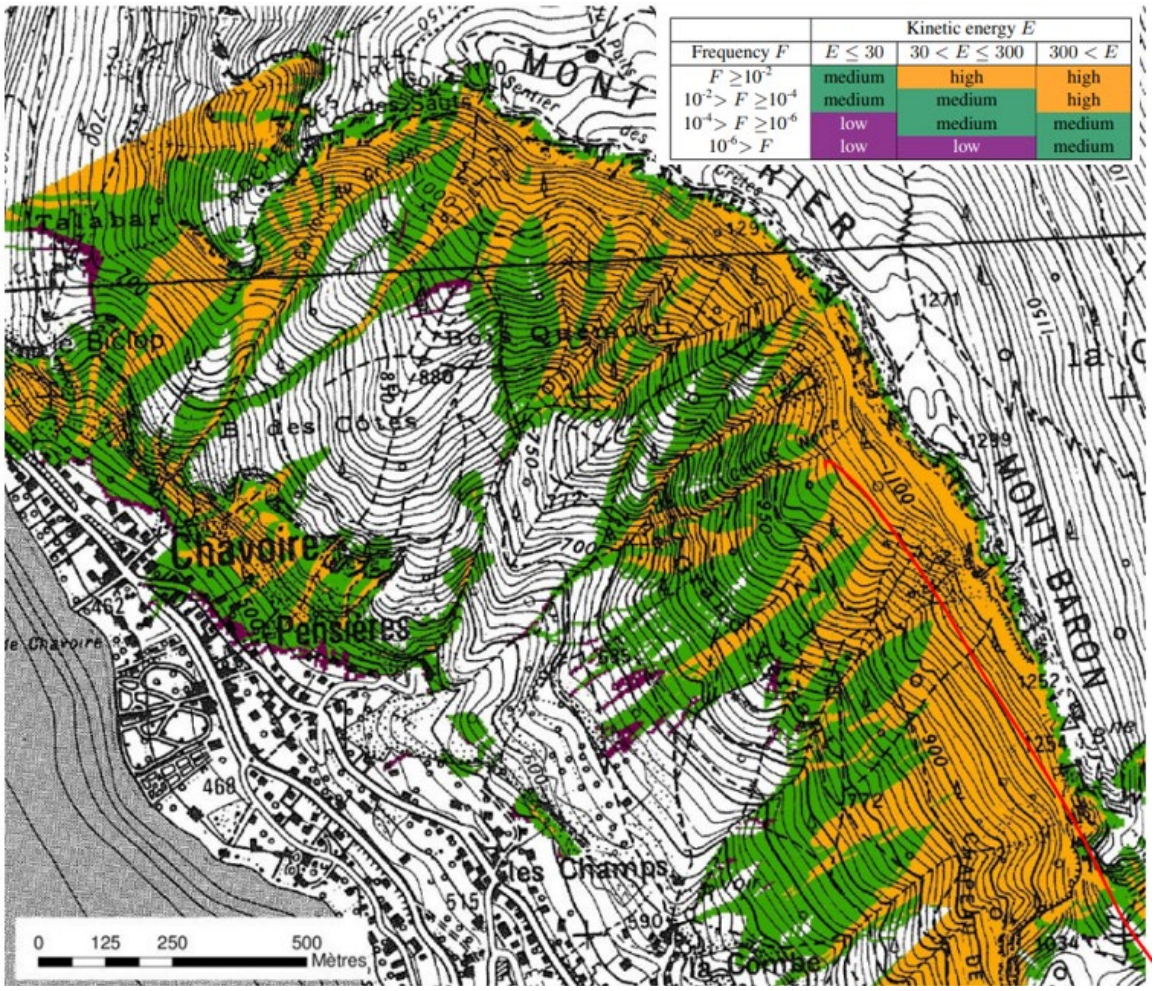

Figure 2.9b: Hazard Map with the Effect of Vegetation Considered

2.8 Chapter Summary

Rock slope instability is controlled by discontinuities. Rockfall occurs in a number of geological conditions which include near vertical or vertical jointing, steep slopes, and undercut slopes. Rock toppling involves flexural toppling, block toppling, or a combination of the two. Rockfall events occur after rock block detachment. Rockfall behavior is a combination of impact and trajectory which can be difficult to predict. The behavior of rockfall can be simplified into four categories: free fall, bouncing, rolling,

and sliding. All of these movements are influenced by the slope geometry and characteristics and properties of the materials.

Rockfall simulations can be used to identify rockfall hazards. These simulations can be performed in either 2D or 3D and can provide information on energy, runout distance, and other results. Simulations are either conducted using the Lumped Mass method or the Rigid Body method. Historically, the Lumped Mass method is most often used.

There are many different parameters involved in the modeling of rockfall which are a function of the analysis method. The parameters include normal and tangential restitution, rolling and dynamic friction, vegetation, mass, and shape. The rock shape is a factor that is often overlooked and can be more influential than mass (Caviezel et al. 2021).

Rockfall hazard maps are used for a variety of purposes. They have been used to estimate future events (Stock and Collins 2014) and investigate the impact of deforestation caused by increased development (Monnet et al. 2010).

CHAPTER THREE: STUDY LOCATION AND SITE DATA

This chapter presents the description of the study geography and collected field data. The study location is in Southeast Boise, Idaho which is located on the Snake River Plain. The study site is located on Whitney Terrace, which is bound on one side by a vertical columnar jointed basalt cliff and associated talus deposits. The study area is a subsection on Whitney Terrace where field observations and surveying took place. Included in this chapter is a description and use of publicly available LiDAR data, the geo-location of boulders in the study area, and boulder volumes determined through photogrammetry of calibration boulders. This chapter answers the research question "Can publicly available LiDAR data be used for a calibrated rockfall model and the development of predictive rockfall maps?"

3.1 Study Location

The Snake River Plain is a large geological feature that stretches throughout southern Idaho. From satellite imaging, the plain looks to be homogeneous; however, it can be dissected into the western Snake River Plain and the eastern Snake River Plain. These features were formed through different geologic processes, leading each plain to have its distinct structure, lithology, and age (Maley 2019). The western Snake River Plain was created through large gravity faults at the north and south boundaries, forming a large structural basin. The geology of the western plain ranges from sand dunes to volcanic rock.

Boise, Idaho is located on the western Snake River Plain. It has columnar basalt terraces throughout the area. Columnar jointed basalt is best described as a series of

columns that are hexagonal in shape that are formed from cooling lava flows (Zhang et al. 2020). Examples of columnar jointed basalt can be found throughout the western Snake River Plain and Boise.

The most prominent areas of basalt are located around Lucky Peak Reservoir. Researchers have mapped cross-sectional areas of the Boise River Canyon near Lucky Peak Reservoir shown in Figure 3.1 (Othberg and Gillerman 1994). Prominent pillow basalts and layers of basalt flows along Highway 21 are noted in their findings.

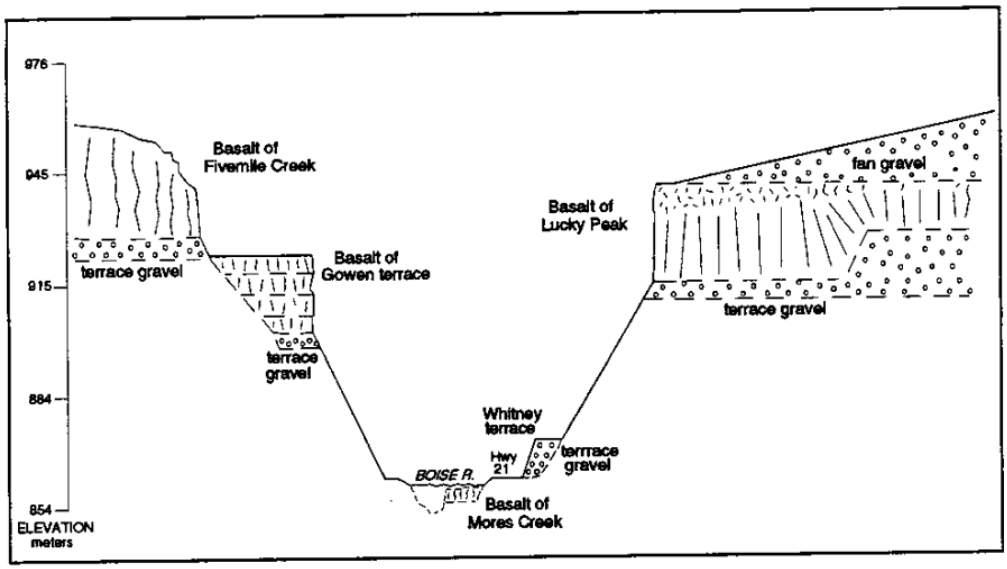

Figure 3.1: Cross-sectional Areas in Boise River Canyon (Othberg and Gillerman 1994)

The study location is in Boise, south of the Boise River near Lucky Peak Reservoir, as shown in Figure 3.2. The Boise River has prominent columnar jointed basalt features alongside the river and Highway 21 in this area. This study site is located

on Whitney Terrace, to the south of State Highway 21. A geological cross-sectional map of the area is shown in Figure 3.3.

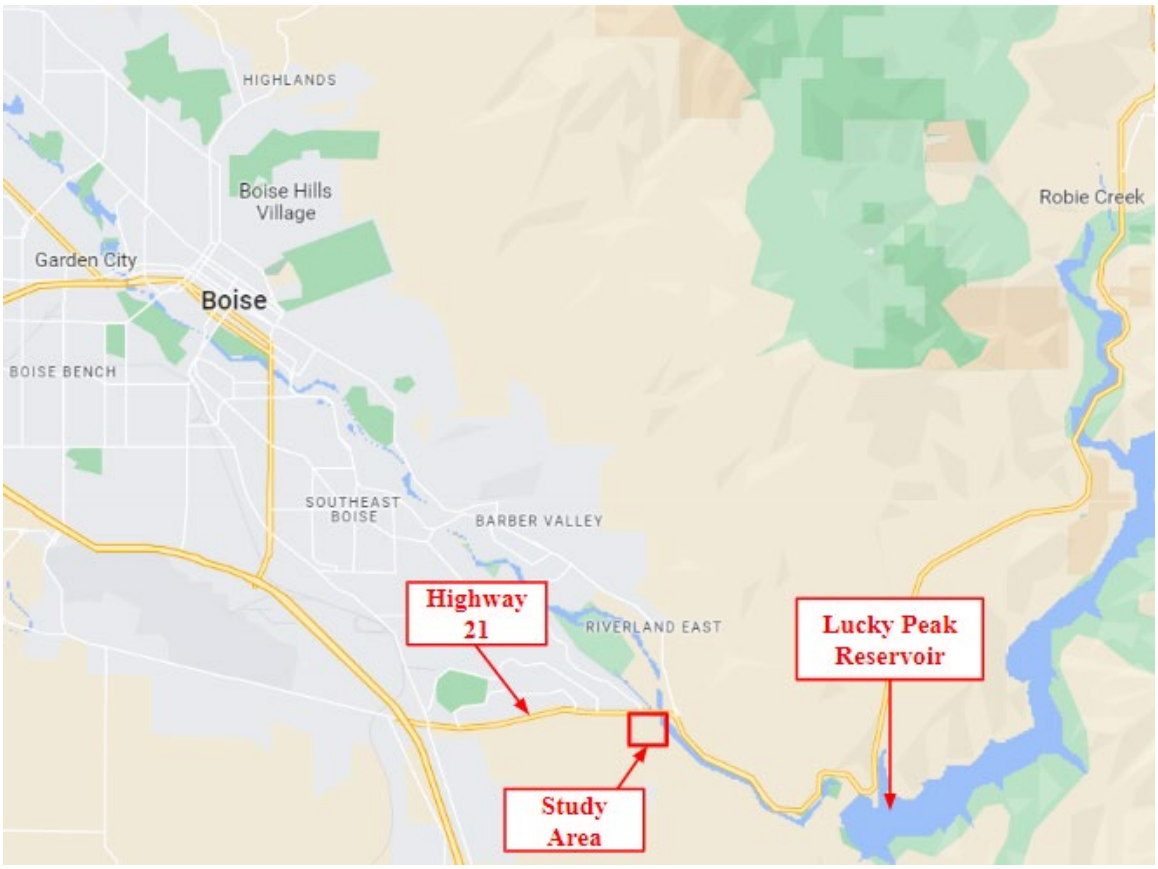

Figure 3.2: Approximate Location of Study Site (Google Maps 2023)

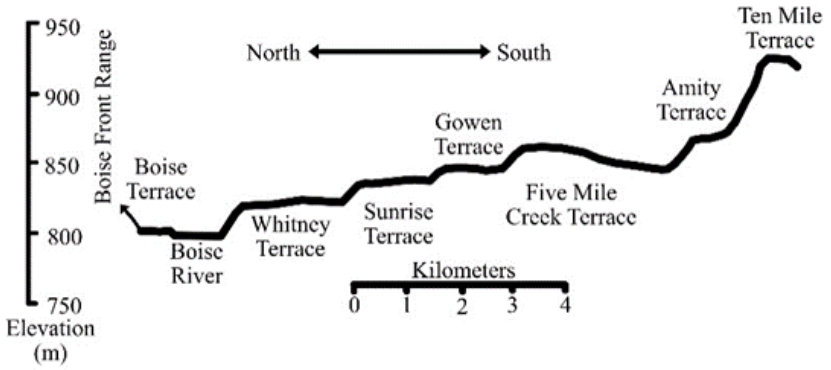

Figure 3.3: Terraces South of Boise River (Hudyma et al. 2022)

The columnar basalt cliff face at the study site, shown in Figure 3.4, consists of both vertical and horizontal discontinuities. UAV photogrammetry from previous investigations at Whiney Terrace revealed the cliff face is vertical and is between five and seven meters in height. The figure shows biological weathering at the site shown by the lichen and small vegetation on the rock face. The most prominent weathering at the site is most likely physical weathering. This is due to the freeze-thaw cycles that occur during late fall through early spring in Boise.

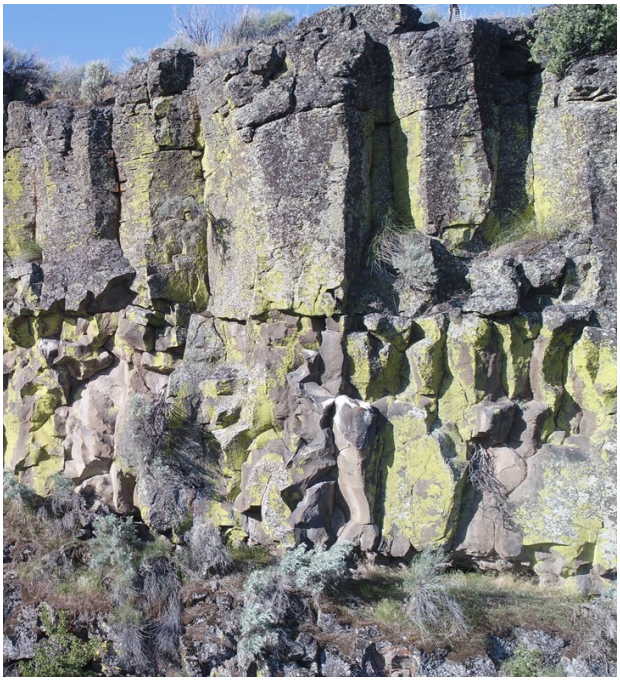

Figure 3.4: Columnar Jointed Basalt Cliff Face at Study Area

This study area in Whitney Terrace was selected because of the large number of boulders that had detached from the cliff face that had come to rest within the site boundaries. The study area, outlined in magenta in Figure 3.5, is approximately 3474 square meters (0.35 ha or 0.86 acres). It is oriented with the long axis from northwest to southeast. The long axis is approximately 23 meters in length and the short axis is approximately 14 meters in length. The columnar basalt cliff face is located approximately 40 meters upslope from the study area. Between the cliff face and the upper boundary of the study area, there are a series of chutes and talus deposits. Talus deposits are zones where boulders have detached from the cliff face and accumulated. Between the talus deposits are chutes, which are characterized by the lack of talus deposits (or poorly formed talus deposits) and the presence of vegetation. The USDA

Web Soil Survey (https://websoilsurvey.nrcs.usda.gov/app/) shows around a 3.5 ft depth to bedrock for the study area. The Canyon Point subdivision is located approximately 12 meters from the end of the study area. The study area outline and site characteristics can be found in Figure 3.5 and Figure 3.6.

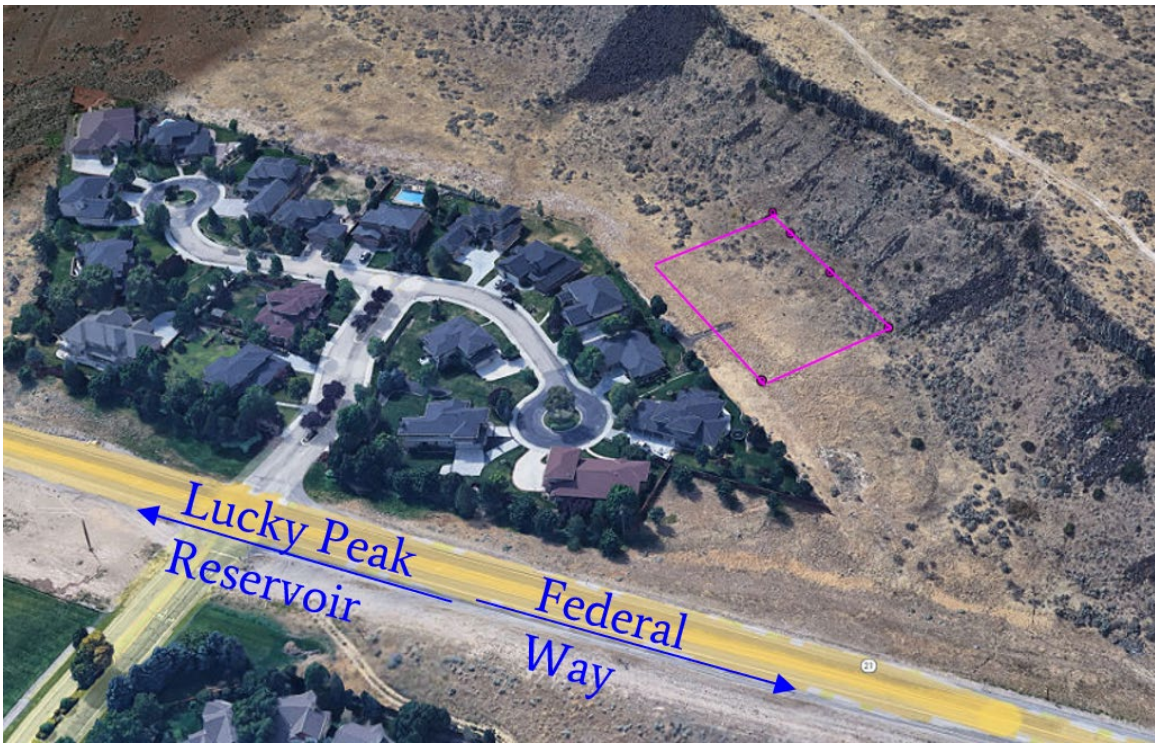

Figure 3.5: Study Area Outline Near Canyon Point Subdivision on Whitney Terrace (Google Earth 2023)

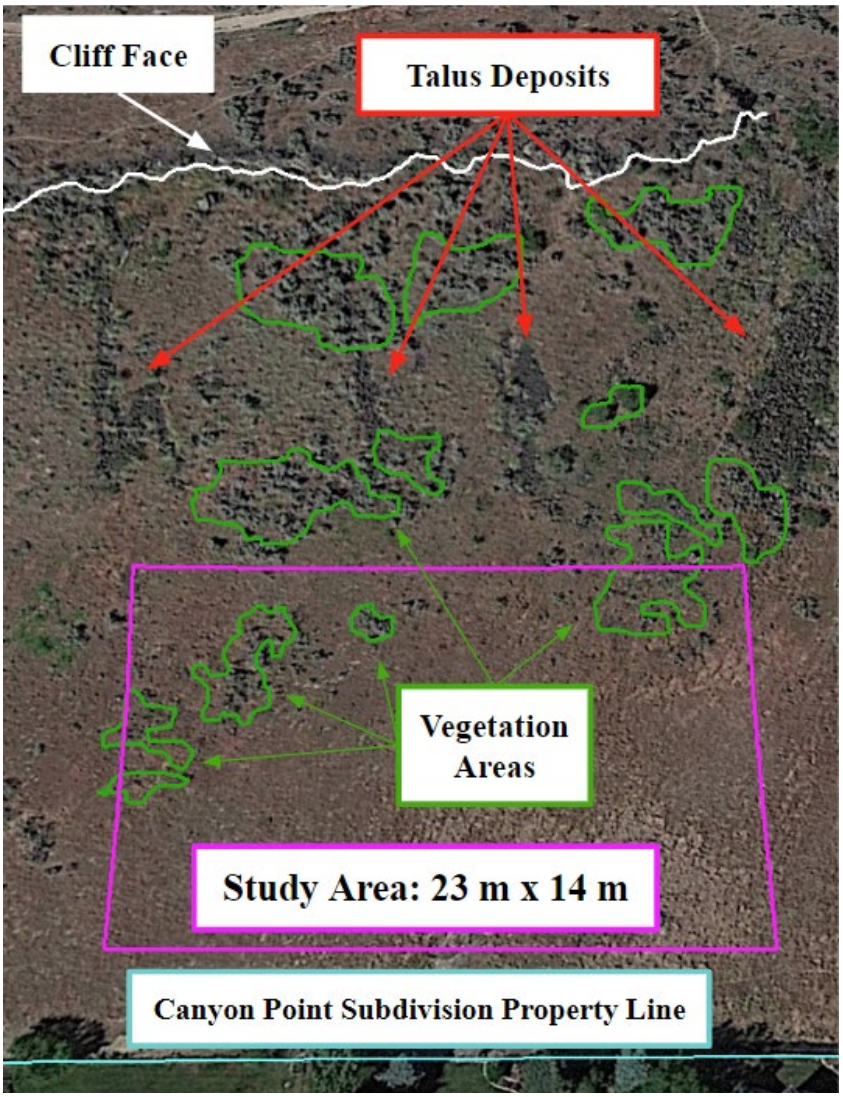

Figure 3.6: Study Area Characteristics (Google Earth 2023)

3.2 LiDAR Data

One of the research questions is "Can publicly available LiDAR data be used for rockfall modeling?". LiDAR point clouds were downloaded from the Idaho LiDAR Consortium ("Boise River 2015" 2016). The airborne LiDAR was collected in 2015 for the Boise River site consisting of 143.8 square kilometers (35,539 acres) along the Boise River and in the Boise foothills. These data were collected with a Leica ALS80 LiDAR

sensor and the target quality of these data were greater than or equal to 8 points per square meter.

The raw LiDAR data are a point cloud that includes points representing ground, vegetation, buildings, and other above-ground objects. To have an accurate slope for the rockfall simulation, the non-ground LiDAR points were removed. These data were imported as a LAS file into CloudCompare, an open-source point cloud editing software, and were filtered to a bare-earth digital elevation model (DEM). In the bare-earth DEM, vegetation was digitally stripped away to reveal the ground surface. The bare-earth DEM was imported into Surfer (by Golden Software) where the data were plotted as a contour map. Within Surfer, cross-section elevations and distances were extracted. An example of a cross-section extracted from the DEM is shown in Figure 3.7.

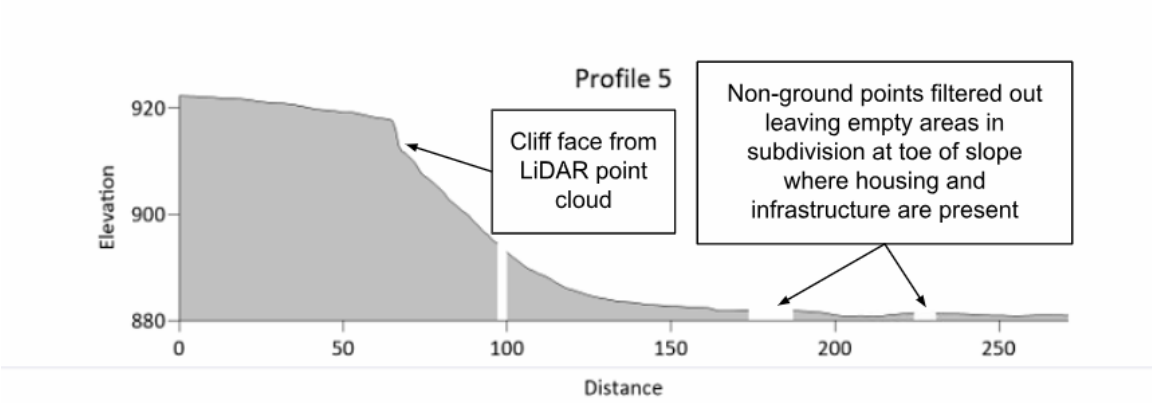

Figure 3.7: Example Slope from Bare Earth DEM

The slopes extracted from the DEM have missing data. The bare earth DEM has missing LiDAR points from the houses in the subdivision and vegetation on areas of the

slope. These points were manually entered to create a continuous slope. Previous studies at Whitney Terrace revealed the cliff face to be 5-7 meters in height and vertical. The LiDAR data show a steeply dipping but not vertical cliff face. The LiDAR points were adjusted to create a vertical cliff face.

When assessing the LiDAR data, it was noted that the boulders at the site and study area were not detected. This is likely due to the target point density being insufficient. This means that the boulder locations beneath the cliff face had to be geolocated using surveying techniques because they could not be determined from the LiDAR data.

At this site, publicly available LiDAR can be partially used to create a rockfall model. While the slope geometry is relatively reliable, there are specific aspects that need to be augmented. This includes manually adjusting the slope so that the cliff face is vertical, which is consistent with field observations, and adding data points where the bare earth model had blank areas. Additionally, the LiDAR data were not able to detect the boulders that had been detached from the cliff face. Boulder locations are an important part of a calibrated rockfall model.

3.3 Boulder Geolocations and Volumes

Seventy-five boulders were geolocated within the study area boundaries using a real-time kinematic (RTK) survey system. The locations of the boulders are shown in Figure 3.8. The study site is outlined in magenta and the cliff face is outlined in white. The majority of the boulders are located in the upper-central portion of the area boundary with groupings of boulders in the lower right-hand side, upper right-hand side, and along

the upper left-hand side of the boundaries. The majority of the boulders at the site were small, most likely less than 50 kg in mass, and embedded in the sagebrush vegetation. The survey locations of the boulders and corners of the study area boundary can be found in Appendix A. Seven boulders are highlighted in Figure 3.8. These boulders had a range of sizes and were not embedded in sagebrush vegetation. These boulders are the calibration boulders. Photogrammetry was conducted on the calibration boulders to determine their volumes.

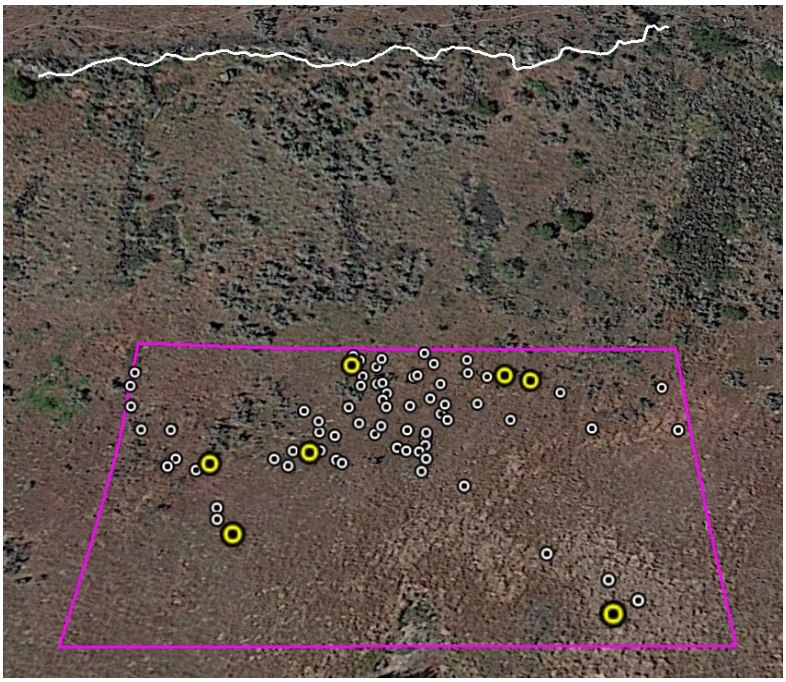

Figure 3.8: Study Area with All Geolocated Boulders

Photogrammetry, which is the science of making accurate measurements of physical objects based on images, was used to determine the volume of the boulders. PhotoModeler Premium, by PhotoModeler Technologies, was the software chosen to create models of the seven boulders and extract volume measurements. To conduct the photogrammetry the native grasses surrounding the boulder were removed to reveal the

bare sides of the boulders. Coded targets were placed around the boulders to create a scale. For each boulder, up to one hundred visible light digital images were taken of the boulder and coded targets, as shown in Figure 3.9. In Photomodeler, the centers of the coded targets are automatically recognized and by inputting the distance between target centers, a scaled surface model was created.

a. Visible Light Image b. Photogrammetry Surface Model

Figure 3.9: Visible Light Image and Surface Model of a Boulder at the Study Site

Figure 3.9 shows both the digital image (left side) and the surface model (right side). Figure 3.9a and Figure 3.9b are indistinguishable from each other. However, the surface model can be manipulated in point cloud viewing software, and measurements, linear, area, and volume, can be made. Table 3.1 contains the location and volume of the seven calibration boulders.

Table 3.1: Geolocation, Volume, and Mass Results.

Calibration Boulder	Calibration Boulder Slope	Distance from Cliff (m)	Volume (m^3)	Mass (kg)
1	M	85.22	0.529	1534.1
20	L	47.69	0.04	116
5	K	46.81	0.045	130.5
HH	H	45.66	0.077	223.3
P	G	58.79	0.034	98.6
A	E	73.70	0.13	377
D	D	62.99	0.161	466.9

The density of basalt ranges between 2.0 g/cm^3 (Kuhn et al. 2010) and 2.9 g/cm^3 (Bolger et al. 1999) based on the amount of vesicular porosity within the basalt. This study used a density of 2.9 g/cm^3. The mass was calculated using the density and volume based on photogrammetry results.

3.4 Calibration Boulder Slopes

Each of the calibration boulders was located on an associated slope. Each of the slopes was taken as a straight line approximately perpendicular to the cliff face. The slope name associated with each calibration boulder is shown in Table 3.1. Figure 3.10

shows the locations of the calibration boulders with respect to the cliff face and study area boundaries.

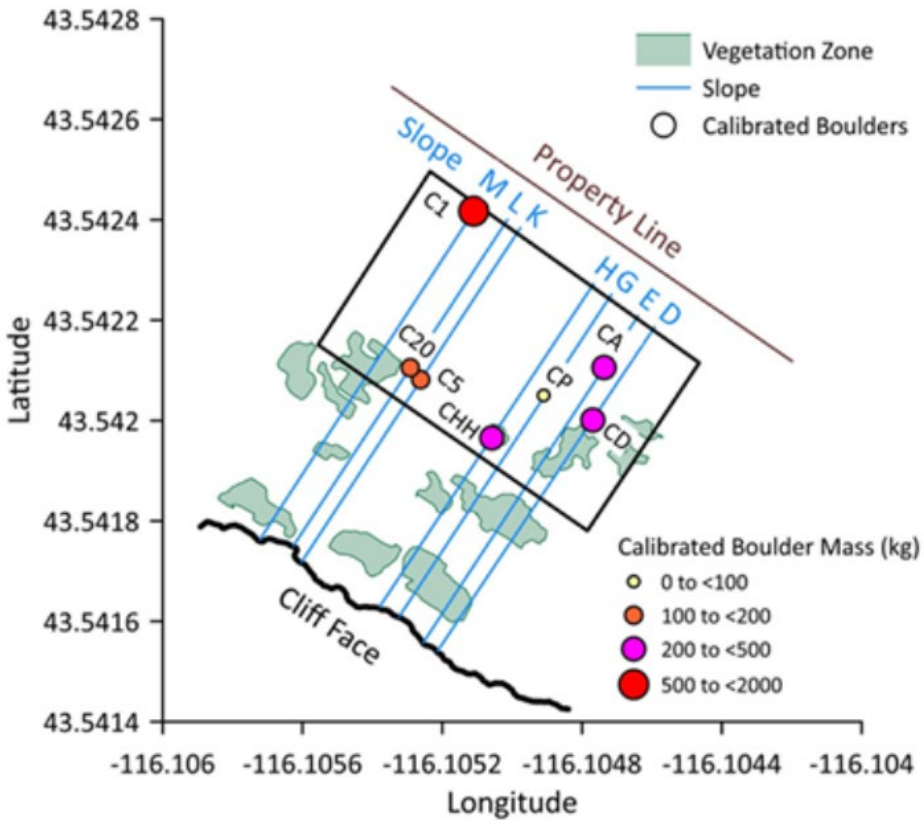

Figure 3.10: Location of Calibration Boulders in Study Area

The calibration boulders are spread throughout the study area boundaries and are located at different distances from the cliff face. The plot symbols are scaled to the calibration boulder mass.

3.5 Chapter Summary

The study area was located on Whitney Terrace in southeast Boise, Idaho. The study site has prominent columnar jointed basalt cliffs, and the site has experienced

previous rockfall events as shown by the talus deposits and a large number of runout boulders. The study area is 322 square meters (twenty-three by fourteen meters) and is located at the base of the slope and vertical cliff face and next to a property line of the Canyon Point subdivision. Within the study area, seventy-five boulders were geolocated. The volumes of seven of the boulders, termed calibration boulders, were determined through photogrammetry. The locations of calibration boulders spanned across the study area. The calibration boulder masses ranged from approximately 100 to 1500 kg.

For this research, publicly available LiDAR data can partially be used for rockfall modeling. The data had a resolution of greater than 8 points per square meter. This resolution was sufficient to obtain slope geometries; however, this resolution was insufficient to capture the location of boulders within the study area. Additionally, the airborne LiDAR data did not adequately capture the vertical cliff face at the study location. To address these deficiencies, the geometry of the cliff face had to be adjusted and boulders had to be geolocated within the study area.

CHAPTER FOUR: ROCKFALL MODEL CALIBRATION

To produce a predictive rockfall runout map for the study area, a rockfall model must be calibrated. This chapter presents the procedures followed to develop a calibrated rockfall model. Seven calibration boulders and their runout slopes were used for the calibration of the rockfall model. Using the boulder volumes and mass, as well as their slope geometries, an informed sensitivity analysis was performed to determine the slope parameters for the rockfall model. With the 2D analysis, each calibration boulder was assumed to have fallen straight down from the cliff face; therefore, each rock has a unique slope profile and calibration parameters. Each rockfall model was considered calibrated for its respective boulder once the results of the calibration resulted in the mean runout distance within one-half of the standard deviation, σ, of the true geolocated distance. This chapter answers the research questions "Is the Lumped Mass or Rigid Body analysis method more appropriate for the columnar jointed basalt at the study site?" and "How is a rockfall model considered calibrated?"

4.1 Rockfall Simulation Software and Calibration Procedure

RocFall2 by Rocscience was used to produce the calibrated rockfall model. This is a two-dimensional analysis software which means that rocks are modeled as moving down a linear path and the rock is not allowed to deviate from the path. Users input a slope geometry, define slope materials, add forest damping (if required), and add rockfall barriers (if required). This software has two different analysis methods, Lumped Mass and Rigid Body, and the two analysis methods use different calculations and inputs. The software can output rock endpoint locations, rock parameters (energy, velocity, and

bounce height), and histograms of endpoint locations and rock parameters (RocFall2 User Guide 2023).

The calibration procedure used can be described as an informed calibration. Data collected from the study site were used to determine the slope properties. The data collected from the site consisted of seven calibration boulders (known volumes, mass, and location from the cliff face), the slope geometries associated with each of the calibration boulders, and the general geology of the site were inputs to the calibration procedure. The geology of the site, including materials and stratigraphy, provided a starting point for estimating the slope properties. Slope properties were systematically varied for each of the calibration boulders' slopes so the mean runout distance from the simulation matched the measured runout distance of the calibration boulder. Slopes were considered calibrated when the difference between the simulated mean runout distance and the known location is within one-half the standard deviation of the runout distances. The calibration procedure resulted in seven sets of slope parameters.

4.2 Calibration of Slope Properties for Matching Calibration Boulder Runouts

As previously described, there are two methods in RocFall2 for two-dimensional rockfall simulation. The Lump Mass method is a well-researched and well-established method that has simpler slope parameters than the Rigid Body method. There are parameters that are common to both methods. These parameters are described below.

4.2.1 Common Input Parameters

There are general input parameters that are required for either Lump Mass or Rigid Body methods. These parameters are the coefficient of restitution and seeder properties. The coefficient of restitution is defined as the retarding capacity of the slope surface and is one of the most influential parameters in rockfall behavior (Peng 2000). This coefficient is split into two parameters, normal restitution and tangential restitution, R_t and R_n, respectively. These coefficients are used to represent the effect of surface conditions on the rockfall model. Both coefficients are based on the change of velocities during a rockfall. Table 4.1 presents values of normal and tangential restitution for different slope materials that are applicable to the thin soil veneer study site.

Table 4.1: Example Restitution Coefficients

Description	**Normal Restitution**	**Tangential Restitution**	**Source**
Bedrock or boulders with little soil vegetation	0.330 - 0.370	0.83 - 0.87	Pfeiffer and Bowen 1989
Rock Slope	0.487	0.910	Chau et al. 1998
Bedrock	0.5	0.95	Giani 1992
Clean Hard Bedrock	0.53 (STDV=0.04)	0.99 (STDV=0.04)	RocFall2 User Manual
Top-soil with vegetation	0.3 (STDV=0.06)	0.8 (STDV=0.06)	RocFal12 User Manual

STDV is the standard deviation.

The tangential restitution has higher values and has less range of values than the normal restitution coefficients. Based on the data in Table 4.1, vegetation reduces the values of normal and tangential restitution. The values in Table 4.1 were used as a starting point for the calibration.

Seeders are either points or lines on the slope where rocks will originate and move downslope. Seeders were added to the rockfall simulation after the cliff face was edited to a vertical face. A line seeder was placed along the cliff face that provided multiple areas of detachment of boulders as shown in Figure 4.1. The two different colors in Figure 4.1 represent the two different materials; gray represents the basalt bedrock and brown represents the thin veneer of soil over rock. Since the detachment areas of these boulders are unknown, a line seeder is the most appropriate option to provide a wider range of results. The seeder properties also include a mass and density for both Lumped Mass and Rigid Body methods and a shape for the Rigid Body method.

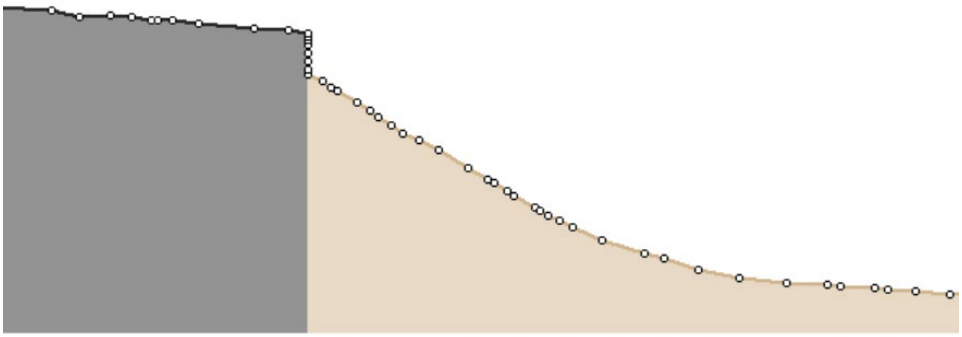

Figure 4.1: Line Seeder Along Cliff Face

4.2.2 Lumped Mass Method

To perform the Lumped Mass calibration, the slope geometries for each calibration boulder were uploaded into RocFall2. A calibration for each of the calibration boulders was performed. This was performed by altering the normal and tangential restitution coefficients until the runout distance matched the location of the calibration boulder. The friction angle was calculated by RocFall2 based on the tangential restitution coefficient. The mass and density of each calibration boulder were used in the seeder properties. The initial conditions which include horizontal velocity (m/s), vertical velocity (m/s), and rotational velocity (degree/sec) were set to zero. Ten thousand rocks were simulated, and the distribution of the runout distances was plotted. An example of a distribution for the Lumped Mass method (Slope M calibration boulder C1) is shown in Figure 4.2.

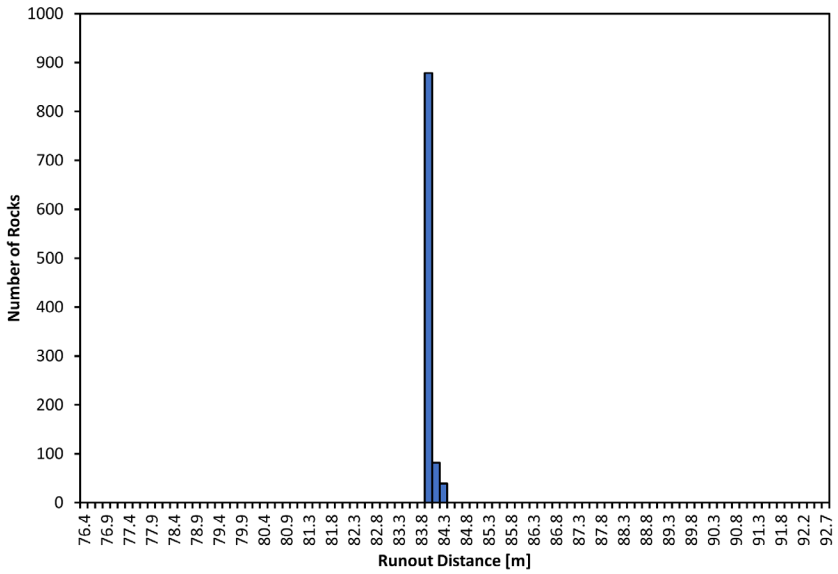

Figure 4.2: Distribution of Runout Distances for Lumped Mass Method Slope M Calibration Boulder C1

The mean calculated runout distance (83.6 meters) almost matches the geolocated runout distances (85.2 meters) using a normal restitution of 0.45 and a tangential restitution of 0.89. The results for all calibration boulders were similar in that there was little if any variation of predicted runout distances. During field reconnaissance, there was a distribution of actual runout distances for observed boulders of similar size in the study area, as noted in Figure 3.7. Consequently, the results of the Lumped Mass model were considered not realistic, and it was determined the Rigid Body method resulted in more accurate runout distances.

4.2.3 Rigid Body Method without Vegetation

The Lumped Mass method assumes the rocks to be spherical particles. This assumption is not appropriate for columnar jointed basalt boulders which are formed by two orthogonal sets of joints, creating a rectangular boulder shape. To improve on the results from the Lumped Mass method, the Rigid Body method was performed. In the Rigid Body method, the seeder properties have three inputs: density, mass, and shape. The boulders in the study area have variable shapes; however, they are best described as blocky with few rounded edges. RocFall2 has a variety of shapes the user can choose and the “Super Ellipse^4 (2:3)” shape most closely matched the geolocated boulders. This shape has a generally rectangular shape with rounded corners as shown in Figure 4.3.

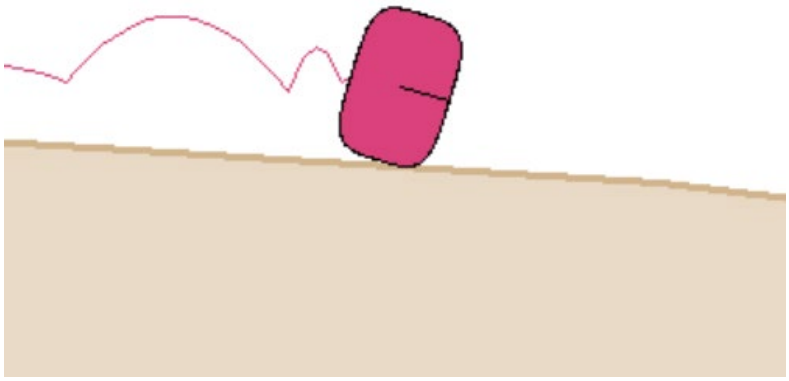

Figure 4.3: Rock Shape (Super ellipse ^4 2:3) in RocFall2

In addition to the restitution values, the Rigid Body method requires coefficients for dynamic and rolling friction. The initial values chosen were 0.56 for dynamic friction (Chau et al. 1998) and 0.6 for rolling friction (Azzoni and de Freitas 1995). These were the recommended values based on the RocFall2 User Guide and they were not part of the calibration process.

For Rigid Body analysis, the input properties for the seeder include the number of rocks, horizontal velocity, vertical velocity, rotational velocity, initial rotation, and rock type. Ten thousand rocks were used for calibration runs. All velocity and rotation parameters were set to zero. This is because we believe there is no initial rotation or velocity before the rockfall occurs. Initial velocity would usually occur during a seismic event or explosion. Likely, the rockfall happening on site is caused by weathering, mostly due to the freeze-thaw cycle, with no associated initial velocities or rotations.

The single boulder calibrations involved systematically changing the coefficients of restitution and friction coefficients until the mean runout distances for each calibration

boulder converged to the observed runout distance from the cliff. Ten thousand rocks were simulated, and the distribution of the runout distances were plotted. An example of a distribution for the Rigid Body method (Slope M Calibration Boulder 1) is shown in Figure 4.4. For this calibration, the normal restitution is 0.5, the tangential restitution is 0.95, the dynamic friction is 0.56, and the rolling friction is 0.6. The histograms for all calibration boulders and associated slopes can be found in Appendix B.

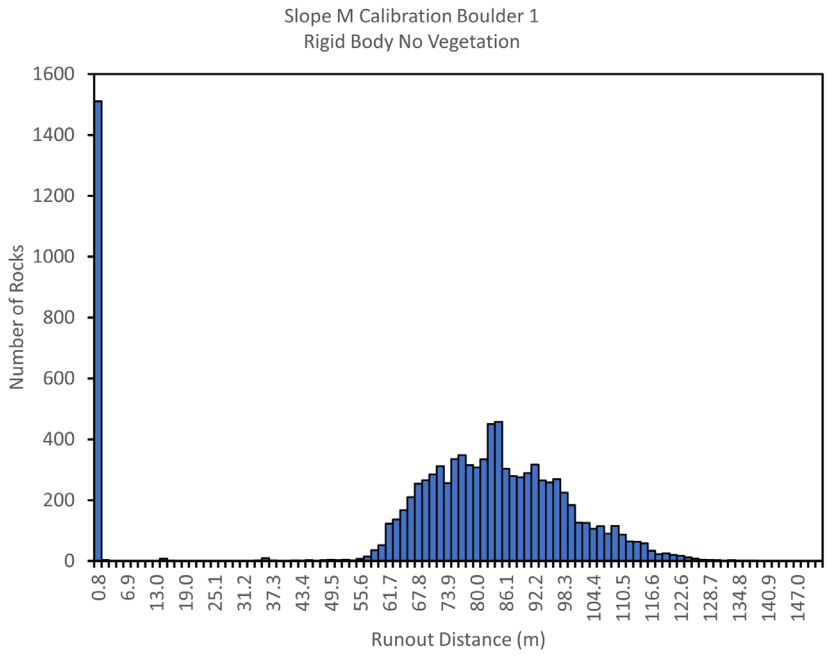

Figure 4.4: Rigid Body Method Runout Distribution Distances for Slope M Calibration Boulder C1

The distribution of the runout distances for 10,000 rocks shows a number of rocks that did not move downslope, represented by the initial spike in the histogram. Some rocks moved further downslope, as shown by the small number of rocks between the initial spike and well-formed distribution at runout distances between approximately 48

meters and 138 meters. The mean runout distance of the distribution was 82.8 meters and the actual runout of the calibration boulder was 85.2 meters.

Is it unrealistic to assume the mean of the simulated runout distribution will be exactly the same value as the measured runout of the geolocated calibration boulder. For this research, a model is considered calibrated when the measured runout distance of the calibrated boulder falls within one-half of the standard deviation of the mean of the simulated runout distribution from the rockfall model. For this calibration, the one-half standard deviation is 5.9 meters, so the geo-located calibration boulder falls within the one-half standard deviation. This slope is considered calibrated.

After the runout distances for several calibration boulders were matched with the mean runout distance for the simulation, it was decided to hold the friction coefficients the same for all calibration runs since it had little effect on the results. The friction coefficients were 0.56 for dynamic friction and 0.6 for rolling friction. Table 4.2 shows the results of all calibration boulder simulations.

Table 4.2: Rigid Body Restitution Values without Vegetation Calibration Results

Calibrated Boulder	Restitution		Runout (m)		
	Normal	Tangential	Measured	Mean Simulated	One-Half Standard Deviation
1	0.50	0.95	85.22	82.82	5.89
20	0.45	0.72	47.69	49.13	1.93
5	0.4	0.74	46.81	48.13	2.07
HH	0.45	0.70	45.66	46.51	1.99
P	0.50	0.80	58.79	57.46	2.78
A	0.50	0.93	73.70	72.26	5.16
D	0.45	0.83	62.99	61.49	2.48

The normal restitution values ranged from 0.4 to 0.5. The tangential restitution varied between 0.7 and 0.95. All of the calibrated boulder locations were within one-half of a standard deviation from the mean simulated rock location.

Once the Rigid Body method calibrations were completed, rocks with different masses were simulated to determine their runout distances. Slope M was used as a test case and one thousand simulations of 50 kg rocks and one thousand simulations of 10,000 kg rocks were performed. The results are shown in Figure 4.5.

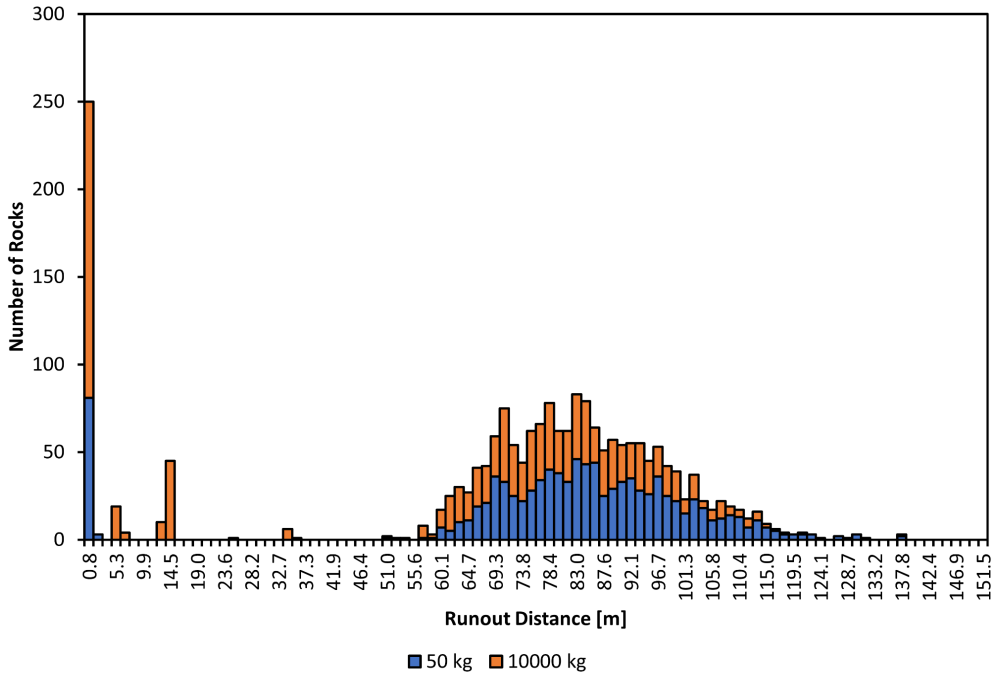

Figure 4.5: Rigid Body Method for Slope M Showing Runout Distances of 50 kg and 10000 kg Rocks

Surprisingly, the well-formed runout distance distribution for the 50 kg and 10000 kg rocks was approximately the same. Intuitively, smaller rocks should travel shorter distances than larger rocks. This was observed at the study area during site reconnaissance. The site was revisited, and historic Google Earth imagery was used to observe that it is likely vegetation was affecting the runout distance of these rocks. Thus, it was decided to use forest-damping slope properties to model vegetation for the calibration models.

4.2.4 Rigid Body Method with Vegetation

The Rigid Body method provided reasonable results in that there was a spread of runout distances associated with each mass of simulated rock. However, it was noted that rocks having less mass had similar runouts as rocks with larger masses. This did not

reflect the field conditions at the site and is not in agreement with commonly accepted rules of behavior. To address this issue, vegetation was incorporated into the rockfall model.

To account for the effect of vegetation, the location of vegetation within the study areas had to be determined. Using Google Earth Pro, satellite imaging of the site was examined, vegetated areas were identified, and the coordinates of their outlines were recorded. There was a total of thirteen areas with recurring vegetation, as shown in Figure 4.6.

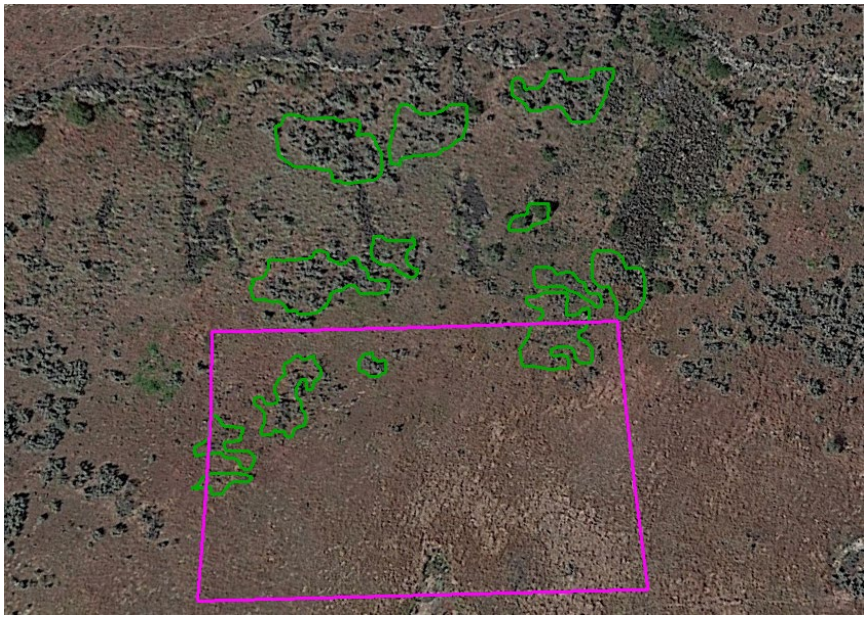

Figure 4.6: Outlines of Vegetated Areas and Study Area

The outline coordinates of the vegetated areas were translated into the location on each slope profile. This was performed using the Google Earth ruler tool. Once all of the locations of vegetation were known, the vegetation was input into the RocFall2 models.

RocFall2 has recommended damping values for vegetation for open, medium, and dense forest vegetation. Since the vegetation on site consisted of sagebrush that is fairly scattered, the open forest density was chosen. This option uses a value of 20 m^2/ha Basal Area for the open forest option. Basal area is defined as the total cross-sectional area of tree trunks and stems per hectare (RocFall2 User Guide 2023). Within the defined area, a drag coefficient is applied throughout the zone of 500 kg/s. The forest density and drag coefficient are RocFall2 recommended values. An example of the added vegetation is shown in Figure 4.7 for Slope M. The vegetation is represented by the green bands.

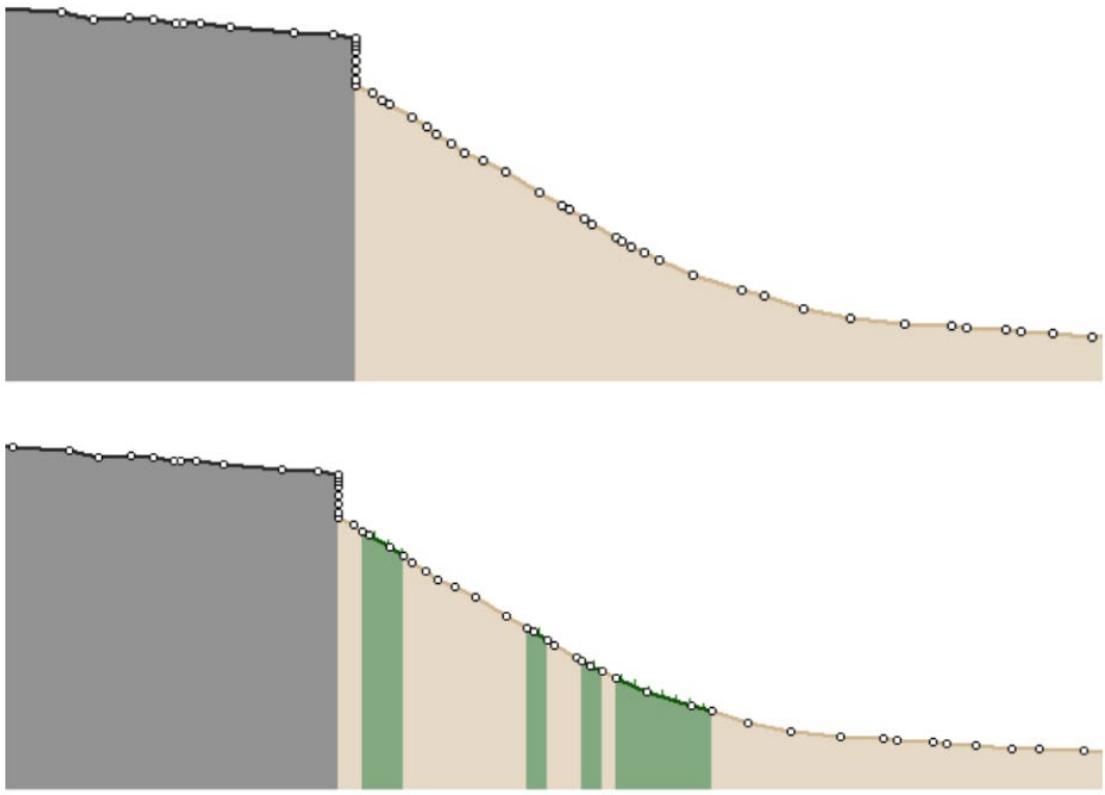

Figure 4.7: Slope M without and with Vegetation

Calibrations were performed for all calibrated boulders and their associated slopes. As with the Rigid Body method without vegetation, the friction coefficients were 0.56 for dynamic friction and 0.6 for rolling friction. The single boulder calibrations with vegetation involved systematically changing the coefficients of restitution and friction coefficients until the runout distances for each calibration boulder converged to the observed runout distance from the cliff. Ten thousand rocks were simulated, and the distribution of the runout distances were plotted. An example of a distribution for the Rigid Body method (Vegetated Slope M calibration boulder C1) is shown in Figure 4.8. For this calibration, the normal restitution is 0.5, the tangential restitution is 0.96, the dynamic friction is 0.56 and the rolling friction is 0.6. The histograms for all calibration boulders and their associated vegetated slopes can be found in Appendix C. Slope K and Slope L did not have vegetation.

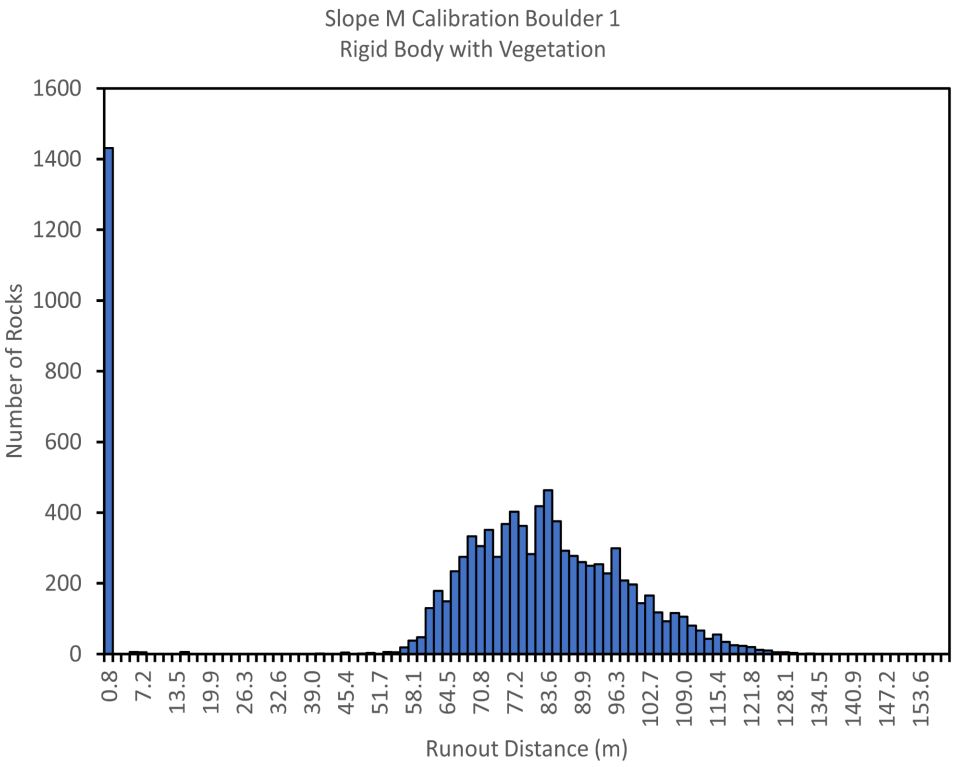

Figure 4.8: Runout Distance Results for Vegetated Slope M

The initial spike shown in Figure 4.8 are rocks that have detached but did not move downslope. After the initial spike, there are rocks that have traveled downslope but do not fall within the large distribution. The large distribution has a minimum runout distance of 53 meters and a maximum runout distance of 144 meters. The average runout distance is 83.5 meters with a standard deviation of 13.1 meters.

Table 4.3 is a comparison of the restitution values for non-vegetated and vegetated calibration slopes for the Rigid Body method. The majority of the results had increased coefficients of restitution values after the calibration. This is due to the vegetation acting as a drag coefficient. Since increases in the coefficient of restitution increase runout distance, it makes sense that the values needed to increase in order to meet the geolocation.

Table 4.3: Comparison of Restitution Values for Non-Vegetated and Vegetated Calibration Slopes (Rigid Body Method)

Calibrated Boulder	Non-Vegetated Slope		Vegetated Slope	
	Normal Restitution	Tangential Restitution	Normal Restitution	Tangential Restitution
1	0.5	0.95	0.5	0.96
20	0.45	0.72	0.45	0.72
5	0.4	0.74	0.4	0.74
HH	0.45	0.7	0.45	0.82
P	0.5	0.8	0.55	0.98
A	0.5	0.93	0.55	0.98
D	0.45	0.83	0.5	0.9

Since the non-vegetated slope Rigid Body method showed rocks of different masses having the same runout distances, it was decided to repeat that analysis to see if the vegetation affected runout distances for different masses of rocks. The same masses, 50 kg and 10000 kg were used. The results are shown in Figure 4.9a for the 50 kg rocks and Figure 4.9b for the 10000 kg rocks.

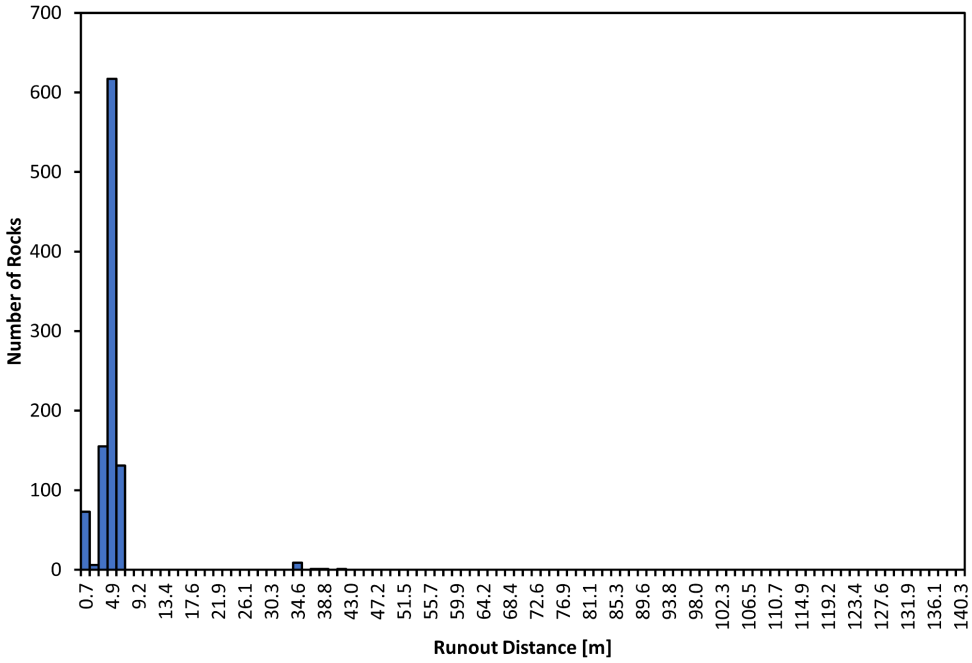

Figure 4.9a: Runout Distance for 50 kg Rock on Vegetated Slope M

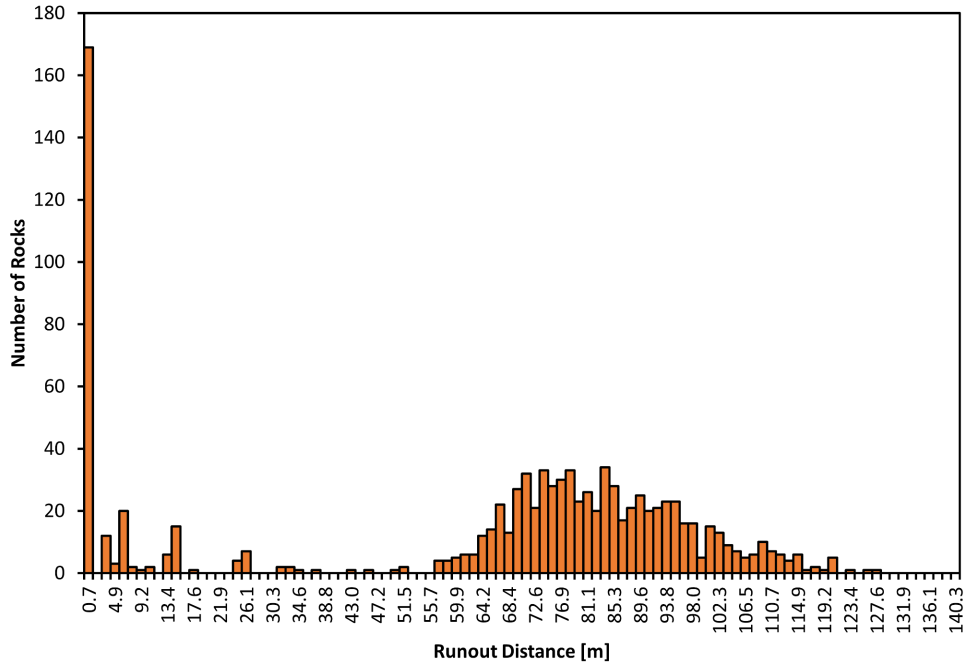

Figure 4.9b: Runout Distance for 10000 kg Rock on Vegetated Slope M

The results show that larger masses travel further downslope than smaller masses for a vegetated slope. The smaller 50 kg rocks have less energy than the larger 10000 kg rocks and the smaller rocks are more influenced by the vegetation.

4.3 Chapter Summary

The calibration process evolved from using the Lumped Mass method to using the Rigid Body method. When the Lumped Mass method was used, there was minimal or no distribution of the runout values along the calibration slopes. This did not match the information gathered during site reconnaissance activities and subsequently, the Rigid Body method was used. When using the Rigid Body method using a Super ellipse ^4 2:3 rock shape, a distribution of runout distances was achieved. The friction coefficients were held constant and restitution coefficients were systematically varied until the calibration boulders fell within one-half of a standard deviation of the furthest grouping of the runout distances, meaning the slope was calibrated. However, further investigations revealed that rocks of different masses had the same runout distances, which was not a logical result. A review of the site reconnaissance data prompted the use of vegetated slopes with the Rigid Body method. Historical areas of vegetation were identified on Google Earth and were incorporated into RocFall2 using vegetation-damping parameters. The slopes were recalibrated, and the results showed larger rocks traveled further than smaller ones which matched reconnaissance of the study area. For the vegetated slope Rigid Body method, the normal restitution values ranged between 0.4 and 0.55 and the tangential restitution values ranged between 0.72 and 0.98.

CHAPTER FIVE: PREDICTIVE ROCKFALL RUNOUT MAPS

In this chapter, the development of the predictive rockfall runout maps is discussed. The rockfall models to create the runout maps were based on the results from the vegetated slope calibrated models. The range of values from the calibrated slope parameters, restitution and friction coefficients, were used to create the runout maps for a range of boulder sizes. This chapter presents the process of creating the runout maps. The research question, "What is the best way to produce a predictive runout map when the potential block size at the site is variable?" is answered in this chapter.

5.1 Parameters for Predictive Rockfall Runout Maps

Predictive rockfall runout maps were developed for different boulder masses to determine if they would settle within the study area boundaries or beyond the study area boundaries. The masses used were 50 kg, 100 kg, 400 kg, 800 kg, and 1500 kg. This range of rock masses represents the estimated masses of boulders seen within the study area boundaries during site reconnaissance activities. Runout maps were developed using the vegetated slope Rigid Body method. This section details the input components used to develop the runout maps.

5.1.1 Slope Profiles

Fifteen slope profiles were extracted from the DEM produced from the publicly available LiDAR data. Of the fifteen slope profiles, seven of the slope profiles were from the calibration boulders. As a result, the slope profiles for the runout maps were not evenly distributed throughout the site study area. Similar to the calibrations, the slope

profiles were adjusted. The cliff face was adjusted to be vertical and gaps within the slopes were filled for all slope profiles.

5.1.2 Slope Properties

The slope properties used for the runout maps were based on the vegetated slope Rigid Body method calibrations. The runout maps were meant to determine runouts for the entire site; therefore, the slope properties for all calibrated slopes were used. From the vegetated Rigid Body calibration process, the coefficients of normal restitution ranged from 0.40 to 0.55 and the coefficients of tangential restitution ranged from 0.72 to 0.98. These restitutions were assumed to be normally distributed and mean values and standard deviations were computed. The friction coefficients were held constant with values of 0.56 for dynamic friction and 0.6 for rolling friction. The vegetated properties were set to open forest damping. Two of the slopes, K and L, were found to not pass through any vegetation. The remaining thirteen slopes all encountered at least one vegetation area. The slope properties used to develop the predictive rockfall runout maps are shown in Table 5.1.

Table 5.1: Slope Properties Used for Predictive Rockfall Runout Maps

Slope Material Parameter	Value	Standard Deviation

Normal Restitution	Mean Value 0.47	0.025
Tangential Restitution	Mean Value 0.85	0.043
Dynamic Friction	Constant Value 0.56	N/A
Rolling Friction	Constant Value 0.60	N/A
Vegetation	Open Forest Damping	N/A

The friction values determined in the calibration process remained constant; therefore, the values were held as their calibrated values of 0.56 (dynamic friction) and 0.6 (rolling friction) for the predictive runout maps. The minimum and maximum values of the restitution coefficients from the calibrations were used for the runout maps. The mean and standard deviations shown in Table 5.1 were used to fit all values between the calculated minimum and maximums from the calibration. By using the chosen mean and standard deviation values, 99.9% of data should fall within three standard deviations of the mean. This was chosen to account for all restitution values from the calibration under a normal distribution.

5.1.3 Rock and Seeder Parameters

The masses of the rocks used to produce the runout maps were 50, 100, 400, 800, and 1500 kilograms. The shape of the rocks was the “Super ellipse ^4 2:3”. The density of the rocks was 2.9 g/cm^3. Five thousand rocks for each mass were simulated for every slope. The seeder was placed along the vertical cliff face using a line seeder with multiple points.

5.2 Developing Predictive Rockfall Runout Maps

To develop the predictive rockfall runout maps, the fifteen slopes covering the study area were used. The slopes were lettered A through O. A rockfall model using the parameters in Table 5.1 was produced for each slope using the five masses of rocks. Five-thousand rocks were simulated for each mass on each slope. Figure 5.1 shows the fifteen slopes within the study area. Also included are the vegetated zones, the calibrated and surveyed boulders, and the property line for the subdivision. The property line is based on the wooden picket fence separating lawns from native grassland.

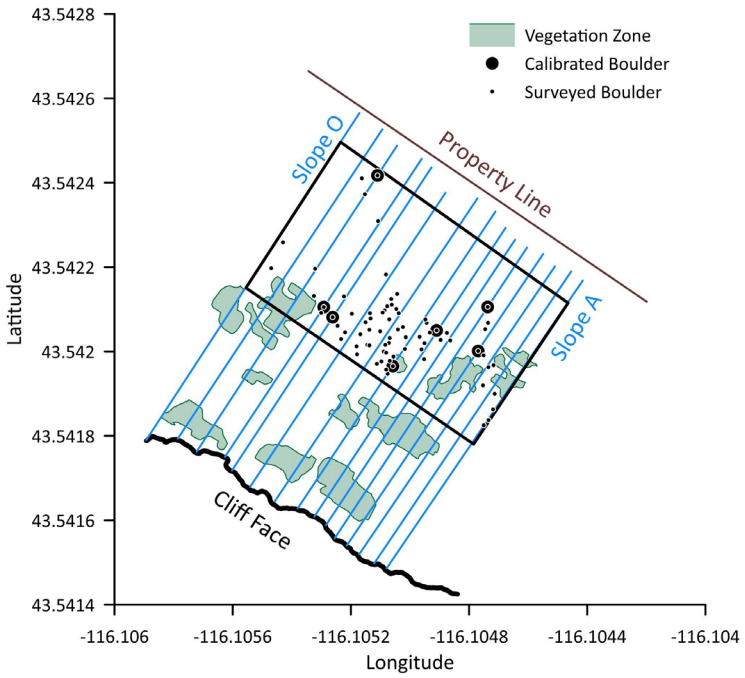

Figure 5.1: Site Map Displaying Cliff Face, Slopes, Study Area, and Property Line

The runout distribution for each of the masses was computed and presented as a histogram. The histogram for Slope H is shown in Figure 5.2. The histograms for all rock masses and vegetative slopes can be found in Appendix D.

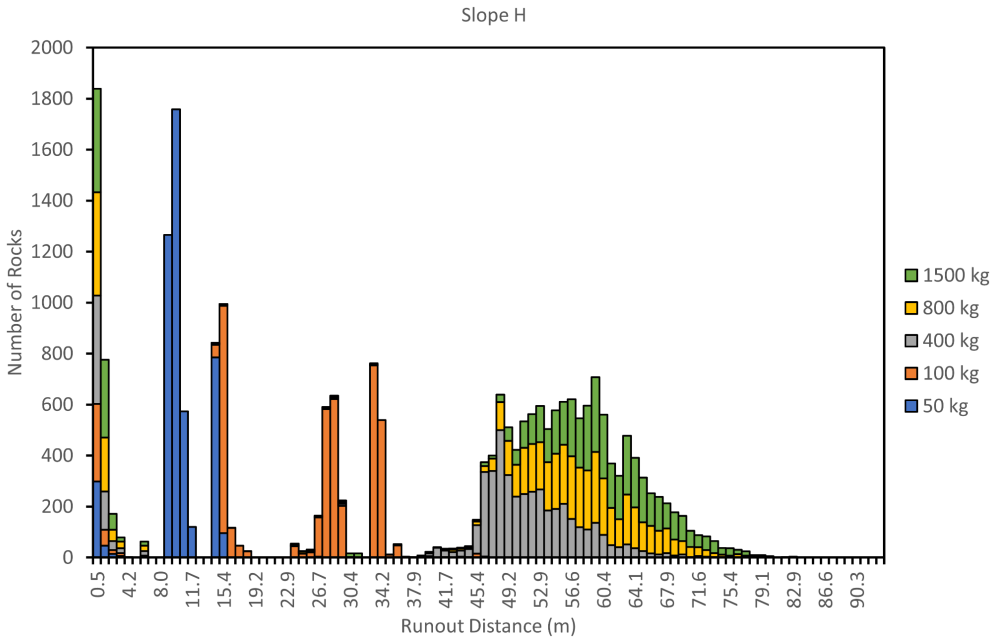

Figure 5.2: Histogram of Rock Runout Distances for Slope H

In Figure 5.2, all rock mass histograms have an initial spike indicating the rocks that did not travel downslope. The majority of the 50 kg rocks traveled approximately ten meters downslope. The 100 kg rocks traveled between 15 and 35 meters downslope. Based on the histogram, the mean runout distance for the furthest traveling groups of 50 kg and 100 kg rocks are 26 and 44 meters, respectively. The 400, 800, and 1500 kg rocks travel the furthest and form a grouping located the furthest distance from the cliff. Within the grouping, the histogram shows the 1500 kg rocks traveled the furthest and the 400 kg traveled the least distance.

To produce the predictive rockfall runout maps, the furthest traveling grouping for each rock mass was identified. The minimum and maximum runout distance runout distances were determined and used to calculate the average runout distance for the groupings. For slope H, the mean runout distances for the 400 kg, 800 kg, and 1500 kg rocks are approximately 52, 58, and 60 meters, respectively. Ultimately, each of the fifteen slopes had minimum, average, and maximum runout distances computed for each of the five rock masses. These values were plotted along their slopes to form the predictive runout maps.

5.3 Runout Map Results

Five runout maps were produced for the study area. Each of the maps corresponds to the mass of the simulated rocks. All runout maps are presented in Appendix E. This section presents comparisons of the 50,100, 800, and 1500 kg maps. The 50 and 100 kg maps were chosen because there are a significant number of small boulders throughout the study area. The 800 kg map was chosen because it is most likely the upper limit of the mass of a boulder that would detach from the cliff face. The 1500 kg map was chosen because it closely matches the largest calibration boulder in the study area. The runout maps are presented in Figure 5.3.

As expected, the runout maps show that larger masses move further downslope than smaller masses. As the rock mass is increased, more rocks land within the study area and, more importantly, beyond the study area. The effect of vegetation and areas of concern are two important aspects that are readily apparent within the runout maps. These aspects are described below.

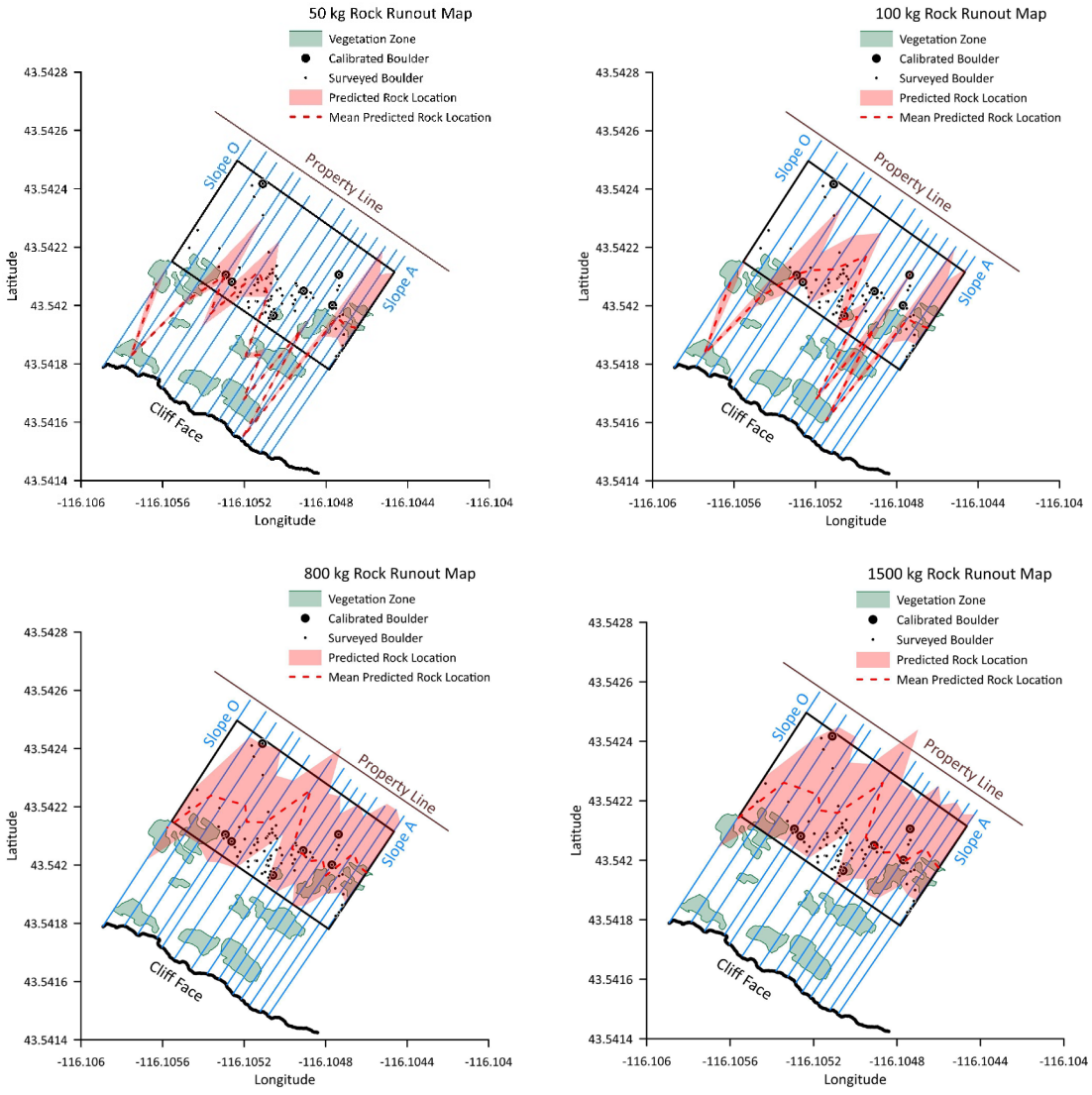

Figure 5.3: 50, 100, 800, and 1500 kg Predictive Rock Runout Maps

5.3.1 Effect of Vegetation

As seen in Figure 5.3, many of the 50 and 100 kg rocks come to rest in vegetated areas just below the cliff face. Slope N and Slope C are of particular interest. For Slope N, which has a large amount of vegetation, the mean runout distances for 50, 800, and 1500 kg rocks were 4.7 meters, 60.2 meters, and 62.1 meters. The difference in runout distances between the larger masses is minuscule compared to the runout distances between the 50 and 800 kg rocks. This indicates that vegetation has a significant effect on rocks with smaller masses compared to larger masses.

While vegetation seems to act as a barrier, it does not act the same across the entire site. For Slope C, the 50 kg rocks runout into the study area and pass through the vegetation in their path. One possible explanation could be slope geometry. Steeper slopes would impart higher energies meaning rocks could pass through the vegetation. Another possibility could be the nature of the rockfall movement. In some cases, the rockfall may bounce over vegetation or bounce fewer times within the vegetated area causing it to encounter less vegetation compared to other simulated rocks. This may explain why some groupings of rocks can travel downslope while the majority are caught in areas of vegetation. At the study site, sagebrush vegetation acts as a natural barrier for the 50 and 100 kg rocks.

5.3.2 Areas of Concern

The most useful aspect of the runout maps is identifying areas of concern or areas where rockfall boulders may negatively impact infrastructure. At this study site, the concern is what mass of rock may come out of the cliff face and runout past the property lines. The runout maps developed for this research display the furthest traveling groups of rocks for each slope. Some of the runout maps show rocks passing the property line

resulting in concern for the safety of the subdivision. In general, the 1500 kg resulted in the furthest traveling rocks which pose the most danger due to the distance and size of the rocks.

Slope I has the greatest runout distances of any slope analyzed. For this slope, both the 800 kg and 1500 kg masses have the possibility of traveling into private property. These large rocks potentially pose a hazard to the subdivision.

One other concern at the study site would be the removal of vegetation. Monnet et al. (2010) showed the risk and hazards associated with rockfall increased after deforestation. At the study site, deforestation is not a concern, but wildfires are a concern. If a wildfire occurred, the sagebrush vegetation could be destroyed, and boulders could move further downslope. Since the vegetation acts as a barrier, slowing the energy of the rocks, and removal of vegetation would lead to rocks with greater energy and runout distance. This would be very influential in the results of the hazard map and would pose an even greater hazard to the subdivision.

5.4 Chapter Summary

Predictive rockfall runout maps were developed for the study site using the vegetated slope parameters and the Rigid Body method. The rockfall models used to develop these maps were based on the calibration parameters, coefficients of restitution and friction, found during the individual boulder calibration process. As expected, rocks with larger masses travel further than rocks with smaller masses. Rocks having masses of 800 kg and 1500 kg almost fill the study area. The runout maps indicate that vegetation impacts the 50 kg and 100 kg rocks. The vegetation either acts as a barrier that stops their

runout or reduces runout distance. The larger rocks used in this research were not impacted by the vegetation. The predictive rockfall runout maps can be used to visualize potential hazards at the site that the furthest traveling groupings of rocks pose to the subdivision below. For this research, the potential hazard is rocks having runout distances that pass the property line. For the study site, Slope I poses the greatest hazard to the subdivision. On Slope I, the 400 kg, 800 kg, and 1500 kg rocks all crossed over the property line.

CHAPTER SIX: SUMMARY AND FUTURE WORK

This chapter focuses on the findings of this research and ideas for future work. The findings include the process of field data collection, analysis of data, rockfall calibration process, and development of predictive rockfall runout maps. The results of the runout maps are also discussed. This chapter concludes by discussing some of the many steps that can be taken to improve or expand the current research. All four of the research questions posed in section 1.2 of this thesis are addressed in this chapter.

6.1 Summary and Findings

The initial step for this thesis was the collection of data. There were three parts to data collection: preliminary work, using publicly available LiDAR data, and field data collection. The preliminary work consisted of identifying a suitable study area. The study area was chosen because rockfall events had taken place and there were a variety of runout boulder sizes to investigate. Using the publicly available LiDAR data, a bare earth DEM was created. Unfortunately, the LiDAR did not have a significant resolution to identify single runout boulders but could be used to extract slope geometries. The field data collected included surveying the boundaries of the study area, geolocating the runout location of numerous boulders in the study area, and using photogrammetry to determine the volume of seven boulders that were used for rockfall model calibrations. Once the calibration boulders were geolocated, slope geometry was extracted for each calibration boulder by taking the profile perpendicular to the boulder and cliff face using the bare earth DEM. The slopes had missing data points because of vegetation and the cliff face

was not vertical. Both of these issues were corrected by manually editing the slopes. The slopes were entered into RocFall2 for calibration.

The calibration process greatly altered the pathway of the originally proposed research. Originally, it was assumed a Lumped Mass method was appropriate for rockfall models. When using this method, the mean runout distance was nearly the same for every rock simulated even though the mass of the rocks varied greatly. The simulation results were different from what was observed at the site. The observations made on the site were that the rocks were not all located in one area, and they were spread throughout the entire slope with large groupings towards the toe of the slope and cliff face. This prompted the use of the Rigid Body method for the rockfall model calibrations. The Rigid Body method required additional parameters for the simulations. These included frictional coefficients and a simulated rock shape. Caviezel et al. (2021) noted the shape of rocks plays an important factor in the results of rockfall runout distance and spread. The columnar jointed basalt has a regular shape which is best described as rectangular with rounded corners, which was used for the calibrations. Five thousand simulated rocks were used to calibrate the slope properties for each calibration boulder. To perform the calibrations, the restitution coefficients were systematically varied until the difference between the mean runout distance of the furthest traveling grouping of simulated rocks and the actual location of the calibrated boulder was within one-half of the standard deviation for the simulated rocks. All slopes were successfully calibrated. However, additional studies showed that simulated rocks of different masses would travel the same distances along the slope, which did not agree with field observations. This prompted the use of vegetation in the Rigid Body method calibrations.

Historical Google Earth imagery was assessed and areas of prominent vegetation at the study site were incorporated into the calibration slopes. The segments of the calibration slopes with vegetation were assigned open forest damping properties. The slopes were recalibrated, and new values of the restitution coefficients were determined. Incorporating the effects of vegetation corrected the issue of different rock masses having the same runout distances. The restitution coefficients were not the same for each calibration slope; rather, there was a range of restitution coefficients.

After the individual slope calibrations using vegetated Rigid Body method were completed, rockfall models for the predictive runout maps were developed. It was noted in the calibration process that the friction parameters were relatively insensitive to the model while the restitution coefficients were very sensitive and greatly impacted the runout distances. The predictive runout models used the range of values for the restitution coefficients from the calibration models. The middle value of all of the restitution coefficients was determined and a normal distribution was applied to cover the range of values for tangential and normal restitution coefficients. These parameters were used for each of the fifteen slopes across the site. To develop the predictive runout maps, five different rock masses (50, 100, 400, 800, and 1500 kg) were used. These masses represent the range of boulder masses identified at the site. Five thousand rocks were simulated for each mass value on every slope. The furthest runout grouping, including the maximum runout distance, for each mass was used to develop the predictive runout maps. The runout maps displayed the minimum, mean, and maximum runout distances for the furthest traveled groupings of rocks downslope. Each individual slope had its minimum,

mean, and maximum runout distance values plotted to create the runout maps for each rock mass.

The predictive rockfall runout maps showed two interesting results. First at the study site, only the 50 kg and 100 kg simulated rocks were affected by the vegetation whereas the heavier rocks were not affected. Second, although the vegetation seems to act as a barrier for the smaller simulated rocks, it does not act the same across the entire site. This may be due to steeper slope geometry or differences in rockfall movement, rolling versus bouncing, down the site.

There was only one location within the study area where large simulated rocks crossed the property line. At this location, Slope I in the study area, only the 800 kg and 1500 kg simulated rocks crossed the property line, with the potential to create a hazard for the subdivision. If vegetation is reduced, perhaps by wildfire, the hazard potential could increase.

6.2 Answers to Research Questions

The answers to the research questions are presented below. The answers include a discussion, where appropriate.

- Can publicly available LiDAR data be used for a calibrated rockfall model and the development of predictive rockfall maps?

Publicly available LiDAR data can be used but because of its limited resolution, the LiDAR data has to be augmented with field data. For this research, the LiDAR data did not have sufficient resolution to identify historic runout boulders so they needed to be geolocated and their volumes assessed. Additionally, the LiDAR data did not accurately

capture the vertical face of the cliff so it had to be manually altered to reflect the actual site conditions. However, the LiDAR data was of sufficient resolution to capture the slope geometry, and higher resolution public LiDAR data may be available in the future.

- Is the Lumped Mass method or Rigid Body analysis method more appropriate for the columnar jointed basalt at the study site?

For this site, which consists of columnar jointed basalt, the Rigid Body method is more appropriate than the Lumped Mass method. This was shown by the distribution of runout distances during the slope calibration using the calibrated boulders. However, vegetation at the site had a significant influence on runout distances. If the site vegetation is of sufficient stiffness, it is important to consider the effects of vegetation on runout distances.

- How is a rockfall model considered calibrated?

For this research, the model was considered calibrated by observing the furthest grouping of traveling rocks downslope. These groupings were analyzed for their mean runout distance and standard deviation. Each rockfall model was considered calibrated when the geolocated boulder fell within one-half of the standard deviation of the mean of the furthest traveling groupings of rocks. However, there may be other methods to calibrate rockfall models.

- What is the best way to produce a predictive runout map when the potential block size at the site is variable?

In order to account for varying block size at the study area, multiple masses were chosen to be simulated for the rockfall runout maps. These masses include 50, 100, 400, 800, and 1500 kg. The 50, 100, and 400 kg rocks were chosen to simulate due boulders observed

on site having similar masses. The 800 kg rock was chosen due to this being on the upper limit of possibly likely block size. The 1500 kg size was chosen due to the calculated mass of Boulder C1 (1534 kg). Using a variety of masses in the simulations helps to account for the varying masses observed on site. This process could also be done with shape by running a variety of shapes out of the RocFall2 library if shapes varied on site.

6.3 Future Work

There are several ways this research could be expanded and improved. One important improvement is associated with the volume measurements of calibration boulders. Photogrammetry was used to determine the volume of the boulders above the ground surface. There could have been portions of the boulders beneath the ground surface which were not included in the volume measurements.

Another improvement could be made with the slope profiles. While the publicly available LiDAR data seemed to be mostly accurate, there were inconsistencies with the cliff face. This is likely due to the type of LiDAR being used since it captures vertical points. The solution to this problem would be to survey each profile, use a terrestrial LiDAR which could capture points both on the ground and vertical cliff points, or use a drone-based LiDAR system. All potential solutions would provide significantly increased resolution.

Another issue faced was determining the slope parameters. There are numerous studies providing ranges of the friction and coefficients of restitution, but they are mostly associated with the Lumped Mass method. While the calibration procedure used in this research was successful, there may be other combinations of normal and tangential

restitution that would also yield calibrated results. Because these properties can vary across the site, adopting physical measurements of these values would provide more accurate rockfall runout maps. The use of "smart" rocks, which measure acceleration and rotational velocity data, could provide valuable information on rockfall behavior on the slope. This could likely help calibrate the slope providing very accurate restitution and friction coefficients. Another advantage to the smart rocks is understanding the bounce height and rockfall movement behavior (freefall, bouncing, sliding, and rolling). Understanding those behaviors could help understand the rock-slope interaction better which could aid in the design of rockfall models. The vegetation parameters used are also values based on limited research. This research utilized the open forest damping option in certain zones of the slope. Comparing results of a bare, segmented, and fully vegetated slope would provide more understanding on the effect of vegetation. This comparison could provide knowledge on the effect of vegetation throughout seasonal change where there may be dense, sparse, or no vegetation present on site. The change in vegetation should account for differing rockfall runout results.

Lastly, the biggest improvement to the research would be to adopt a three-dimensional analysis software, such as RocFall3. This would account for slope variability across the entire site, and not just using discrete two-dimensional profiles across the site. When using a 2D model, numerical simulations have to be manually interpolated when building a hazard map to account for slope and topographic changes (Monnet et al. 2010). Using a 3D model would provide information on the spread of the rockfall across the site which is not something that two-dimensional analysis provides. This information could be vital in hazard prediction and would create a more accurate end product.

REFERENCES

Alade, S. M., and S. S. Abdulazeez. 2014. “Kinematic Assessment of Rock Slope Stability at Obajana and Ewekoro Quarries.” *Earth Sciences*, 3 (2): 34. https://doi.org/10.11648/j.earth.20140302.11.

Andrew, R. D., R. Bartingale, and H. Hume. 2011. *Context Sensitive Rock Slope Design Solutions*. Federal Highway Administration.

Azzoni, A., and M. H. de Freitas. 1995. “Experimentally gained parameters, decisive for rock fall analysis.” *Rock Mechanics and Rock Engineering*, 28 (2): 111–124. https://doi.org/10.1007/bf01020064.

“Boise River 2015.” 2016. *www.idaholidar.org*. Accessed August 16, 2023. https://www.idaholidar.org/data/boise-river-2015/.

Bolger, J., C. S. Montross, and A. Rode. 1999. “Shock waves in basalt rock generated with high-powered lasers in a confined geometry.” *JOURNAL OF APPLIED PHYSICS*, 86 (10): 5461–5466. https://doi.org/10.1063/1.371546.

Caviezel, A., A. Ringenbach, S. E. Demmel, C. E. Dinneen, N. Krebs, Y. Bühler, M. Christen, G. Meyrat, A. Stoffel, E. Hafner, L. A. Eberhard, D. von Rickenbach, K. Simmler, P. Mayer, P. S. Niklaus, T. Birchler, T. Aebi, L. Cavigelli, M. Schaffner, and S. Rickli. 2021. “The relevance of rock shape over mass—implications for rockfall hazard assessments.” *Nature Communications*, 12 (1). https://doi.org/10.1038/s41467-021-25794-y.

Chau, K. T., R. Wong, and C.-S. Lee. 1998. “Rockfall Problems in Hong Kong and Some New Experimental Results for Coefficients of Restitution.” *Journal of rock mechanics and mining sciences and geomechanics*, 35 (4-5): 662–663. https://doi.org/10.1016/s0148-9062(98)00023-0.

Cláudia Pereira, L., M. Sabino Lana, F. Costa Melo, and P. F. T. Lopes. 2013. “Modeling Aspects of Block Toppling in Rock Slopes.” Proceedings of the 23rd International Mining Congress and Exhibition of Turkey, IMCET 2013 CRSP. 2000. Colorado

Rockfall Simulation Program Version 4.0. <https://geodata.geology.utah.gov/pages/download.php?direct=1&noattach=true&ref=2514&ext=pdf&k=>

Frattini, P., A. Valagussa, S. Zenoni, and G. Crosta (2013). Calibration and validation of rockfall models, EGU General Assembly, 7-12 April 2013 in Vienna, Austria. Id EGU2013-11059

Giani, G. P. 1992. "Rock Slope Stability Analysis.", A.A. Balkema, Rotterdam, Netherlands. *Canadian Geotechnical Journal,* 31(2). https://doi.org/10.1139/t94-039

Highland, L. M., and P. Bobrowsky. 2008. *The Landslide Handbook - A Guide to Understanding Landslides*. Reston, Virginia: U.S. Geological Survey.

Holm, K., and M. Jakob. 2009. "Long rockfall runout, Pascua Lama, Chile." *Canadian Geotechnical Journal*, 46 (2): 225–230. https://doi.org/10.1139/t08-116.

Hudyma, N., N. Walker, and B. Chittoori. 2022. "Mapping and Characterization of Rockfall Runout Talus Deposits from Columnar Basalt Cliffs in Boise, ID." Santa Fe, New Mexico, USA: 56th U.S. Rock Mechanics/Geomechanics Symposium.

Krautblatter, M., and J. R. Moore. 2014. "Rock slope instability and erosion: toward improved process understanding." *Earth Surface Processes and Landforms*, 39 (9): 1273–1278. https://doi.org/10.1002/esp.3578.

Kuhn, B., MacLaughlin, M.M., and Hudyma, N., 2010. "Relationships between unit weight, unconfined compressive strength, and deformation modulus of vesicular basalt", Proceedings of the 44th US Rock Mechanics Symposium, June 27-30, 2010, Salt Lake City, UT, USA.

Kumar, K., P. S. Prasad, Sudhir Mathu, and Shivashish Kimothi. 2010. "Rockfall and Subsidence on Mumbai - Pune Expressway." *International Journal of Geoengineering Case Histories*, 2 (1): 24–39. https://doi.org/10.4417/ijgch-02-01-02.

Maley, T. S. 2019. *Exploring Idaho Geology*. Mineral Land Publications.

Masuya, H., K. Amanuma, Y. Nishikawa, and T. Tsuji. 2009. "Basic rockfall simulation with consideration of vegetation and application to protection measure." *Natural*

Hazards and Earth System Sciences, 9 (6): 1835–1843. https://doi.org/10.5194/nhess-9-1835-2009.

Monnet, J. M., N. Clouet, F. Bourrier, and F. Berger. 2010. "Using geomatics and airborne laser scanning for rockfall risk zoning: a case study in the French Alps."

Othberg, K. L., and W. L. Burnham. 1990. *Geologic Map of the Lucky Peak Quadrangle, Ada County, Idaho*. Idaho Geological Survey.

Othberg, K. L., and V. S. Gillerman. 1994. *Field Trip Guide to the Geology of the Boise Valley*. Moscow, Idaho: Idaho Geological Survey.

Parkash, S., and Gupta. 2014. "Geohazards Risk Management in India."

Peng, B. 2000. "Rockfall Trajectory Analysis - Parameter Determination and Application." University of Canterbury.

Pfeiffer, T. J., and T. D. Bowen. 1989. "Computer Simulation of Rockfalls." *Environmental & Engineering Geoscience*, xxvi (1): 135–146. https://doi.org/10.2113/gseegeosci.xxvi.1.135.

Pfeiffer, T.J.; Higgins, J.D.; Andrew, R.D.; Schultz, R.J.; and Beck, R.B., 1995, Colorado Rockfall Simulation Program Version 3.0a User's Manual: Colorado Department of Transportation, Denver, CO, 60 p.

Pfeiffer, T.J.; Higgins, J.D.; Schultz, R.; and Andrew, R.D., 1991, Colorado Rockfall Simulation Program Users Manual for Version 2.1: Colorado Department of Transportation, Denver, CO, 127 p.

Pierson, L. A., C. F. Gullixson, and R. G. Chassie. 2001. *ROCKFALL CATCHMENT AREA DESIGN GUIDE*. Oregon Department of Transportation and Federal Highway Administration.

Ritchie, A. M. 1963. *Evaluation of Rockfall and Its Control* . Washington State Highway Commission .

RocFall2 User Guide. 2023. <https://www.rocscience.com/help/RocFall/overview>.

Stock, G. M., and B. D. Collins. 2014. "Reducing Rockfall Risk in Yosemite National Park." *Eos, Transactions American Geophysical Union*, 95 (29): 261–263. https://doi.org/10.1002/2014eo290002.

United States Department of Agriculture. Natural Resouces Conservation Services. Web Soil Survey. <https://websoilsurvey.nrcs.usda.gov/app/>.

Wyllie, D. C. 2017. *Rock Fall Engineering*. CRC Press.

Zhang, S., M. He, J. Gu, Z. Cui, J. Wang, L. Zhong, Q. Meng, and H. Wang. 2020. "Rock Mass Classification for Columnar Jointed Basalt: A Case Study of Baihetan Hydropower Station." *Geofluids*, (C. Zhu, ed.), 2020: 1–12. https://doi.org/10.1155/2020/6679317.

APPENDIX A

Coordinates of Study Area, All Surveyed Boulders, and Calibration Boulders

Table A1: Survey Pin Locations

Pin Number	Latitude	Longitude
1	43.54179482	-116.1047839
2	43.54186195	-116.1049121
3	43.5419905	-116.1051756
4	43.54248794	-116.1051789
5	43.54216322	-116.1055346

Table A2: Coordinates of All Geolocated Boulders

Rock	Latitude	Longitude	Rock	Latitude	Longitude
A	-116.104737	43.5421057	Mm	-116.105179	43.5419933
B	-116.104736	43.542068	Nn	-116.105181	43.5420125
C	-116.104745	43.5420533	Pp	-116.105144	43.5420156
D	-116.104769	43.5420012	Oo	-116.105137	43.5420147
E	-116.104751	43.5419912	Qq	-116.105101	43.5420478
F	-116.104717	43.5419678	Rr	-116.10507	43.5420763
G	-116.104734	43.5419628	Ss	-116.105038	43.5420909
H	-116.104753	43.54192	Tt	-116.105047	43.5421011
I	-116.104714	43.5418999	Uu	-116.105062	43.5421109
J	-116.104719	43.5418631	Vv	-116.105044	43.5421364
K	-116.104734	43.5418378	Xx	-116.105063	43.5421243
L	-116.10475	43.5418253	Ww	-116.105081	43.5421823
M	-116.104864	43.5420262	Yy	-116.105077	43.5421074
N	-116.104875	43.5420442	Zz	-116.105087	43.5420976
O	-116.104896	43.5420275	Zza	-116.105092	43.5420925
P	-116.10491	43.5420501	Aaa	-116.105134	43.5420785
Q	-116.104933	43.5420451	Bbb	-116.105136	43.5420908
R	-116.104944	43.5420681	Ccc	-116.105151	43.5420693
S	-116.104951	43.5420198	Ddd	-116.105138	43.5420517
T	-116.104968	43.5420348	Eee	-116.105168	43.542041
U	-116.104961	43.5420049	Fff	-116.105108	43.5423093
V	-116.104952	43.5419817	1	-116.10511	43.5424173
W	-116.105017	43.5420063	2	-116.105153	43.5423727
X	-116.105014	43.5420338	1a	-116.105163	43.5424106
Y	-116.105024	43.5420583	Hhh	-116.104948	43.5420761
Z	-116.105041	43.5420523	Fff	-116.10543	43.5422585
Aa	-116.105068	43.5420321	Ggg	-116.10547	43.5421973
Bb	-116.105071	43.5420206	3	-116.105321	43.5421962
Cc	-116.105084	43.5420158	Jjj	-116.105325	43.5421318
Dd	-116.105089	43.5419998	4	-116.105223	43.5421304
Ee	-116.10508	43.5419973	5	-116.105262	43.5420814
Ff	-116.105068	43.5419781	20	-116.105292	43.5421053
Gg	-116.105056	43.5419879	21	-116.105301	43.5420918
Hh	-116.105058	43.5419654	6	-116.105243	43.5420631
Ii	-116.105075	43.5419474	22	-116.105197	43.5420895
Jj	-116.10508	43.5419572	7	-116.105233	43.5420296
Kk	-116.105097	43.5419764	Kkk	-116.10522	43.5420457

Table A3: Coordinates of Calibrated Boulders

Rock	Latitude	Longitude
C1	-116.105	43.54242
C5	-116.105	43.54208
C20	-116.105	43.54211
CHH	-116.105	43.54197
CP	-116.105	43.54205
CD	-116.105	43.542
CA	-116.105	43.54211

APPENDIX B

Rigid Body No Vegetation Rockfall Calibration Histograms

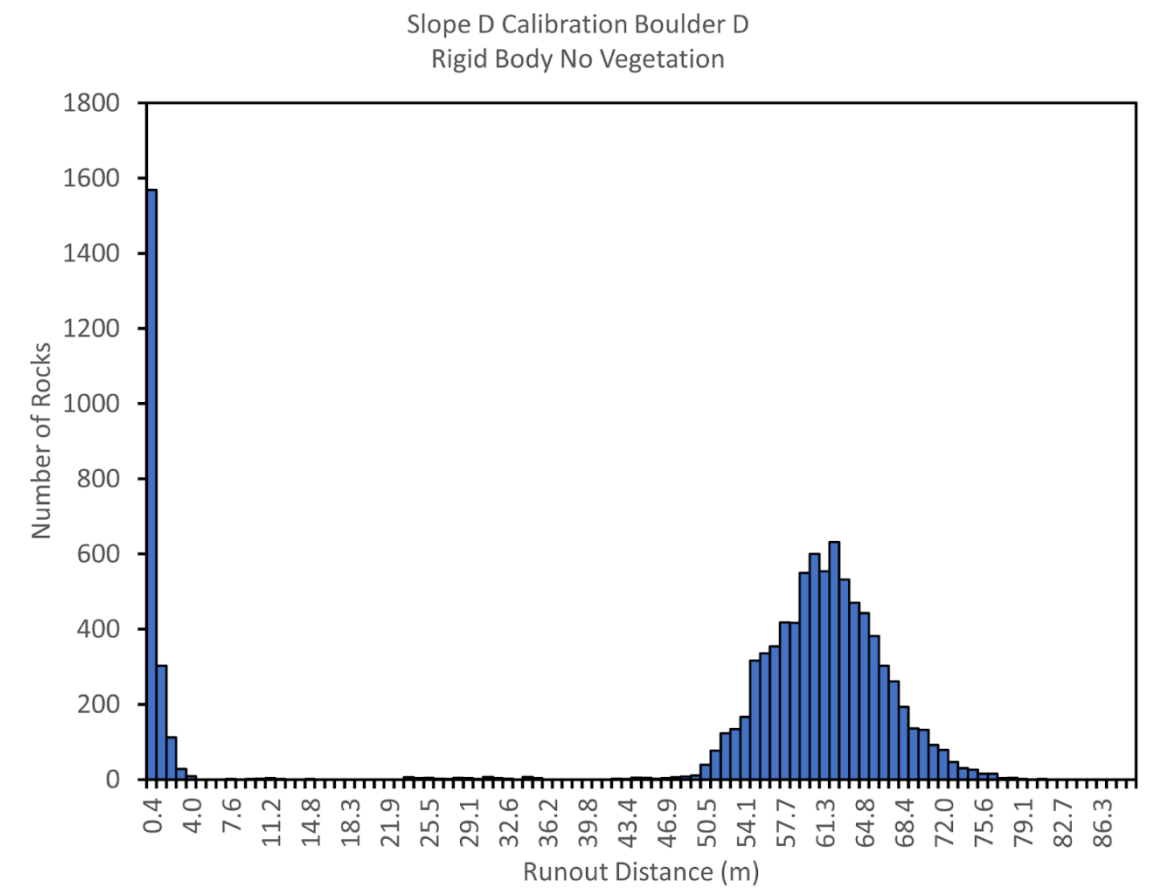
Slope D Calibration Boulder D
Rigid Body No Vegetation
Number of Rocks
1800
1600
1400
1200
1000
800
600
400
200
0
0.4
4.0
7.6
11.2
14.8
18.3
21.9
25.5
29.1
32.6
36.2
39.8
43.4
46.9
50.5
54.1
57.7
61.3
64.8
68.4
72.0
75.6
79.1
82.7
86.3
Runout Distance (m)

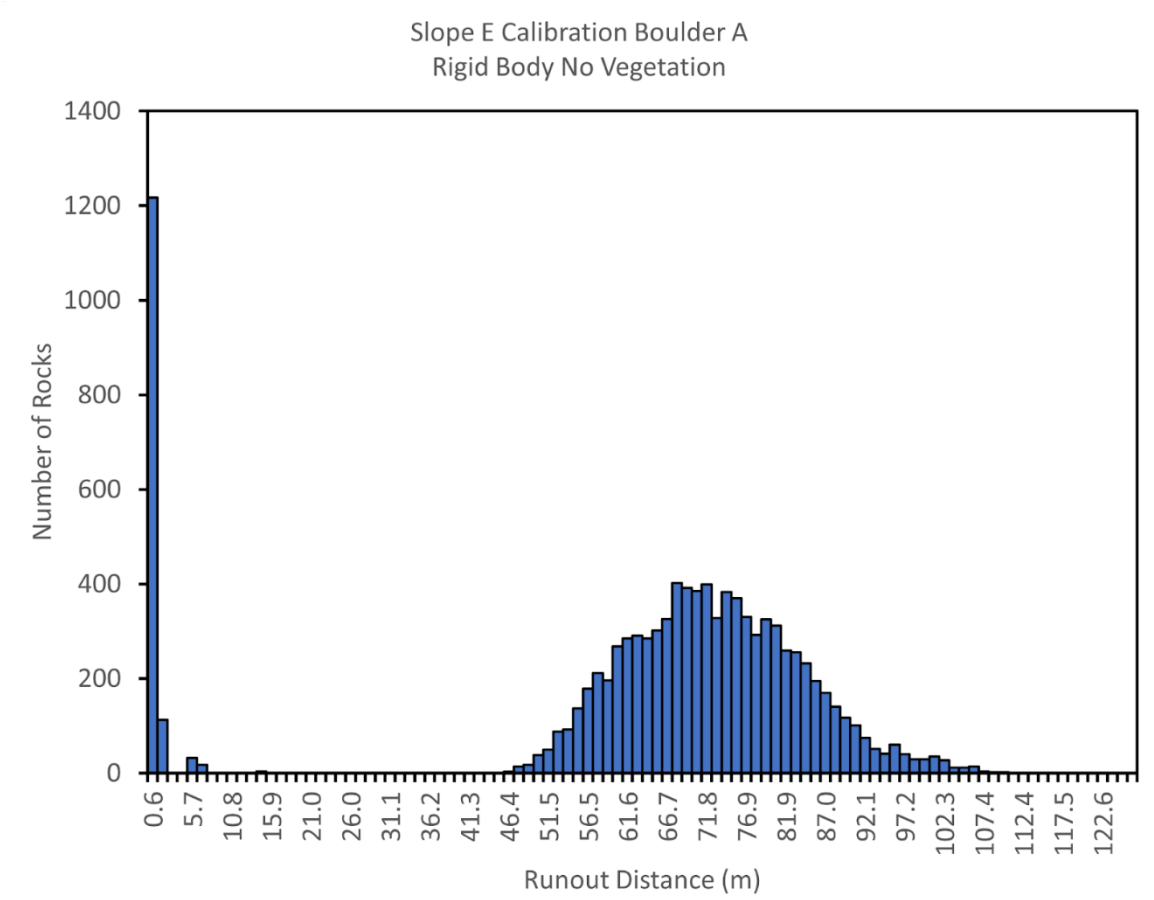
Slope E Calibration Boulder A
Rigid Body No Vegetation
Number of Rocks
1400
1200
1000
800
600
400
200
0
0.6
5.7
10.8
15.9
21.0
26.0
31.1
36.2
41.3
46.4
51.5
56.5
61.6
66.7
71.8
76.9
81.9
87.0
92.1
97.2
102.3
107.4
112.4
117.5
122.6
Runout Distance (m)

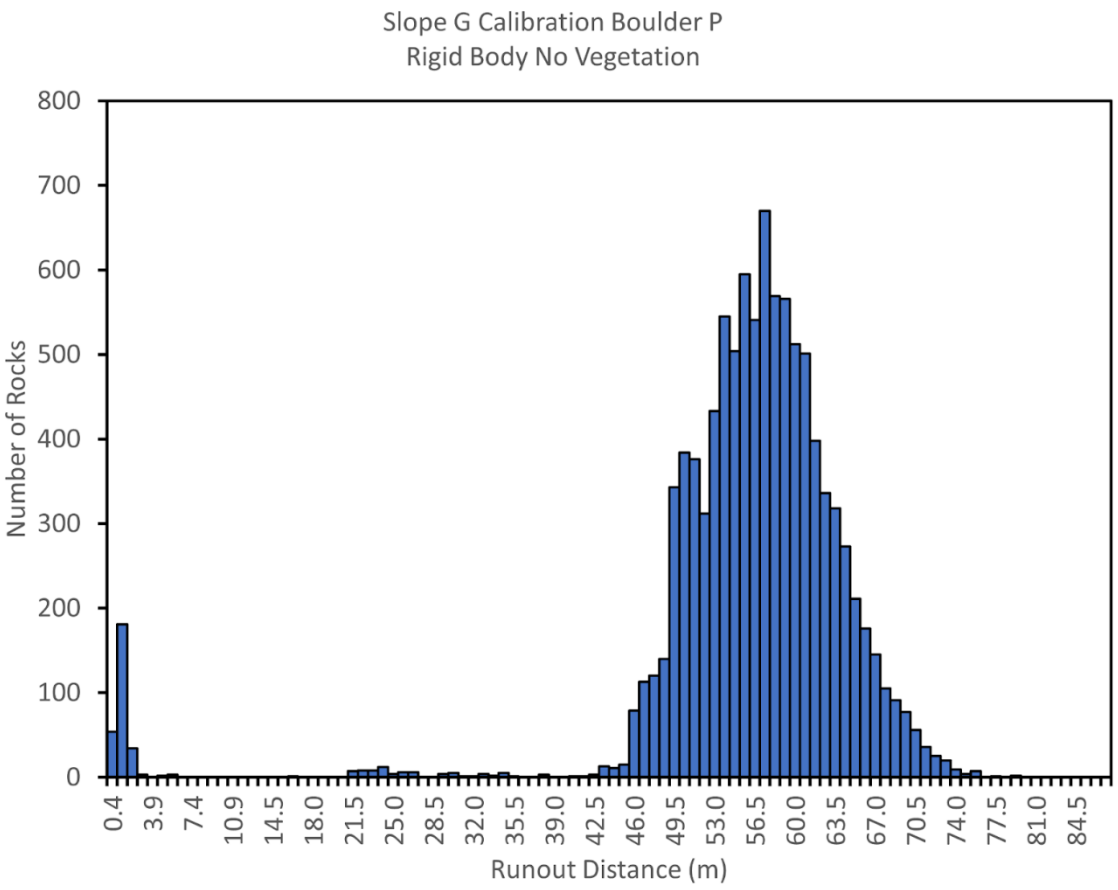
Slope G Calibration Boulder P
Rigid Body No Vegetation
Number of Rocks
800
700
600
500
400
300
200
100
0
0.4
3.9
7.4
10.9
14.5
18.0
21.5
25.0
28.5
32.0
35.5
39.0
42.5
46.0
49.5
53.0
56.5
60.0
63.5
67.0
70.5
74.0
77.5
81.0
84.5
Runout Distance (m)

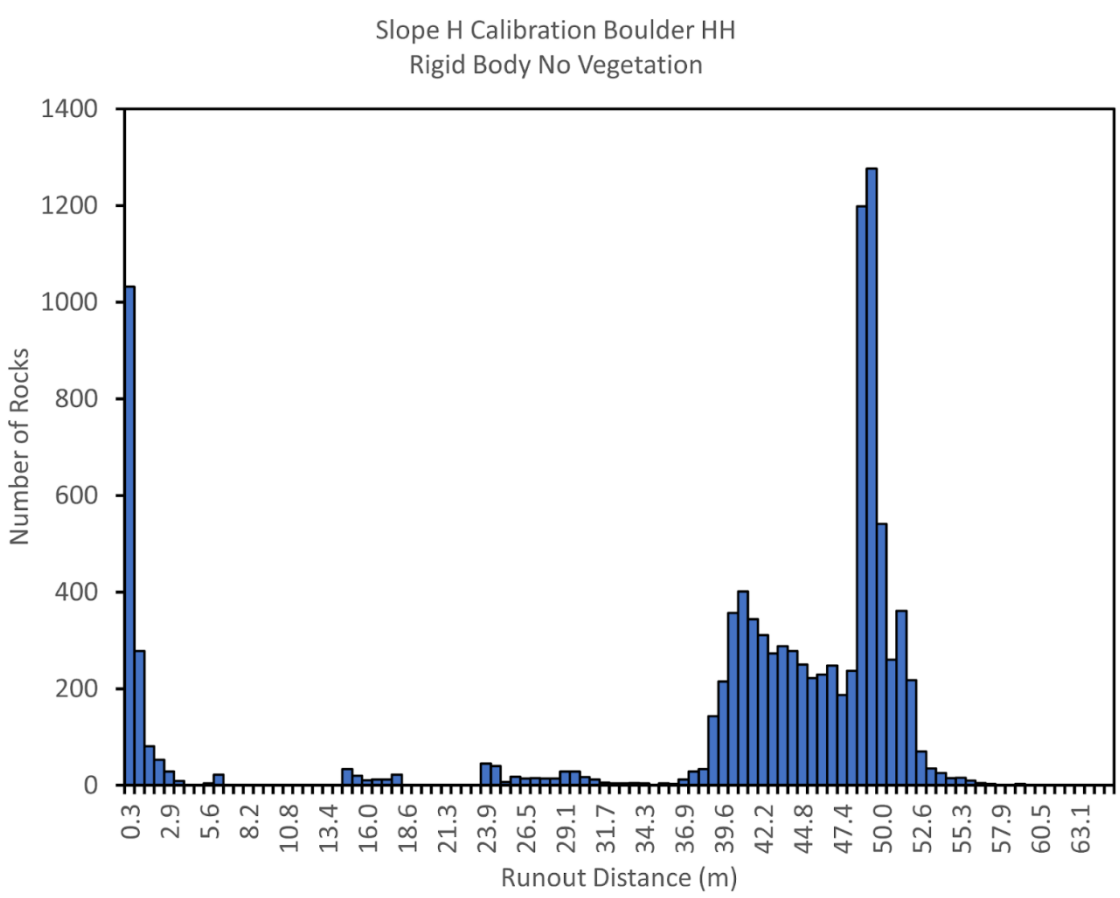
Slope H Calibration Boulder HH
Rigid Body No Vegetation
Number of Rocks
1400
1200
1000
800
600
400
200
0
0.3
2.9
5.6
8.2
10.8
13.4
16.0
18.6
21.3
23.9
26.5
29.1
31.7
34.3
36.9
39.6
42.2
44.8
47.4
50.0
52.6
55.3
57.9
60.5
63.1
Runout Distance (m)

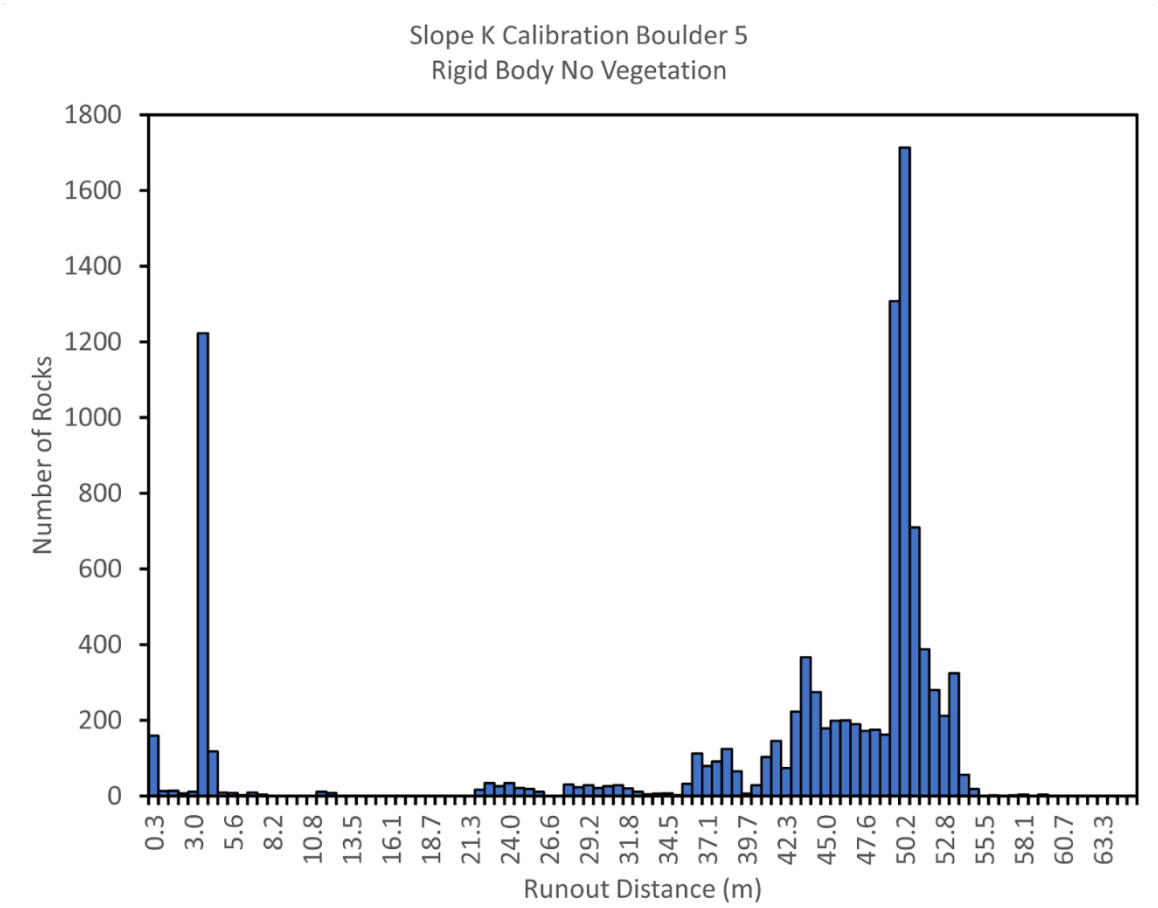
Slope K Calibration Boulder 5
Rigid Body No Vegetation
Number of Rocks
1800
1600
1400
1200
1000
800
600
400
200
0
0.3
3.0
5.6
8.2
10.8
13.5
16.1
18.7
21.3
24.0
26.6
29.2
31.8
34.5
37.1
39.7
42.3
45.0
47.6
50.2
52.8
55.5
58.1
60.7
63.3
Runout Distance (m)

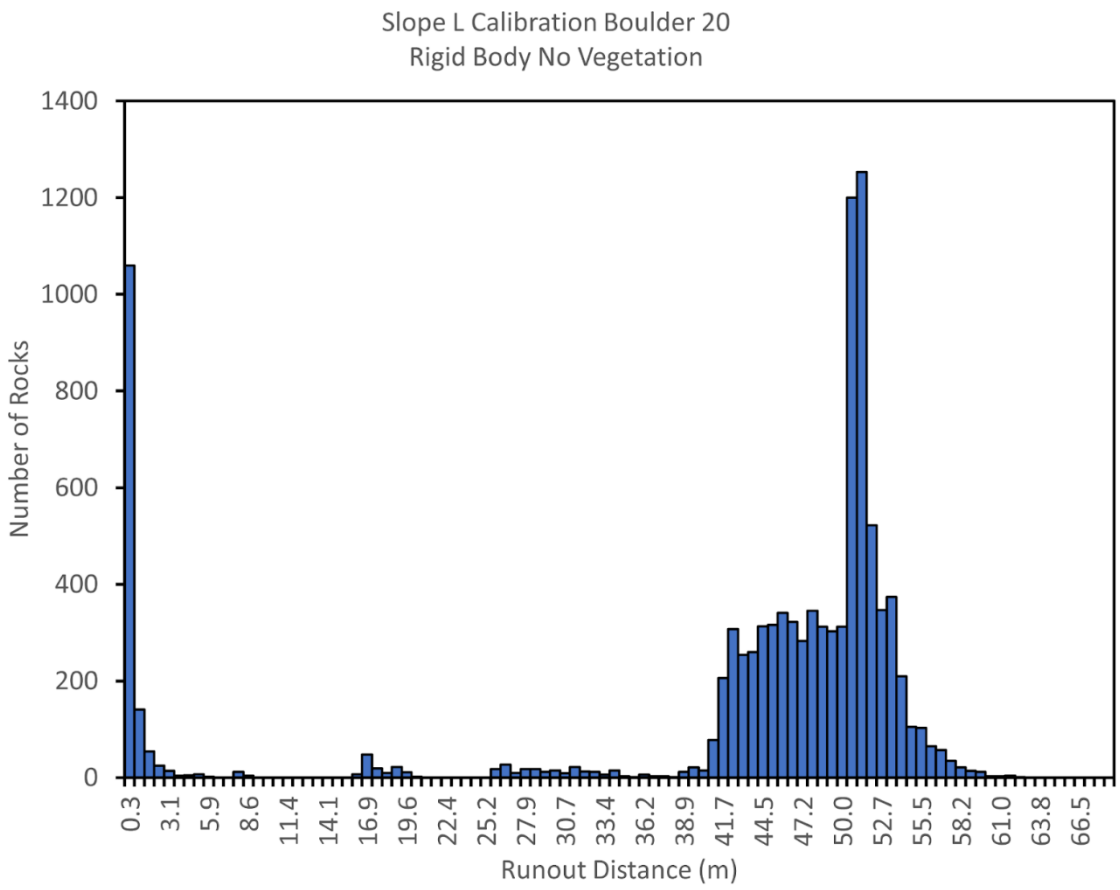
Slope L Calibration Boulder 20
Rigid Body No Vegetation
Number of Rocks
1400
1200
1000
800
600
400
200
0
0.3
3.1
5.9
8.6
11.4
14.1
16.9
19.6
22.4
25.2
27.9
30.7
33.4
36.2
38.9
41.7
44.5
47.2
50.0
52.7
55.5
58.2
61.0
63.8
66.5
Runout Distance (m)

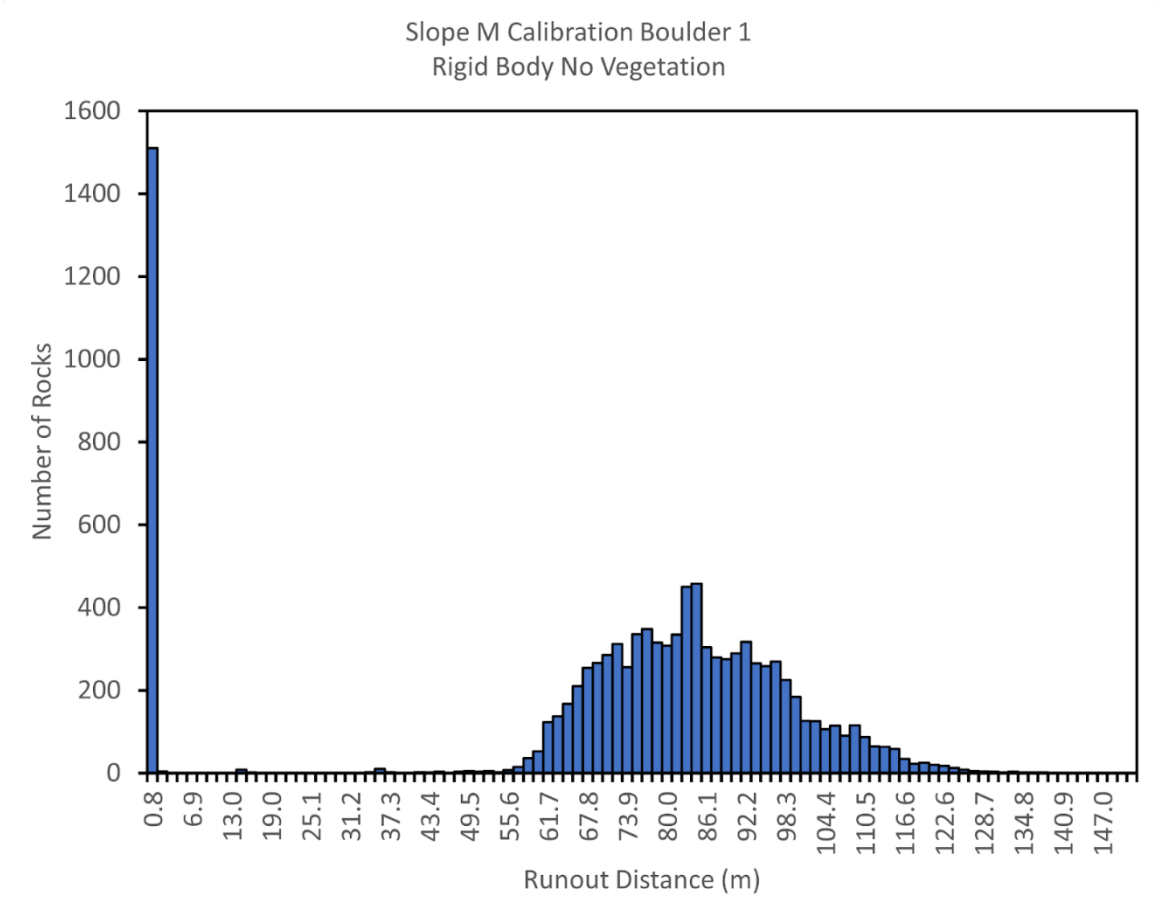
Slope M Calibration Boulder 1
Rigid Body No Vegetation
Number of Rocks
1600
1400
1200
1000
800
600
400
200
0
0.8
6.9
13.0
19.0
25.1
31.2
37.3
43.4
49.5
55.6
61.7
67.8
73.9
80.0
86.1
92.2
98.3
104.4
110.5
116.6
122.6
128.7
134.8
140.9
147.0
Runout Distance (m)

APPENDIX C

Rigid Body with Vegetation Rockfall Calibration Histograms

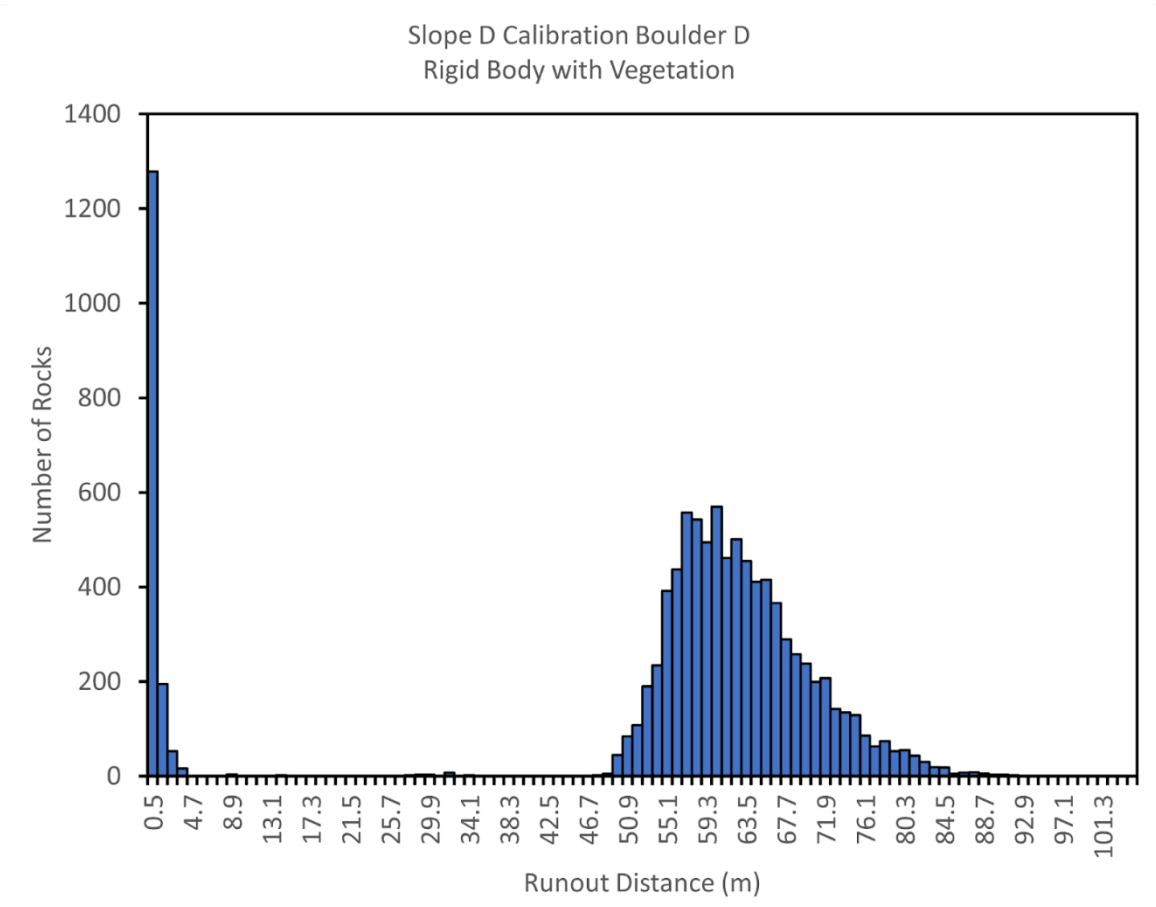
Slope D Calibration Boulder D
Rigid Body with Vegetation
Number of Rocks
1400
1200
1000
800
600
400
200
0
0.5
4.7
8.9
13.1
17.3
21.5
25.7
29.9
34.1
38.3
42.5
46.7
50.9
55.1
59.3
63.5
67.7
71.9
76.1
80.3
84.5
88.7
92.9
97.1
101.3
Runout Distance (m)

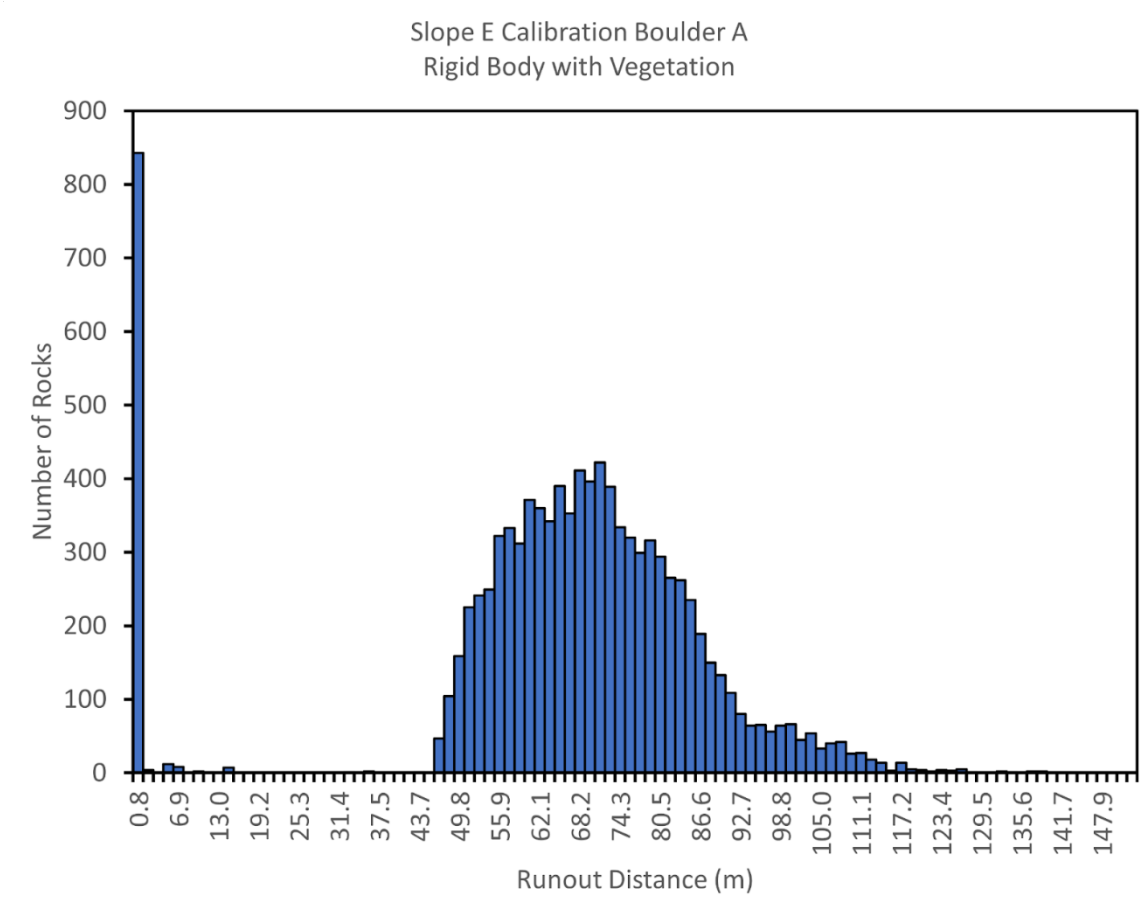
Slope E Calibration Boulder A
Rigid Body with Vegetation
Number of Rocks
900
800
700
600
500
400
300
200
100
0
0.8
6.9
13.0
19.2
25.3
31.4
37.5
43.7
49.8
55.9
62.1
68.2
74.3
80.5
86.6
92.7
98.8
105.0
111.1
117.2
123.4
129.5
135.6
141.7
147.9
Runout Distance (m)

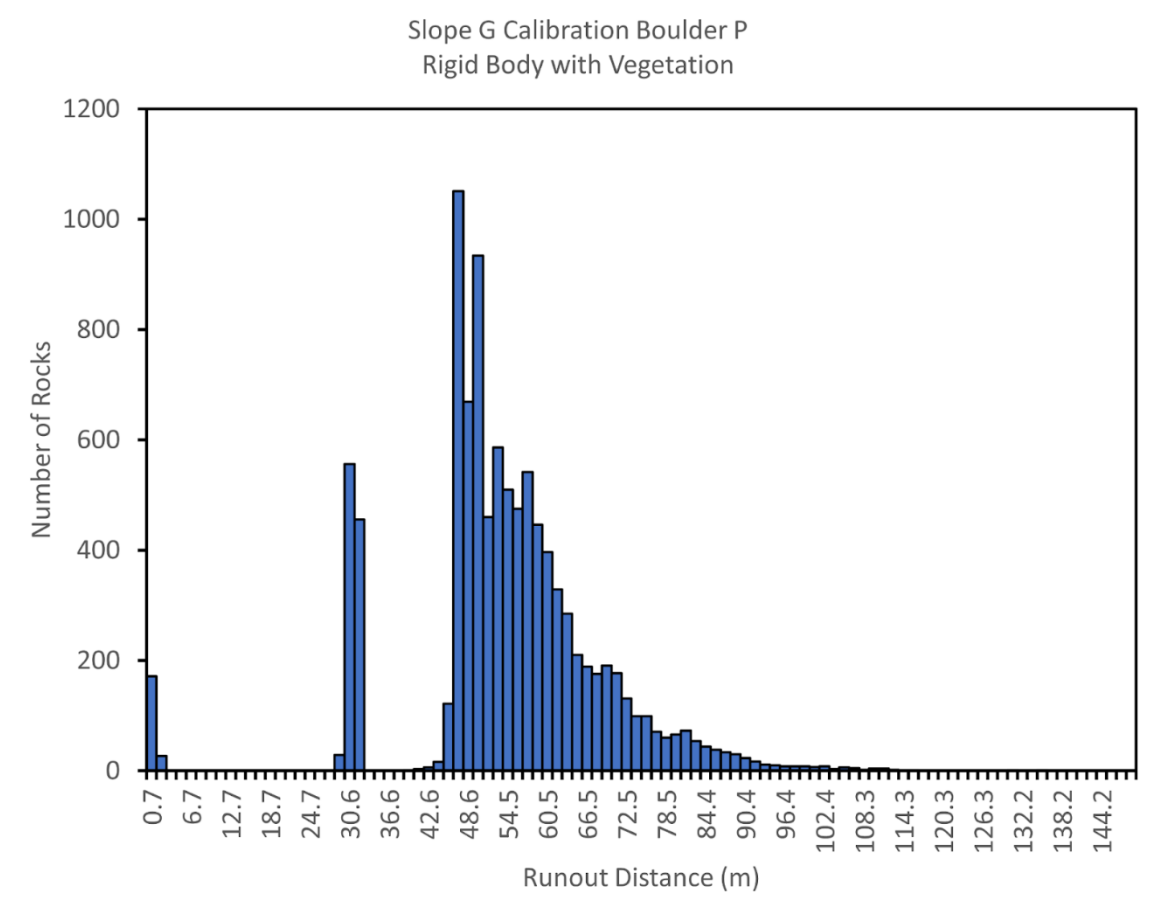
Slope G Calibration Boulder P
Rigid Body with Vegetation
Number of Rocks
1200
1000
800
600
400
200
0
0.7
6.7
12.7
18.7
24.7
30.6
36.6
42.6
48.6
54.5
60.5
66.5
72.5
78.5
84.4
90.4
96.4
102.4
108.3
114.3
120.3
126.3
132.2
138.2
144.2
Runout Distance (m)

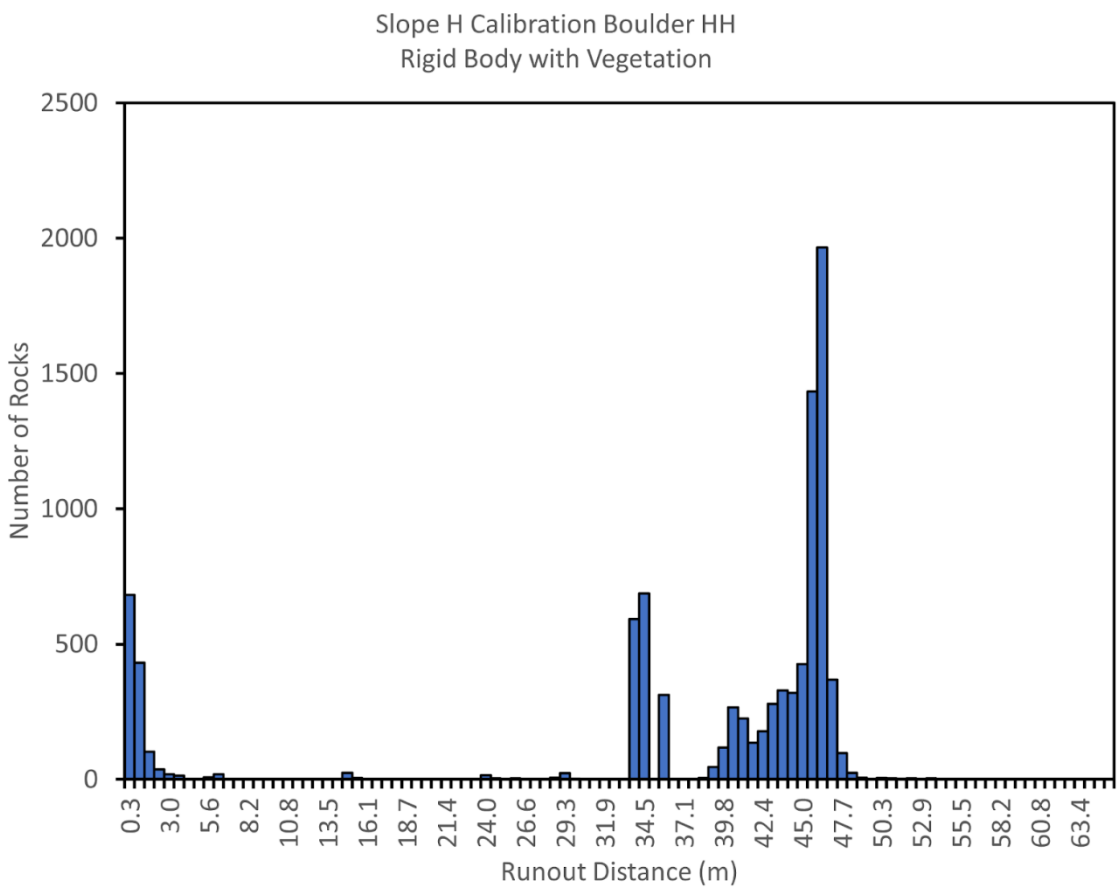
Slope H Calibration Boulder HH
Rigid Body with Vegetation
Number of Rocks
2500
2000
1500
1000
500
0
0.3
3.0
5.6
8.2
10.8
13.5
16.1
18.7
21.4
24.0
26.6
29.3
31.9
34.5
37.1
39.8
42.4
45.0
47.7
50.3
52.9
55.5
58.2
60.8
63.4
Runout Distance (m)

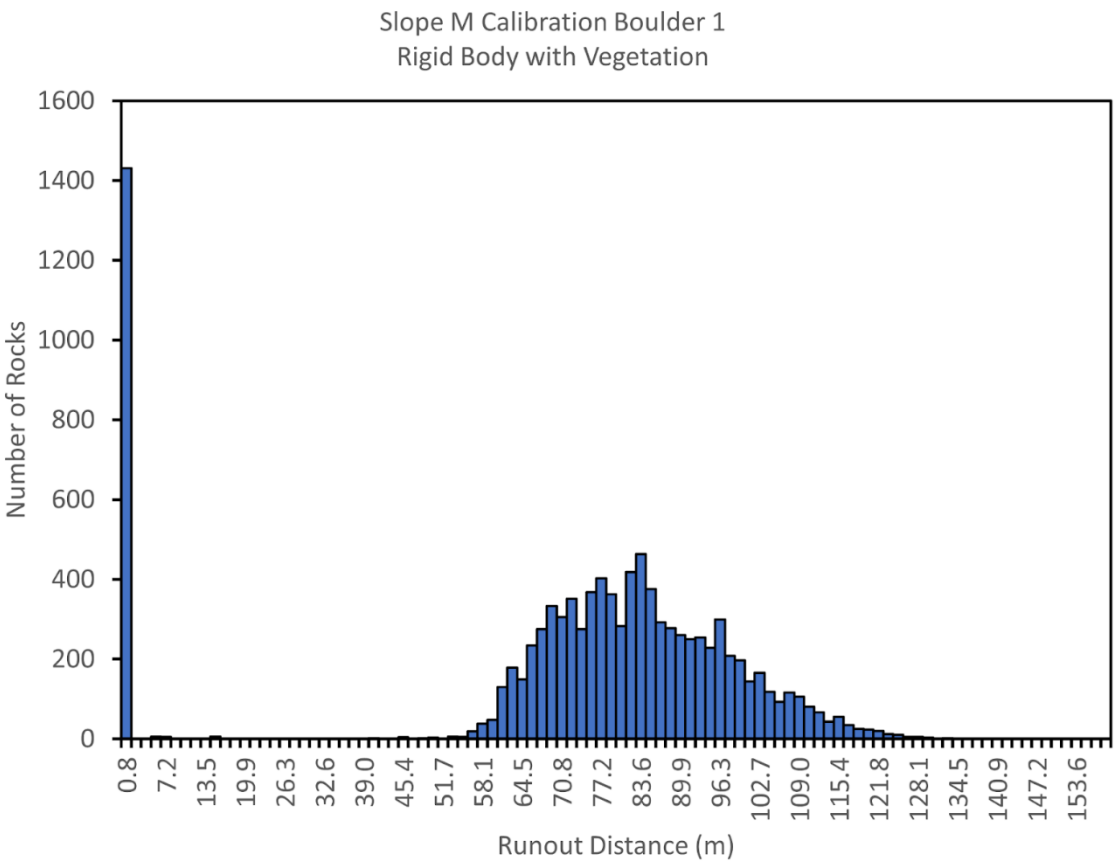
Slope M Calibration Boulder 1
Rigid Body with Vegetation
Number of Rocks
1600
1400
1200
1000
800
600
400
200
0
0.8
7.2
13.5
19.9
26.3
32.6
39.0
45.4
51.7
58.1
64.5
70.8
77.2
83.6
89.9
96.3
102.7
109.0
115.4
121.8
128.1
134.5
140.9
147.2
153.6
Runout Distance (m)

APPENDIX D

Predictive Rockfall Runout Map Histograms

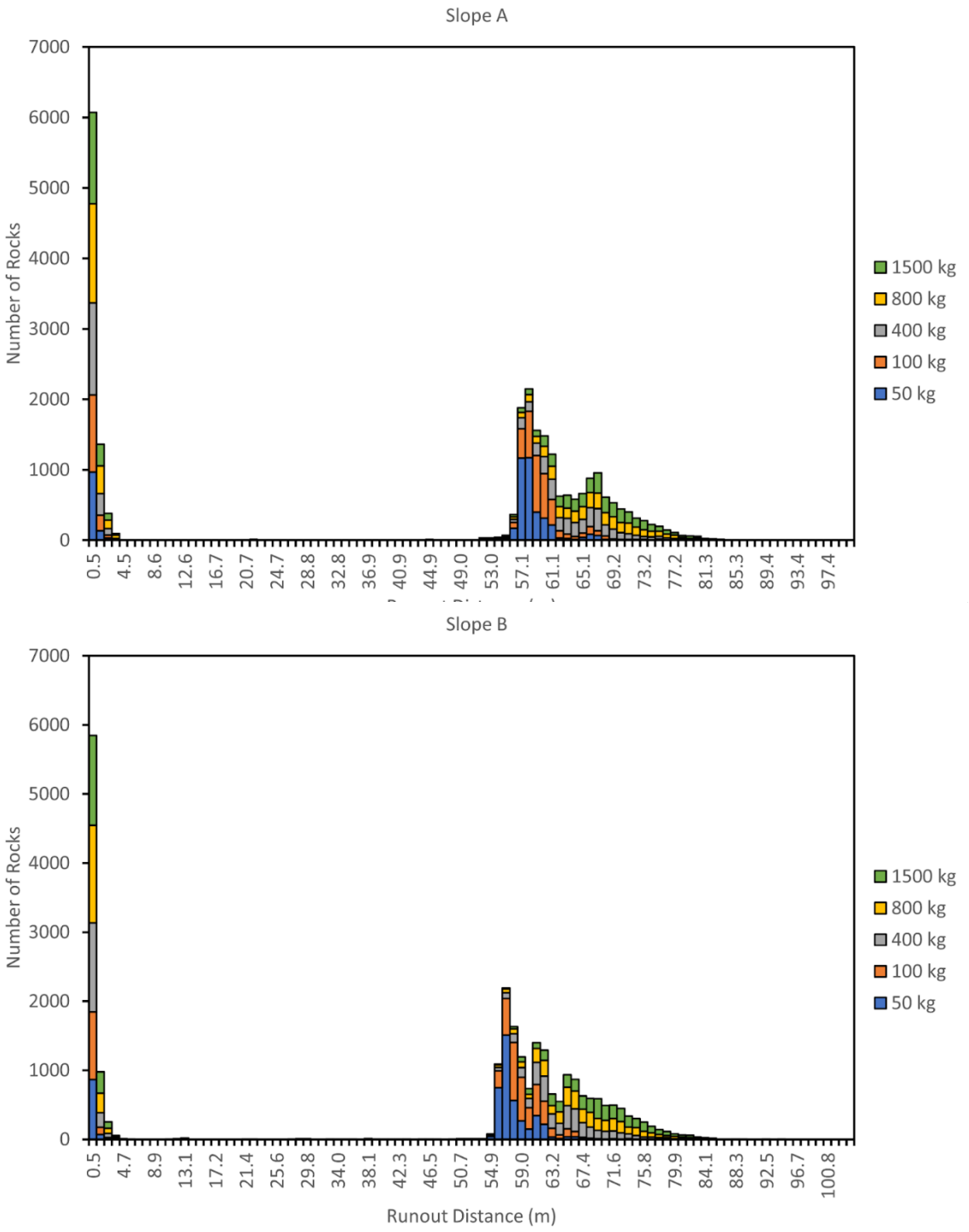
Slope A
Number of Rocks
7000
6000
5000
4000
3000
2000
1000
0
0.5
4.5
8.6
12.6
16.7
20.7
24.7
28.8
32.8
36.9
40.9
44.9
49.0
53.0
57.1
61.1
65.1
69.2
73.2
77.2
81.3
85.3
89.4
93.4
97.4
1500 kg
800 kg
400 kg
100 kg
50 kg
Slope B
Number of Rocks
7000
6000
5000
4000
3000
2000
1000
0
0.5
4.7
8.9
13.1
17.2
21.4
25.6
29.8
34.0
38.1
42.3
46.5
50.7
54.9
59.0
63.2
67.4
71.6
75.8
79.9
84.1
88.3
92.5
96.7
100.8
Runout Distance (m)
1500 kg
800 kg
400 kg
100 kg
50 kg

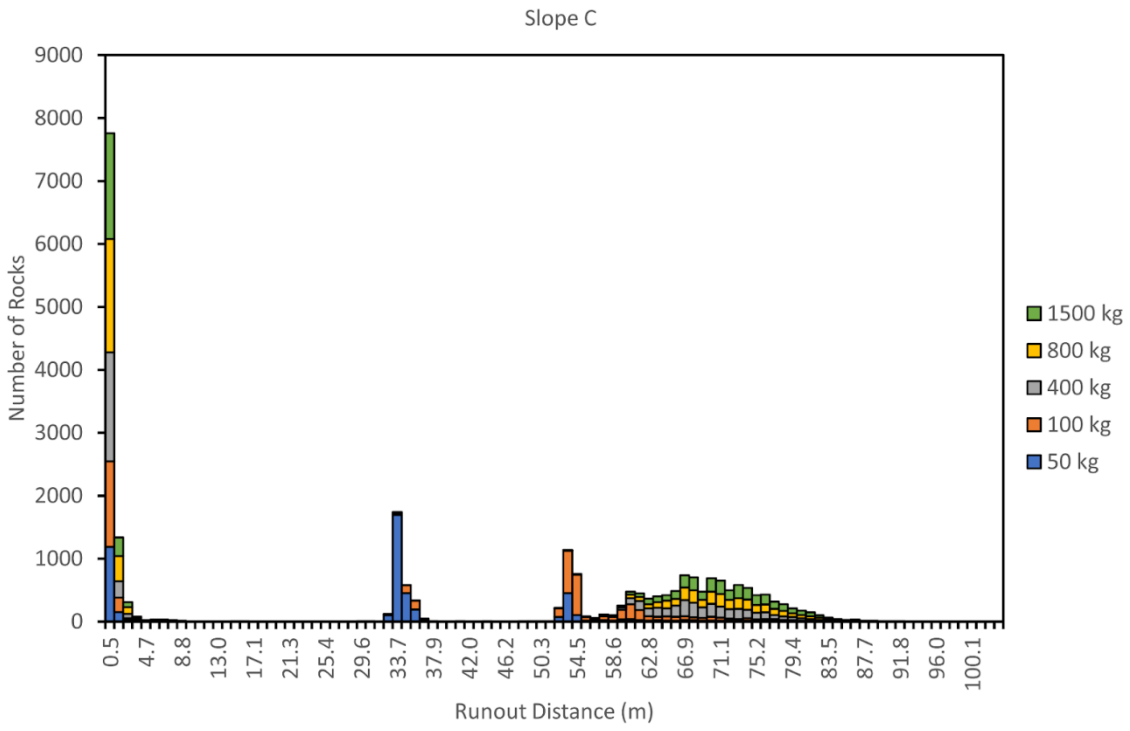
Slope C
Number of Rocks
9000
8000
7000
6000
5000
4000
3000
2000
1000
0
0.5
4.7
8.8
13.0
17.1
21.3
25.4
29.6
33.7
37.9
42.0
46.2
50.3
54.5
58.6
62.8
66.9
71.1
75.2
79.4
83.5
87.7
91.8
96.0
100.1
Runout Distance (m)
1500 kg
800 kg
400 kg
100 kg
50 kg

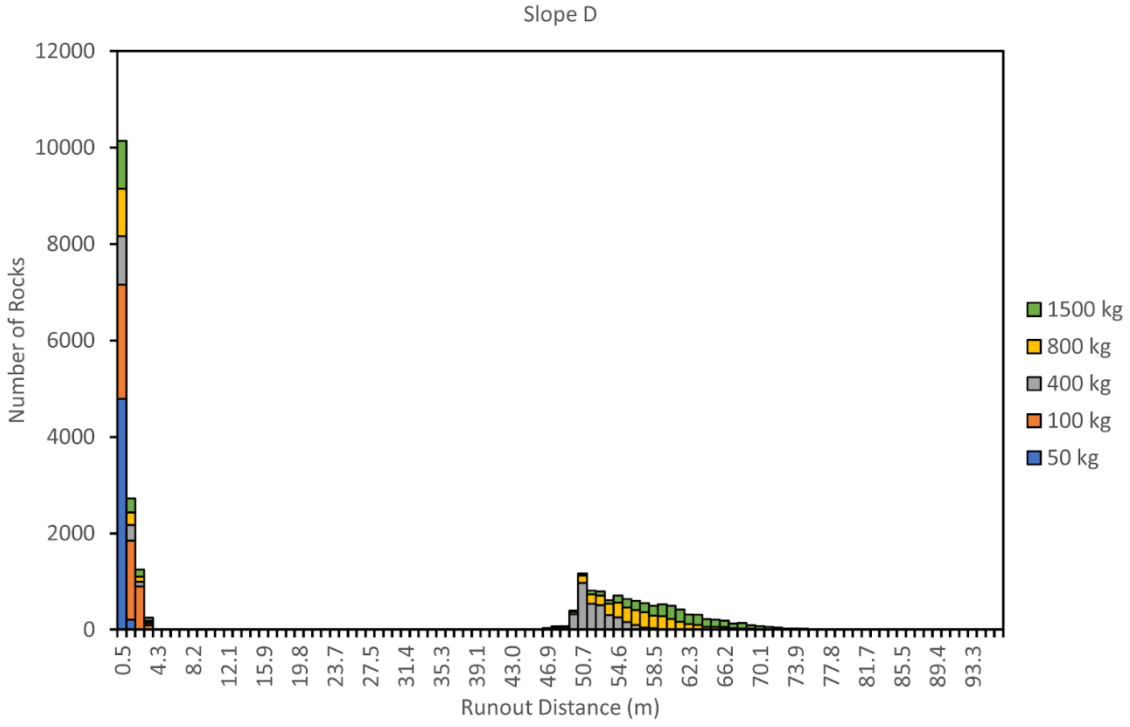
Slope D
Number of Rocks
12000
10000
8000
6000
4000
2000
0
0.5
4.3
8.2
12.1
15.9
19.8
23.7
27.5
31.4
35.3
39.1
43.0
46.9
50.7
54.6
58.5
62.3
66.2
70.1
73.9
77.8
81.7
85.5
89.4
93.3
Runout Distance (m)
1500 kg
800 kg
400 kg
100 kg
50 kg

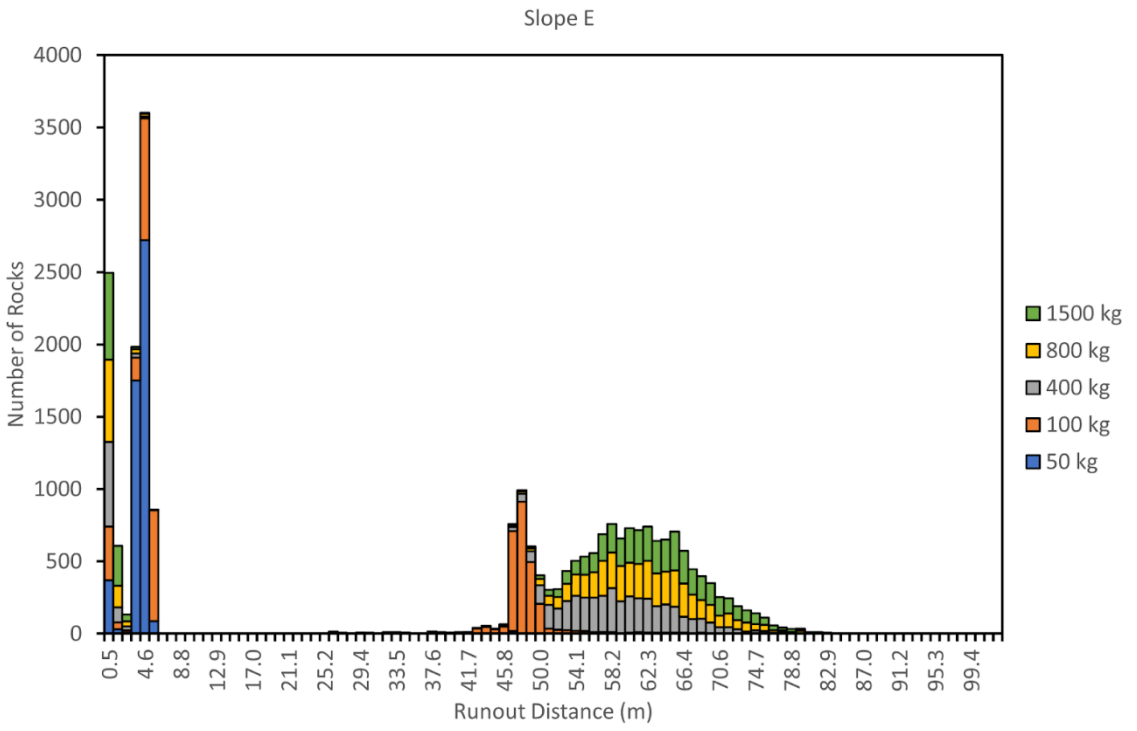
Slope E
Number of Rocks
Runout Distance (m)
1500 kg
800 kg
400 kg
100 kg
50 kg

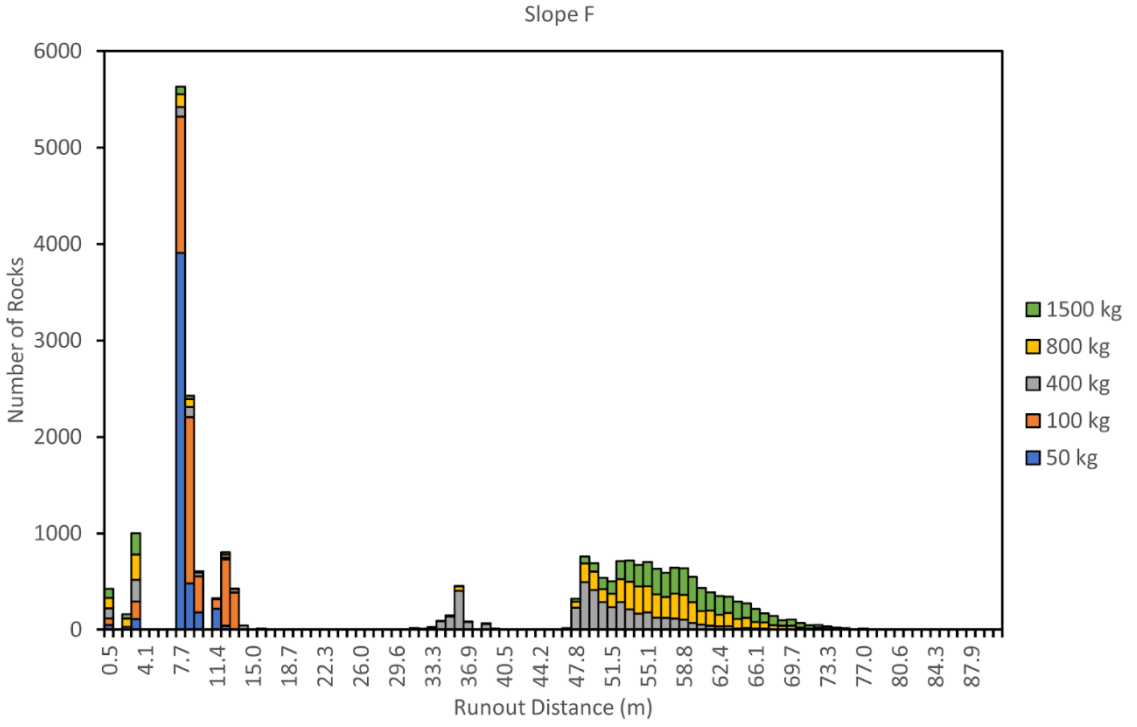
Slope F
Number of Rocks
Runout Distance (m)
1500 kg
800 kg
400 kg
100 kg
50 kg

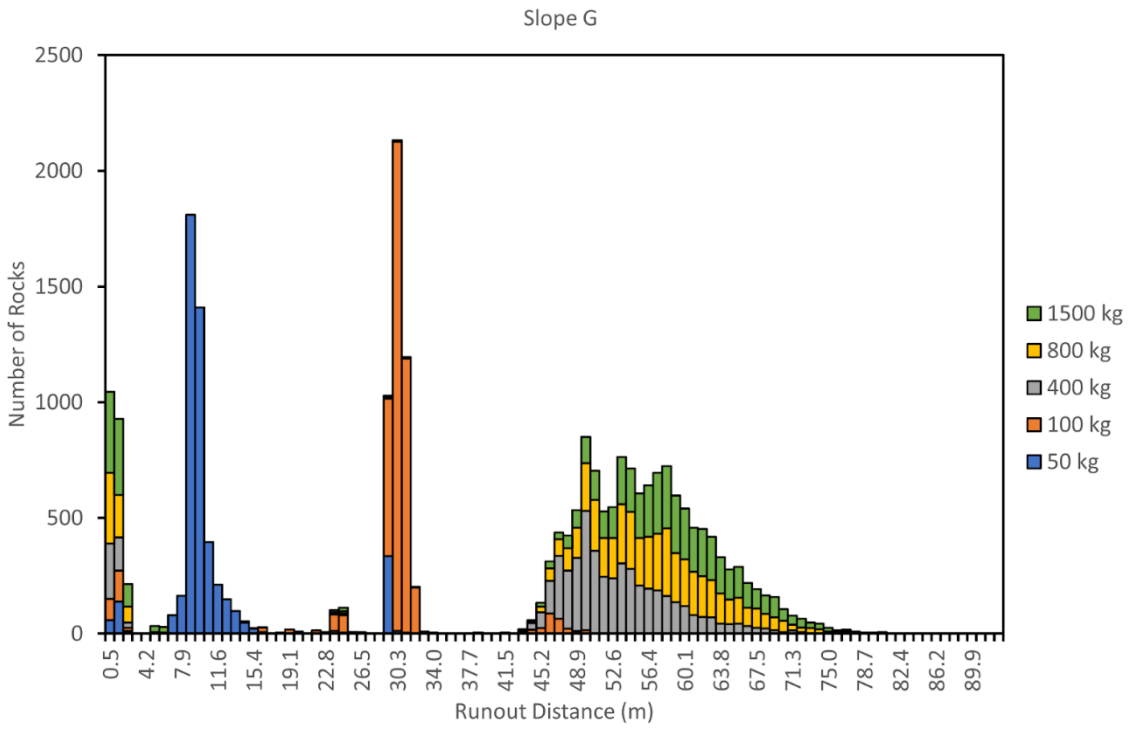
Slope G
Number of Rocks
Runout Distance (m)
1500 kg
800 kg
400 kg
100 kg
50 kg

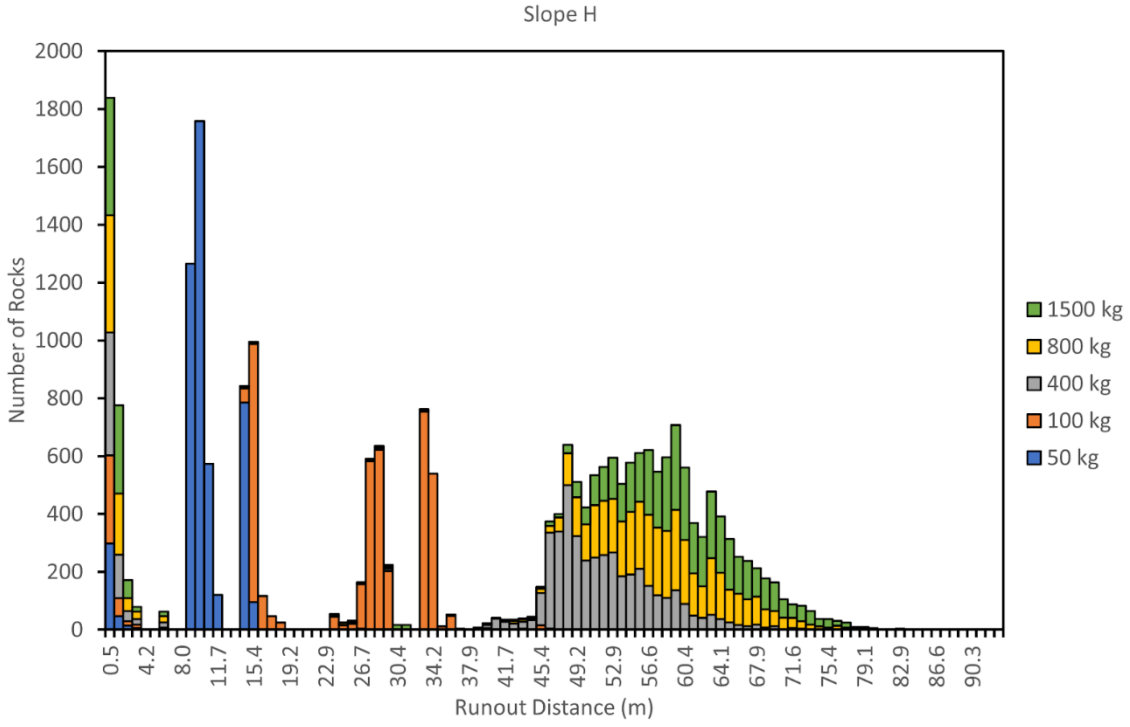
Slope H
Number of Rocks
Runout Distance (m)
1500 kg
800 kg
400 kg
100 kg
50 kg

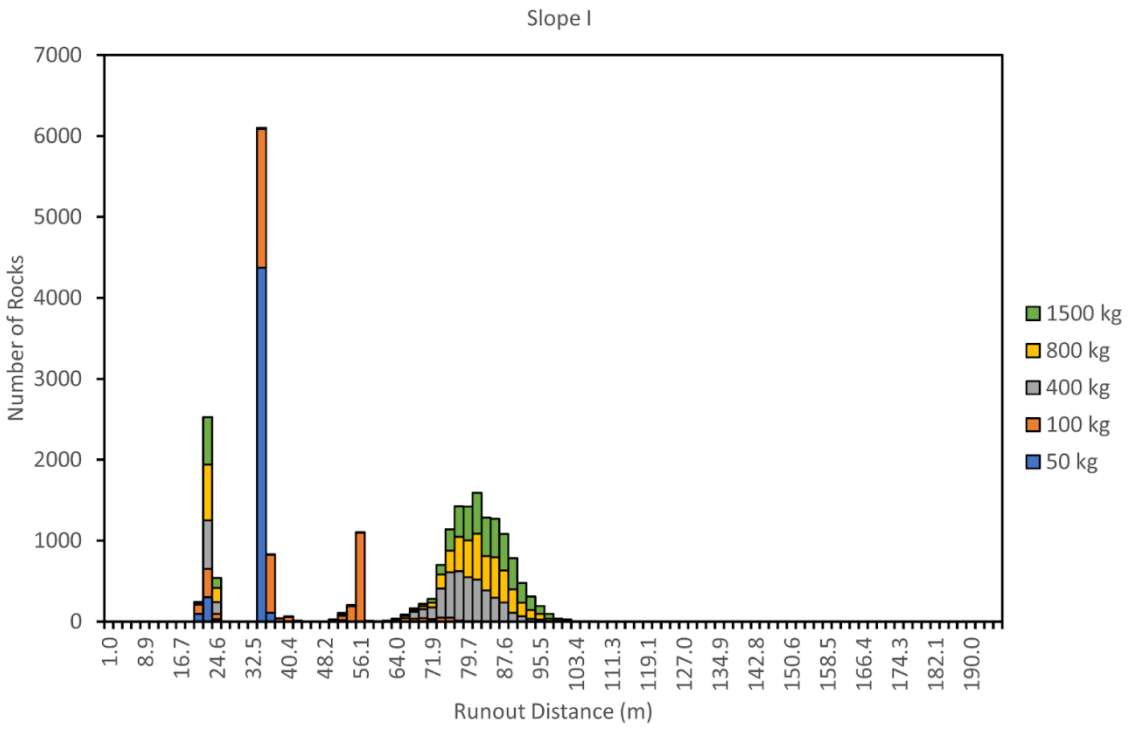
Slope I
Number of Rocks
Runout Distance (m)
1500 kg
800 kg
400 kg
100 kg
50 kg

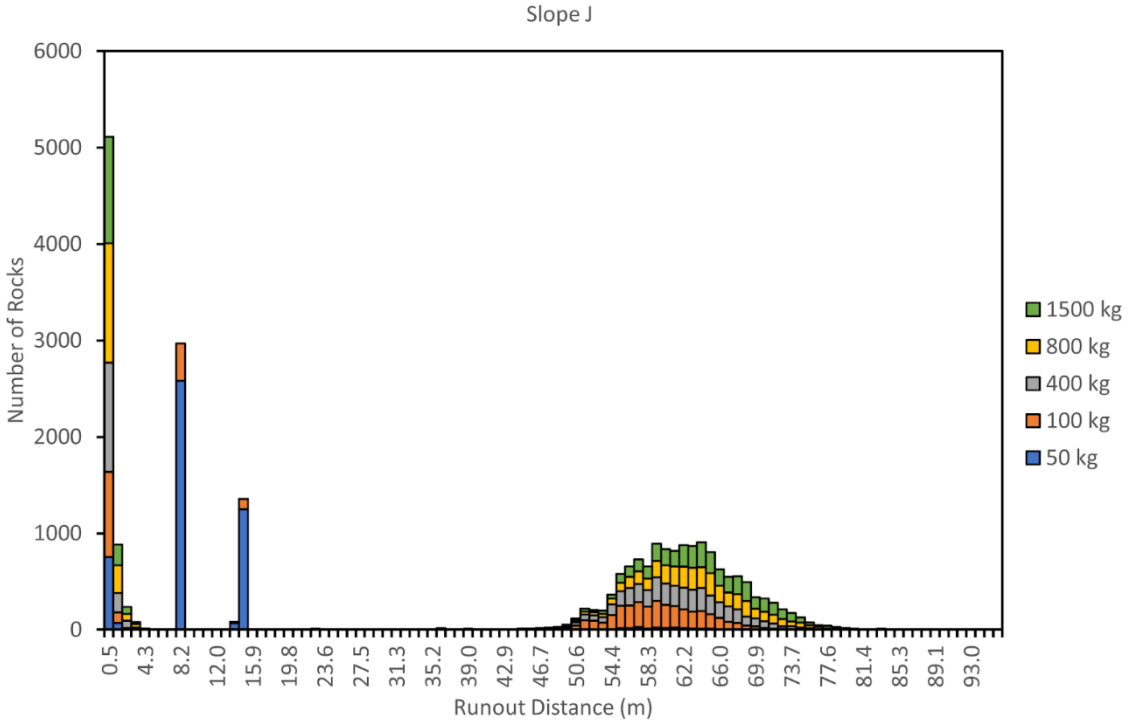
Slope J
Number of Rocks
Runout Distance (m)
1500 kg
800 kg
400 kg
100 kg
50 kg

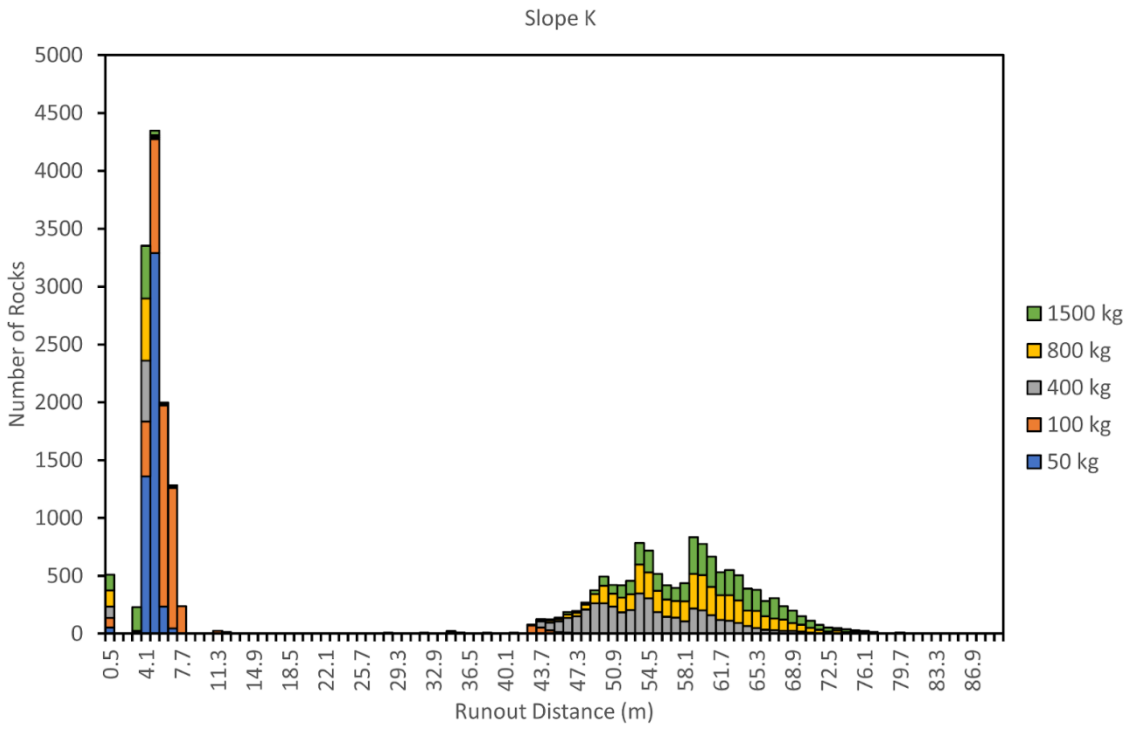
Slope K
Number of Rocks
Runout Distance (m)
1500 kg
800 kg
400 kg
100 kg
50 kg

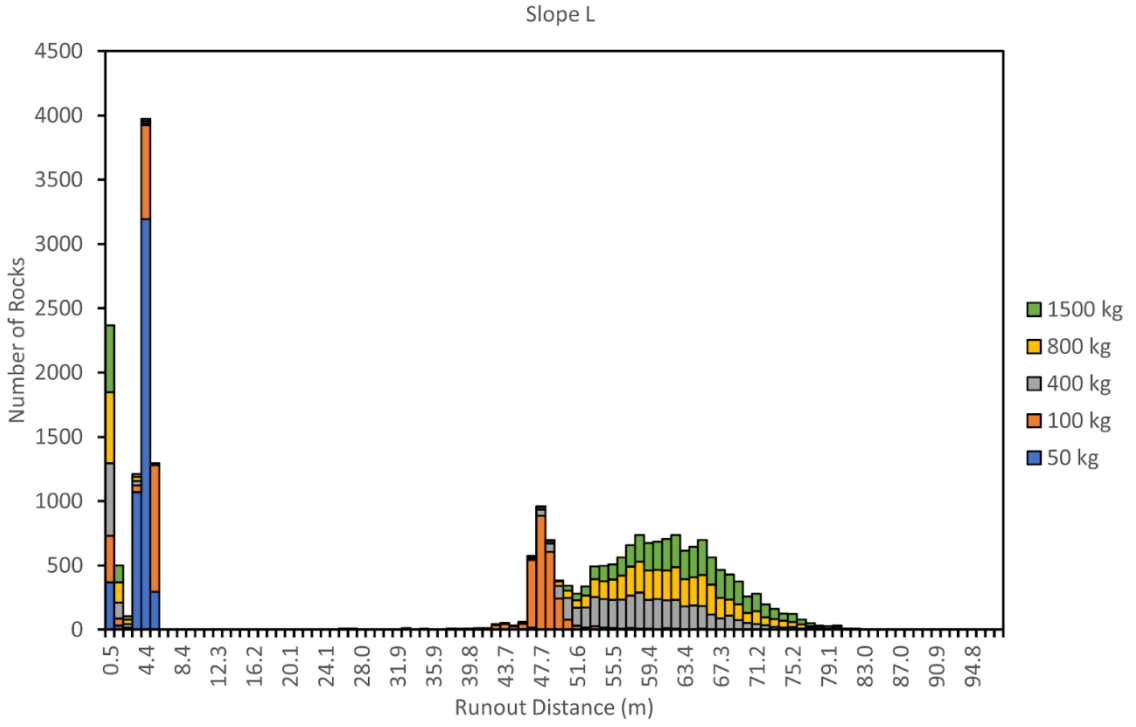
Slope L
Number of Rocks
Runout Distance (m)
1500 kg
800 kg
400 kg
100 kg
50 kg

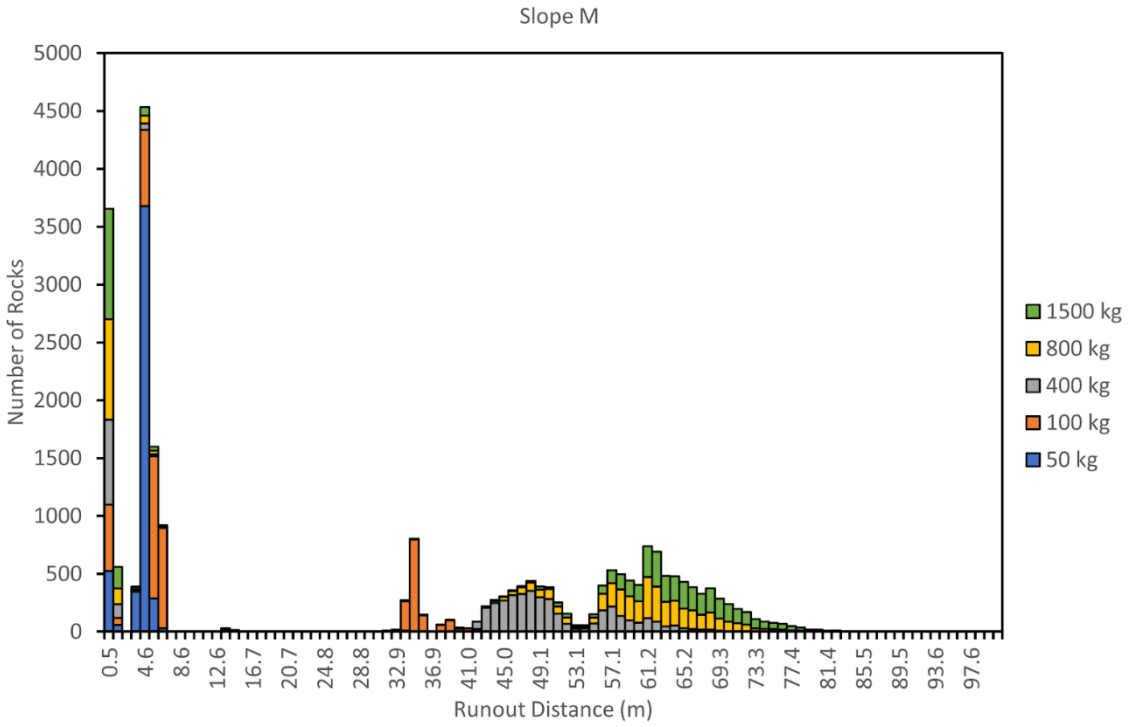
Slope M
Number of Rocks
5000
4500
4000
3500
3000
2500
2000
1500
1000
500
0
0.5
4.6
8.6
12.6
16.7
20.7
24.8
28.8
32.9
36.9
41.0
45.0
49.1
53.1
57.1
61.2
65.2
69.3
73.3
77.4
81.4
85.5
89.5
93.6
97.6
Runout Distance (m)
1500 kg
800 kg
400 kg
100 kg
50 kg

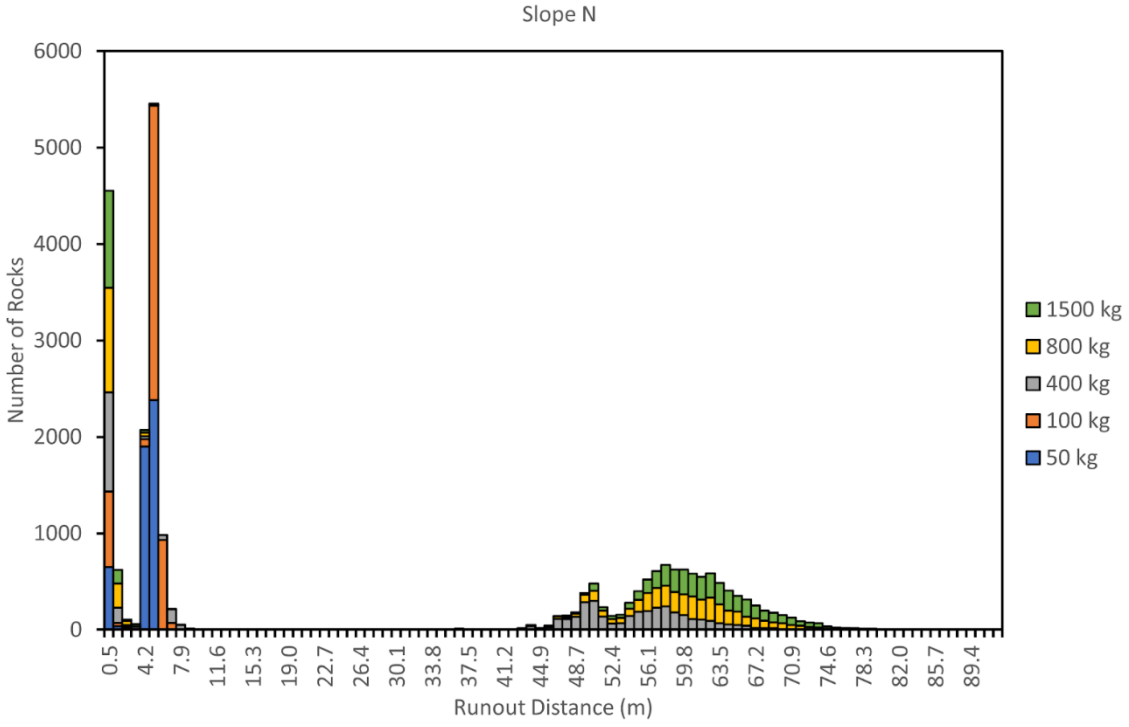
Slope N
Number of Rocks
6000
5000
4000
3000
2000
1000
0
0.5
4.2
7.9
11.6
15.3
19.0
22.7
26.4
30.1
33.8
37.5
41.2
44.9
48.7
52.4
56.1
59.8
63.5
67.2
70.9
74.6
78.3
82.0
85.7
89.4
Runout Distance (m)
1500 kg
800 kg
400 kg
100 kg
50 kg

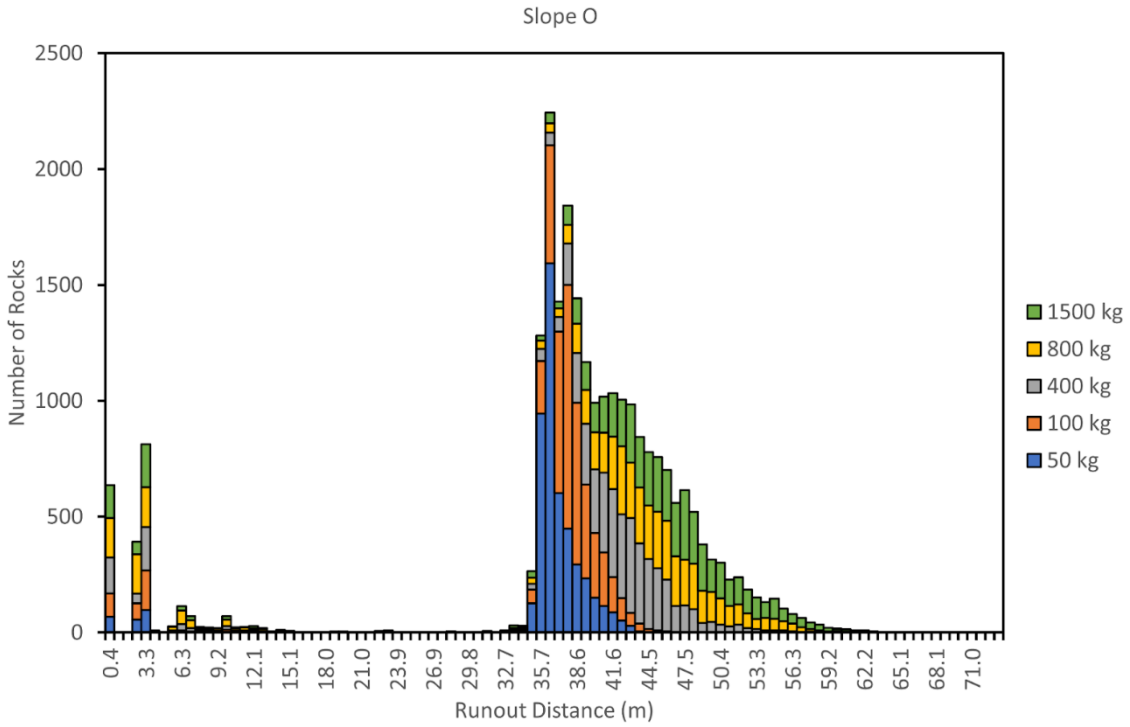
Slope O
Number of Rocks
2500
2000
1500
1000
500
0
0.4
3.3
6.3
9.2
12.1
15.1
18.0
21.0
23.9
26.9
29.8
32.7
35.7
38.6
41.6
44.5
47.5
50.4
53.3
56.3
59.2
62.2
65.1
68.1
71.0
Runout Distance (m)
1500 kg
800 kg
400 kg
100 kg
50 kg

APPENDIX E

Predictive Rockfall Runout Maps

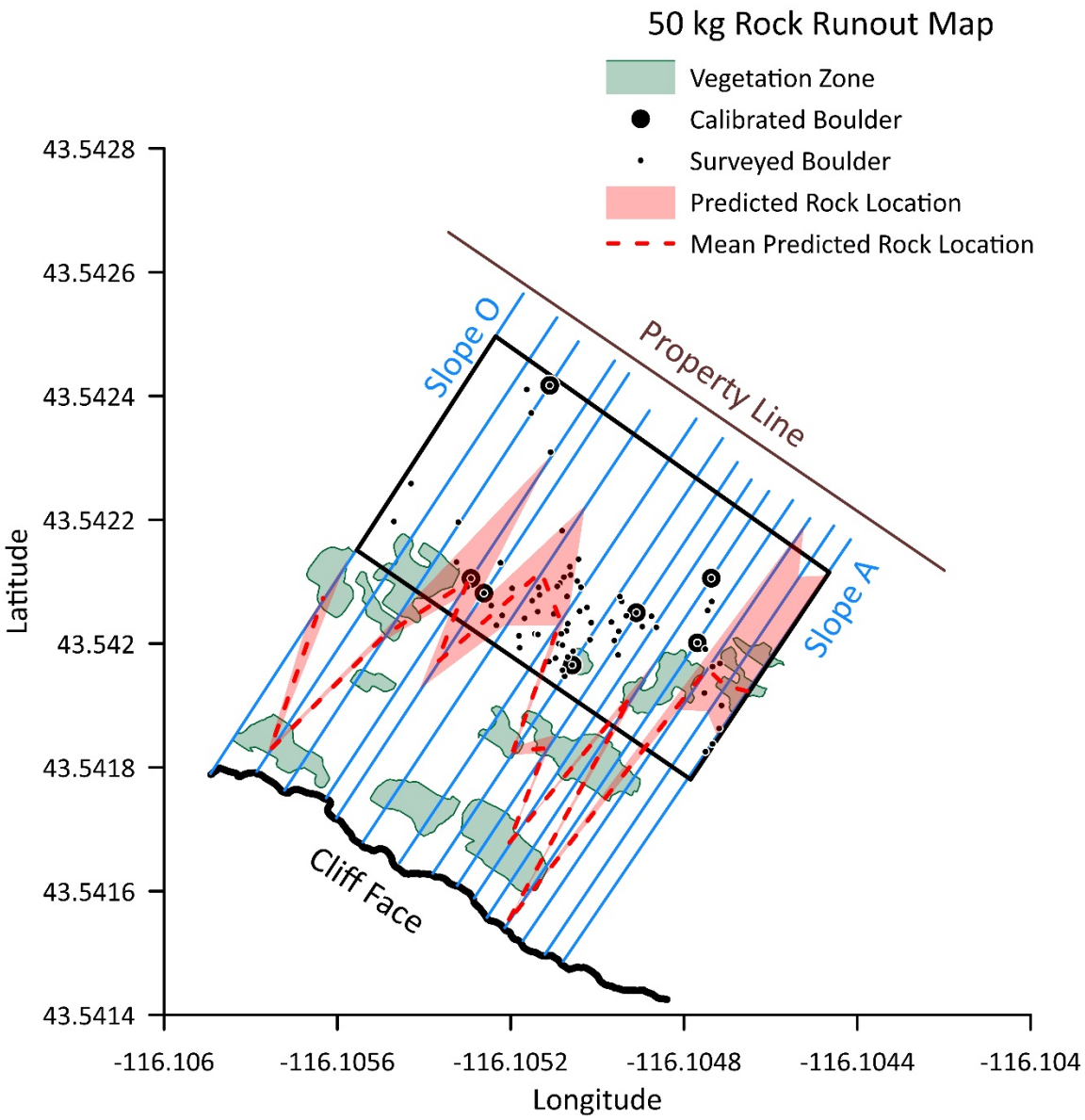
50 kg Rock Runout Map
Vegetation Zone
Calibrated Boulder
Surveyed Boulder
Predicted Rock Location
Mean Predicted Rock Location
Slope O
Property Line
Slope A
Cliff Face
Latitude
43.5428
43.5426
43.5424
43.5422
43.542
43.5418
43.5416
43.5414
-116.106
-116.1056
-116.1052
-116.1048
-116.1044
-116.104
Longitude

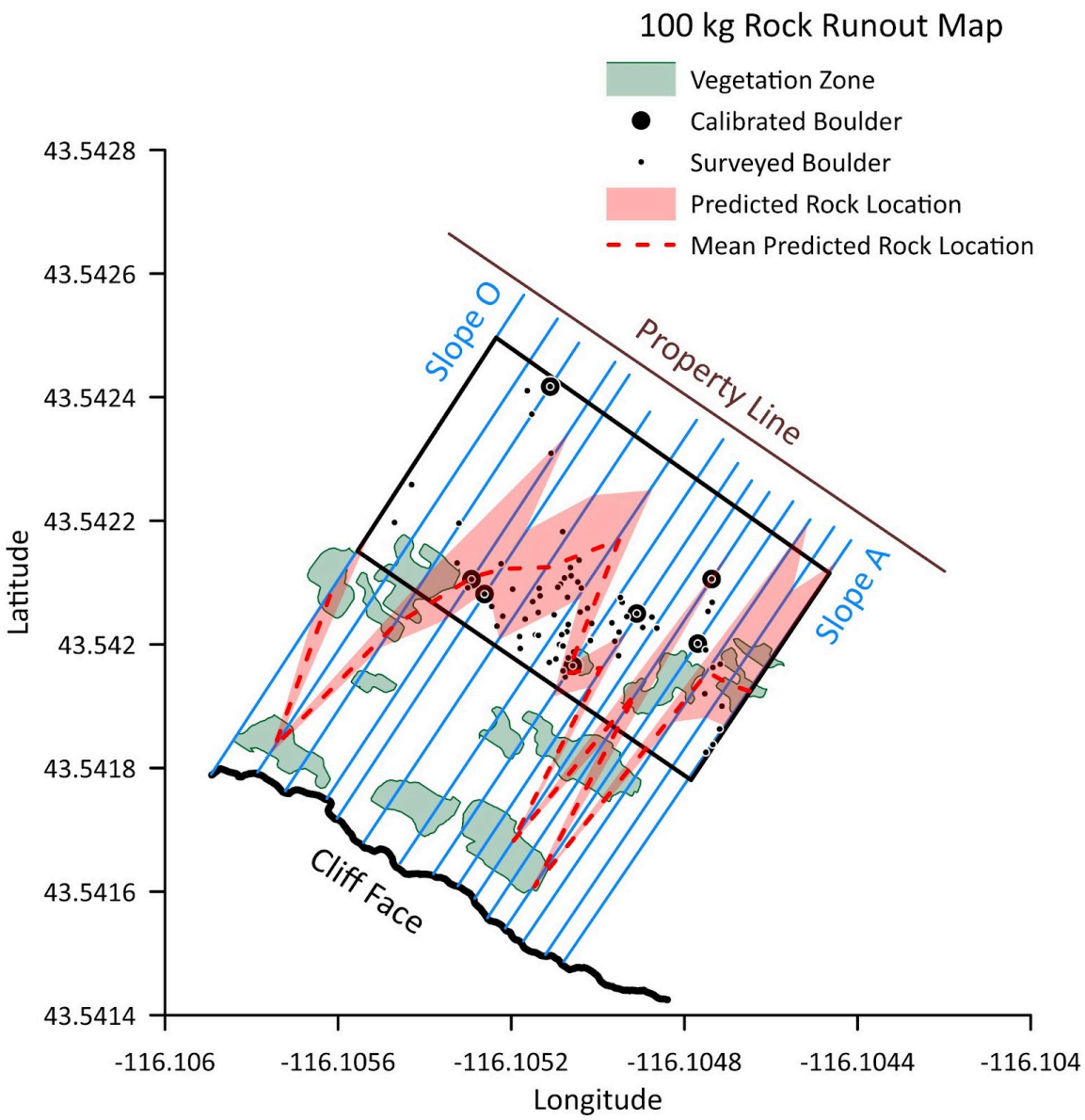
100 kg Rock Runout Map
Vegetation Zone
Calibrated Boulder
Surveyed Boulder
Predicted Rock Location
Mean Predicted Rock Location
Slope O
Property Line
Slope A
Cliff Face
Latitude
43.5428
43.5426
43.5424
43.5422
43.542
43.5418
43.5416
43.5414
-116.106
-116.1056
-116.1052
-116.1048
-116.1044
-116.104
Longitude

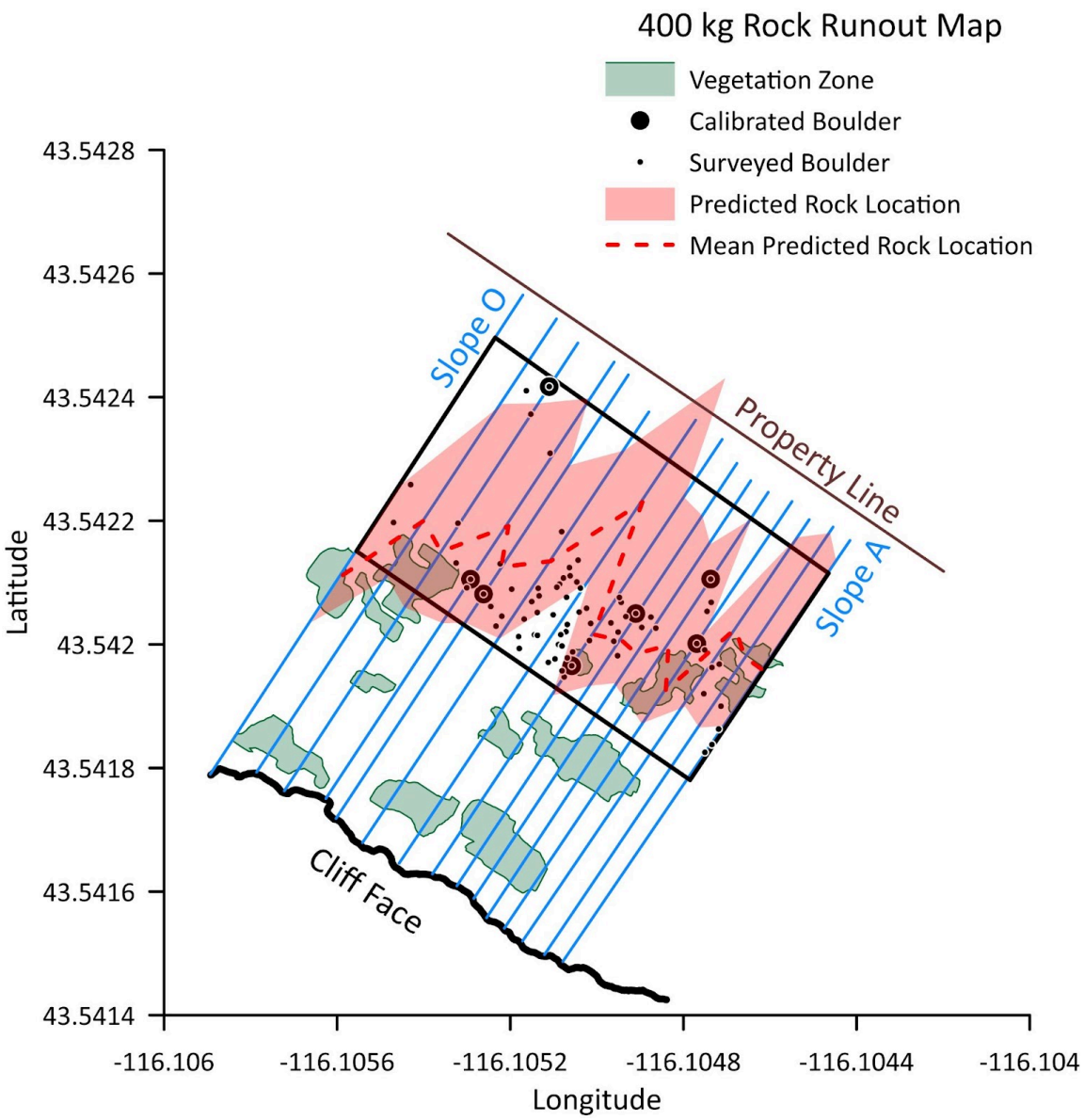
400 kg Rock Runout Map
Vegetation Zone
Calibrated Boulder
Surveyed Boulder
Predicted Rock Location
Mean Predicted Rock Location
Slope O
Property Line
Slope A
Cliff Face
Latitude
43.5428
43.5426
43.5424
43.5422
43.542
43.5418
43.5416
43.5414
-116.106
-116.1056
-116.1052
-116.1048
-116.1044
-116.104
Longitude

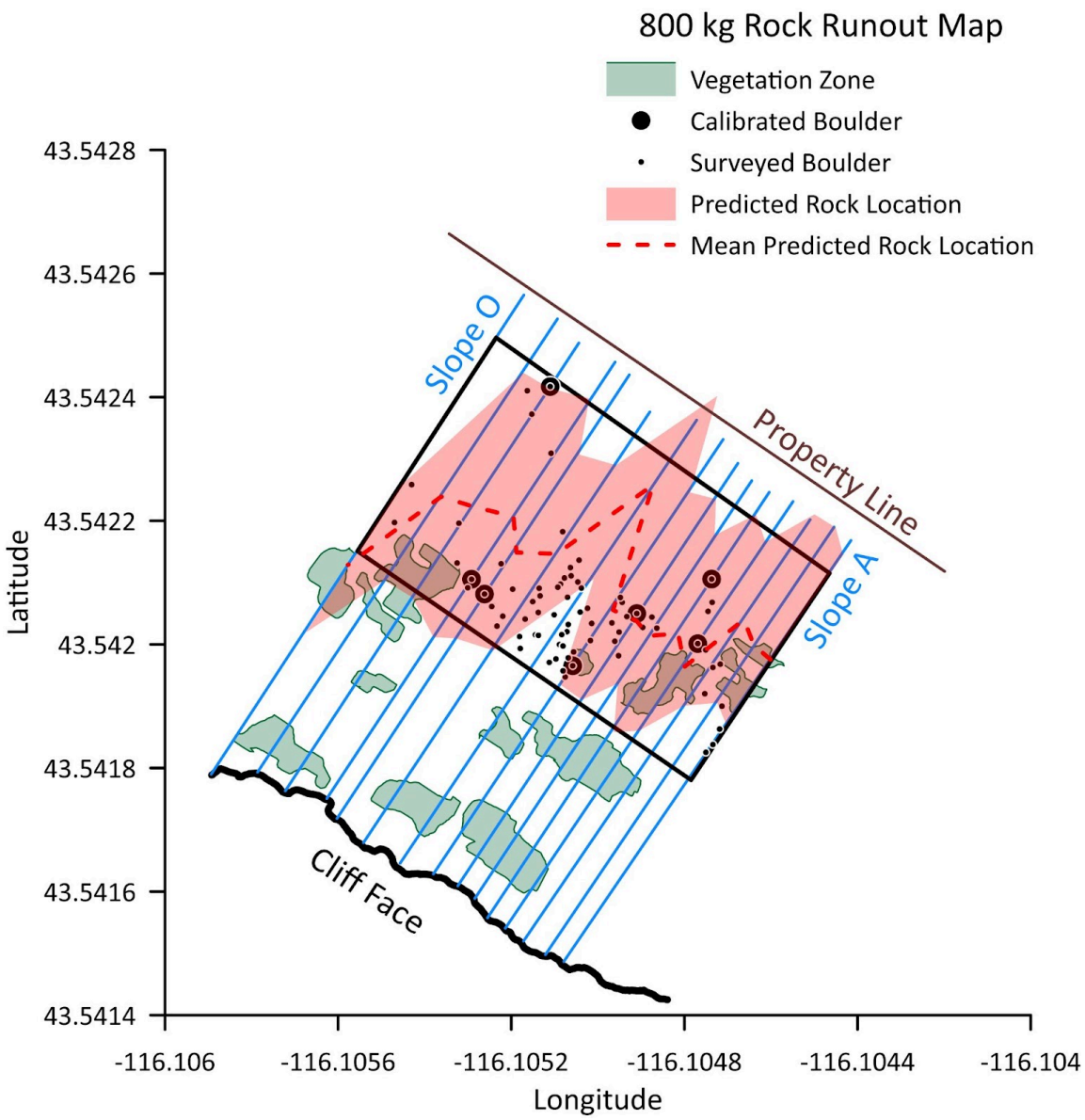
800 kg Rock Runout Map
Vegetation Zone
Calibrated Boulder
Surveyed Boulder
Predicted Rock Location
Mean Predicted Rock Location
Slope O
Property Line
Slope A
Cliff Face
Latitude
43.5428
43.5426
43.5424
43.5422
43.542
43.5418
43.5416
43.5414
-116.106
-116.1056
-116.1052
-116.1048
-116.1044
-116.104
Longitude

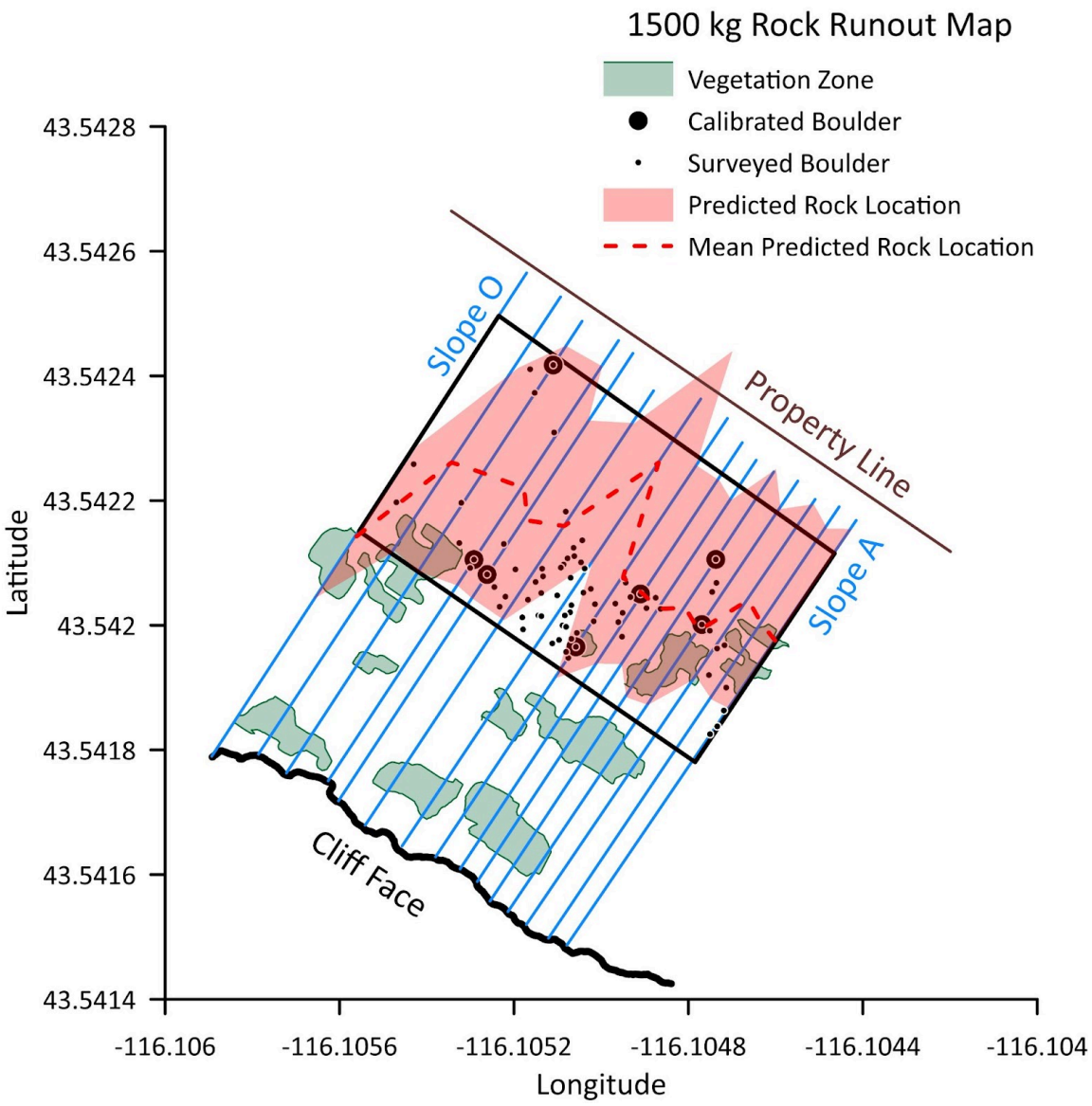
1500 kg Rock Runout Map
Vegetation Zone
Calibrated Boulder
Surveyed Boulder
Predicted Rock Location
Mean Predicted Rock Location
Slope O
Property Line
Slope A
Cliff Face
Latitude
43.5428
43.5426
43.5424
43.5422
43.542
43.5418
43.5416
43.5414
-116.106
-116.1056
-116.1052
-116.1048
-116.1044
-116.104
Longitude